2015

Simulation and Analysis of Air Recirculation Control Strategies to Control Carbon Dioxide Build-up Inside a Vehicle Cabin

Teron James Patrick Matton
University of Windsor

SIMULATION AND ANALYSIS OF AIR RECIRCULATION STRATEGIES TO CONTROL CARBON DIOXIDE BUILD-UP INSIDE A VEHICLE CABIN

by

TERON MATTON

A Thesis
Submitted to the Faculty of Graduate Studies
through the department of Mechanical, Automotive and Materials Engineering
in Partial Fulfillment of the Requirements for
the Degree of Master of Applied Science
at the University of Windsor

Windsor, Ontario, Canada
2015

SIMULATION AND ANALYSIS OF AIR RECIRCULATION STRATEGIES TO CONTROL CARBON DIOXIDE BUILD-UP INSIDE A VEHICLE CABIN

by

TERON MATTON

APPROVED BY:

R. Balachandar
Department of Civil & Environmental Engineering

G. Rankin
Mechanical, Automotive and Materials Engineering

A. Sobiesiak, Advisor
Mechanical, Automotive and Materials Engineering

January 9, 2015

Author's Declaration of Originality

I hereby certify that I am the sole author of this thesis and that no part of this thesis has been published or submitted for publication.

I certify that, to the best of my knowledge, my thesis does not infringe upon anyone's copyright nor violate any proprietary rights and that any ideas, techniques, quotations, or any other material from the work of other people included in my thesis, published or otherwise, are fully acknowledged in accordance with the standard referencing practices. Furthermore, to the extent that I have included copyrighted material that surpasses the bounds of fair dealing within the meaning of the Canada Copyright Act, I certify that I have obtained a written permission from the copyright owner(s) to include such material(s) in my thesis and have included copies of such copyright clearances to my appendix.

I declare that this is a true copy of my thesis, including any final revisions, as approved by my thesis committee and the Graduate Studies office, and that this thesis has not been submitted for a higher degree to any other University or Institution.

Abstract

Using air recirculation inside a vehicle is an effective way to minimize particle pollution and to maximize air conditioning cooling performance, however, prolonged use of air recirculation can cause high levels of carbon dioxide due to occupant exhalation and the lack of fresh air. Using air recirculation strategies can be an effective way of mitigating high carbon dioxide concentrations and poor air quality. Using AMEsim software, this study created a lumped parameter model to predict carbon dioxide concentrations, and analyzed the effects that various recirculation strategies had on the compressor load savings, carbon dioxide concentrations, and thermal environment inside the cabin. Results found fractional and on-off strategies to be effective ways of maintaining carbon dioxide concentrations below 1100 ppm, while timed control strategies produced unacceptable average concentrations above 1200 ppm and 3500 ppm for 1 occupant and 4 occupant scenarios under various driving cycles, consequently resulting in poor air quality.

Dedication

To my family,
your love and support has given me a solid foundation, and with it the determination to achieve my goals.

Acknowledgements

Firstly, I would like to thank the University of Windsor for providing me with the remarkable opportunity to study abroad in Italy, and conduct current research in the automotive industry. This thesis work is the result of a Double Degree Program between the University of Windsor and Politecnico di Torino, and I would like to express my deepest appreciation to Dr. Frise, Dr. Belingardi, Jan Stewart and Mohammed Malik who all played an important role in the coordination of this program. Their support through all the paperwork and necessary requirements made the transition from Windsor to Torino as seamless as possible.

I would also like to thank both my University of Windsor and Politecnico advisors Dr. Andrzej Sobiesiak and Professor Marco Masoero for their constant guidance and support throughout the completion of this thesis. Without their hard work, and dedication, none of this would have been possible.

A thank you goes out to my industry advisors Riccardo Seccardini, Roberto Monforte, and Kevin Laboe, as well as numerous colleagues at both Chrysler and Fiat, for their hospitality, experience and knowledge towards the project. Their assistance throughout my daily activities taught me valuable industry knowledge that was applied towards my project, and can be applied to any future endeavors .

A thank you goes out to Tony Mancini and again Mohammed Malik for organizing and arranging resources and partial funding on behalf of the industry partner for this project.

Finally, I would like to thank my committee members Dr. Gary Rankin, and Dr. Ram Balachandar whose diligent review has helped me refine and improve the quality of my thesis.

Contents

List of Figures

List of Tables

Nomenclature

Symbol	Description
AER	Air Exchange Rate (h^{-1})
AER_D	Determined Air Exchange Rate Using Fractional Recirculation (h^{-1})
AER_{OA}	Air Exchange Rate in Outside Air Mode (h^{-1})
AER_{RC}	Air Exchange Rate in Recirculation Mode (h^{-1})
AGGIH	American Conference of Governmental Industrial Hygienists
C_c	Carbon Dioxide Concentration in Vehicle Cabin
C_{ex}	Carbon Dioxide Concentration in Human Exhalation
C_o	Carbon Dioxide Concentration in Ambient Air
C_s	Carbon Dioxide Concentration in a Space
FR	Fraction of Recirculation
h_1	Specific Enthalpy at point 1
h_2	Specific Enthalpy at point 2
h_{2s}	Isentropic Specific Enthalpy at point 2
h_3	Specific Enthalpy at point 3
h_4	Specific Enthalpy at point 4
h_{ab}	Specific Enthalpy change from points a to b
HVAC	Heating Ventilation and Air Conditioning
IDLH	Immediately Dangerous to Life or Health
$\dot{m}$	Refrigerant Mass Flow Rate
m_a	Mass of Dry Air
m_v	Mass of Water Vapor
NIOSH	National Institute for Occupational Safety and Health
n	Number of Passengers
N	Carbon Dioxide Generation Rate per Person
OA/OSA	Outside Air
OSHA PEL	Occupational Safety and Health Administration Permissible Exposure Limit
ϕ	Relative Humidity (%)
P	Total Pressure of Air Vapor Mixture
P_g	Saturation Pressure of Water at Temperature T
P_v	Partial Pressure of Water Vapor at Temperature T
Q_{ex}	Human Exhalation Volume Flow Rate
Q_H	Heat Transfer with High Temperature Body
q_H	Heat Transfer per Unit Mass with High Temperature Body
Q_L	Heat Transfer with Low Temperature Body
q_L	Heat Transfer per Unit Mass with Low Temperature Body

Q_l	Vehicle Body Leakage Flow Rate
RC	Recirculation
REL	Recommended Exposure Limit
RH	Relative Humidity
R_o	Wheel Radius
S	Source Carbon Dioxide Mass Flow Rate
STEL	Short-term Exposure Limit
TWA	Time-weighted Average
TLV	Threshold Limit Value
UK WEL	United Kingdom Workplace Exposure Limit
T_{db}	Dry-Bulb Temperature
T_H	Temperature of High Temperature Source (K)
T_L	Temperature of Low Temperature Source (K)
T_{wb}	Wet-Bulb Temperature
V	Vehicle Speed (mph)
V_c	Vehicle Cabin Volume
V_o	Outside Ventilation Rate
W	System Work
w	System Work per Unit Mass
$\dot{W}_c$	Compressor Work
$\dot{W}_{in}$	Work Input
ω	Specific/Absolute Humidity

Chapter 1
Introduction

1.1 Background

In the majority of industrialized countries across North America and Europe, the working population generally spends a large amount of time inside vehicles. While a lot of emphasis has been put towards the adverse effects of outdoor pollution, there has been a lack of knowledge and stress towards the interior air pollution and indoor air quality in vehicles that can affect drivers and passengers. Air pollution stemming from the outdoor environment, in-cabin materials, human action, and the air conditioning system remains to be an important component that can adversely affect the health and safety of occupants inside the vehicle [1–9]. As the ideal cabin environment must also provide adequate thermal comfort in addition to proper air quality, factors that may affect the thermal environment must be controlled. Human comfort inside the vehicle cabin is strongly influenced by the temperature as well as relative humidity, thus the vehicle HVAC system must be able to control these parameters to a user-defined value or at least within the appropriate limits of an established human comfort threshold.

As the vehicle travels along the roadway, passengers can be exposed to undesirable outside air pollution through the vehicle HVAC system or through air exchange due to the vehicle body leakage, which can vary depending on the congestion levels of the road in question [2, 7–11]. Newer vehicle HVAC systems include two operating modes: recirculation (RC) and outside air (OSA) modes, which can be driver selected or implemented with an automatic function. Often times, the driver may switch to recirculated air mode in order to mitigate or eliminate the outdoor pollution entering the vehicle cabin [2, 8, 9]. There are also further advantages of using air recirculation mode. One of the main issues for automakers in today's green economy is ensuring their vehicles have the highest fuel economy possible in order to deal with constantly

increasing fuel costs and global fuel economy standards. The air conditioning compressor, one of the largest power consumers on the front end accessory drive of a vehicle, consumes a large amount of energy which will ultimately decrease the vehicle's fuel economy [12, 13]. Using cabin air recirculation has the ability to reduce the air conditioning compressor load, which would result in an increase in fuel economy [2, 8, 9]. However, what the driver may not be aware of, is the build-up of carbon dioxide due to occupant exhalation and the lack of outside fresh air. Over time, this build-up can be potentially hazardous to the health and safety of occupants in the vehicle [2, 8, 9, 14, 15].

As stated above, for an acceptable cabin environment the thermal environment must be controlled inside the vehicle in order to provide ideal human comfort levels. Vehicles with automatic climate control have the ability to monitor and control cabin temperatures, and relative humidity levels to a required value specified by the vehicle passenger. Importantly, relative humidity levels inside the cabin at low values constituting very dry air, or high values constituting very moist air, have the ability to cause discomfort regardless of the cabin temperature. A properly developed system must be able to control cabin air quality without threatening the thermal environment inside the cabin.

With the growing concern and importance of indoor air quality inside vehicles, the research conducted in this thesis provides a simulation tool to better understand aspects of this air quality, specifically carbon dioxide, and how it is affected by different vehicle and human parameters. Furthermore, this simulation tool can also analyze control strategies in order to mitigate any sources of poor air quality entering the vehicle cabin and evaluate the implications of these strategies on the thermal environment inside the cabin, carbon dioxide build-up inside the cabin and the compressor load savings of the air conditioning system.

1.2 Objectives

The objectives of this thesis research were to:

1. Develop a lumped parameter simulation tool using AMEsim in order to predict and quantify CO_2 concentrations inside the vehicle cabin
2. Implement recirculated-air flap control strategies in order to control CO_2 concentrations and relative humidity inside the vehicle cabin
3. Quantify and compare the effects of these recirculation flap management strategies on the vehicle HVAC system, related power consumption, and thermal environment inside the vehicle cabin.

1.3 Thesis Layout

The layout of this thesis includes the following. Chapter 2 is a review of any relevant literature relating to the study of air quality inside a vehicle cabin. This includes a general overview of refrigeration, psychrometrics and human comfort, in addition to the health concerns relating to particle pollution and carbon dioxide. This is then followed by any previous studies to quantify the air exchange rate inside a vehicle cabin under different conditions, and as well apply mode control strategies in order to reduce carbon dioxide build-up and particle pollution inside the cabin. Chapter 3 details the methodology for the simulations, a model sensitivity analysis in determining the most influential parameters, and finally the model integration and application of mode control strategies. Chapter 4 details the simulation results and analysis, including a discussion of the results and any possible limitations and uncertainties affecting the simulation results. Finally Chapter 5 goes on to conclude the results of this thesis study and detail any recommendations for future work.

Chapter 2
Review of the Literature

The following chapter is a review of the available literature pertaining to the control of CO_2 emissions and relative humidity inside a vehicle cabin. Before going into detail about the available literature on the above subjects, it is important to address the fundamentals of refrigeration, psychrometrics and human comfort, which are three main aspects of vehicle HVAC systems. An emphasis will be placed on the temperature and relative humidity ranges that produce optimal thermal comfort. Studies concerning thermal comfort while driving will also be investigated, to further realize optimal conditions of thermal comfort inside a vehicle cabin, and at which thresholds passengers and drivers become affected by thermal discomfort.

Further information in this chapter will discuss the associated health effects, and standards placed on CO_2 exposure. This information will be particularly useful for establishing proper limits for mitigating CO_2 build-up inside the cabin, as a successfully implemented system should be able to control CO_2 build-up to a specified standard found in literature. Lastly, this chapter will focus on studies for predicting the air exchange rate based on different vehicle parameters, and implementing different flap control management strategies for CO_2 control. A large portion of this information will form the base needed to create an accurate CO_2 concentration build-up model.

2.1 Background Theory

2.1.1 Fundamentals of Refrigeration

In order to begin to study refrigeration cycles and the effects of recirculation strategies on the compressor load of the system, it is important to start with a discussion about simple refrigeration cycles and their operating principles. A refrigerator is a cyclic device that allows the transfer of heat from a low-temperature

region to a high-temperature region using a required work input, as shown in Figure 2.1 [16, 17].

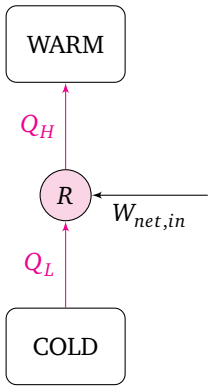

Figure 2.1: A schematic of a refrigeration cycle [16]

The principle cycle involving the process of refrigeration stems from the theoretical thermodynamic cycle known as the Carnot cycle that converts a certain amount of thermal energy into work. The Carnot cycle involves the following isothermal and adiabatic processes:

- Reversible, adiabatic (isentropic) compression and expansion
- Isothermal heat addition and rejection

Since all processes of the Carnot cycle are reversible, by reversing the Carnot cycle, all work and heat interactions in turn are reversed, creating the Carnot Refrigeration Cycle, shown on a T-s diagram in Figure 2.2. Heat is absorbed at the low temperature region, and rejected at the higher temperature region, requiring a work input. The Carnot refrigeration cycle represents the most efficient refrigeration cycle operating between two temperatures, and sets the highest possible coefficient of performance (COP), which can be calculated using Equation 2.1. Since heat is exchanged at constant temperature, T_H=T_2,T_3 refers to the maximum temperature reached by the working fluid in the cycle corresponding to its vaporization temperature, while

T_L=T_1,T_3 refers to the lowest temperature reached in the cycle corresponding to its condensing temperature.

$$COP_R = \frac{Q_L}{Q_H - Q_L} = \frac{1}{\frac{T_H}{T_L} - 1} \tag{2.1}$$

In actuality, the processes involved in the Carnot refrigeration cycle are difficult to attain not only due to the problem of eliminating irreversibilities, but also due to the mechanical issue of compressing and expanding a two-phase fluid. It is for these reasons, that the Carnot cycle is strictly a theoretical thermodynamic cycle and cannot be used in practice [16, 17]. The irreversibilities and mechanical problems

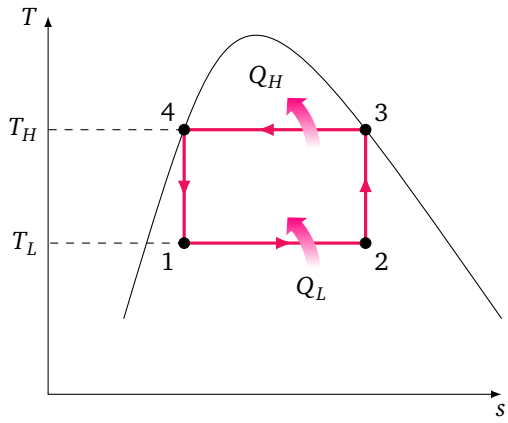

Figure 2.2: The Carnot refrigeration cycle shown on a T-s diagram [16]

associated with the Carnot refrigeration cycle discussed in the previous paragraph can be eliminated by vaporizing all of the working fluid before being compressed, and by replacing the turbine with a throttling device [16, 17]. The resulting cycle, in which most real refrigeration cycles are based on, is known as the Ideal Vapor Compression Cycle shown on a T-s diagram in Figure 2.3a and on a P-h diagram in Figure 2.3b. The ideal vapor compression cycle involves the following processes:

- 1-2_s: Isentropic Compression

- 2_s-3: Constant Pressure Heat Rejection in a Condenser
- 3-4',4: Throttling in an Expansion Device
- 4-1: Constant Pressure Heat Absorption in an Evaporator (Deviation from point 4' to 4 is due to the high irreversibilities of the throttling device)

In an ideal vapor-compression refrigeration cycle, the refrigerant enters the compressor as saturated vapor and is cooled to the point of being a saturated liquid in the condenser. It is then throttled to a lower pressure and vaporizes in the evaporator as it absorbs heat from the refrigerated space.

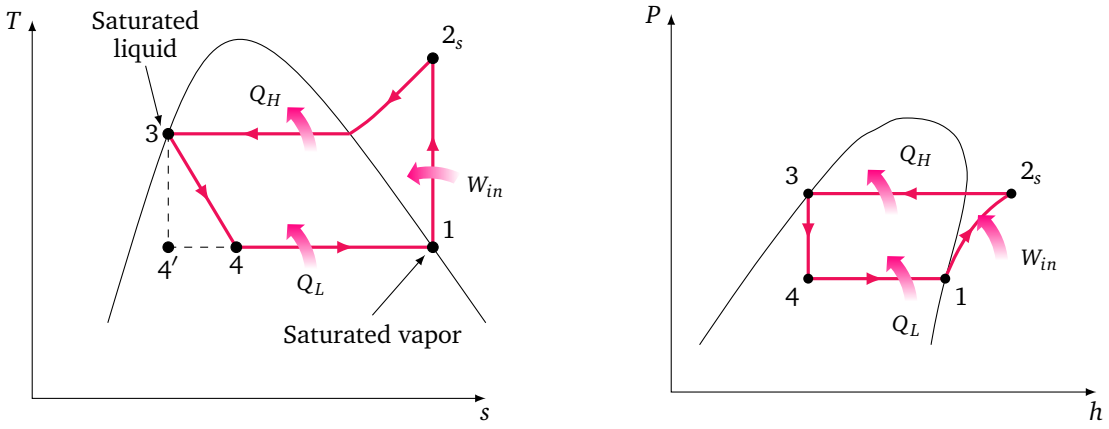

(a) T-s Diagram (b) P-h Diagram

Figure 2.3: Ideal vapor compression cycle shown on a T-s and P-h diagrams [16]

Utilizing the P-h diagram it is useful to define the main parameters of the refrigeration system per unit mass. In order to calculate the heat transfer rate or work, the heat rate or work per unit mass needs to be multiplied by the mass flow rate of the working fluid. The cooling capacity of the system per unit mass, can be defined as the heat absorbed by the working fluid in the evaporator. It is equal to the enthalpy

difference between points 1 and 4, and defined in the following equation:

$$q_L = q_{41} = h_1 - h_4 \tag{2.2}$$

The heat rejected by the working fluid in the condenser per unit mass is equal to the enthalpy difference between points 2 and 3, and can be defined as:

$$q_H = q_{23} = h_2 - h_3 \tag{2.3}$$

Finally, we can define the compressor load or work consumed by the system in the following equation, equal to the enthalpy difference between points 2_s and 1:

$$w_{in} = q_{12s} = h_{2s} - h_1 \tag{2.4}$$

The energy balance of the ideal vapor compression cycle can be defined in the following equation:

$$W - Q = \sum_{i}^{n} h_i \dot{m}_i \tag{2.5}$$

Given the system is closed, the refrigeration cycle has zero work output and an analysis on the entire cycle is undertaken, Equation 2.5 can be simplified into Equation 2.6, where Q_H represents the heat rejected from the working fluid and Q_L represents the heat absorbed by the working fluid.

$$W_{in} = Q_H - Q_L \tag{2.6}$$

The coefficient of performance for the ideal vapor compression cycle can be defined by the ratio of the desired output over the required input. Since the desired output of a refrigeration cycle is to remove heat from the refrigerated space, the coefficient of

performance for the ideal vapor compression cycle can be shown to be:

$$COP = \frac{desired}{required} = \frac{Q_L}{W_{in}} = \frac{h_1 - h_4}{h_{2s} - h_1} \tag{2.7}$$

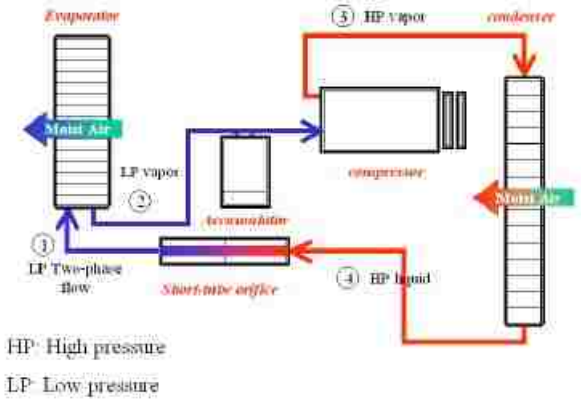

Figure 2.4: Schematic of an actual AC loop - Source: AMEsim Library

A real vapor compression cycle, shown on a schematic in Figure 2.4 differs from the ideal case due to irreversibilities that occur during the cycle. These irreversibilities are mainly attributed to fluid friction causing pressure drops throughout the system, and heat transfer to the surroundings, both of which have an influence on the entropy of the system [16]. The compression from point 1-2_s will no longer be an isentropic process, but a normal compression process as depicted in Figure 2.5. The resulting difference in enthalpies from $h_2 - h_1$ is larger than the difference in $h_{2s} - h_1$, resulting in a decrease of the COP. We can now define the isentropic efficiency of the compressor as the ratio of the ideal cycle compressor work over the real cycle compressor work as follows:

$$\eta_{s,c} = \frac{h_{2s} - h_1}{h_2 - h_1} \tag{2.8}$$

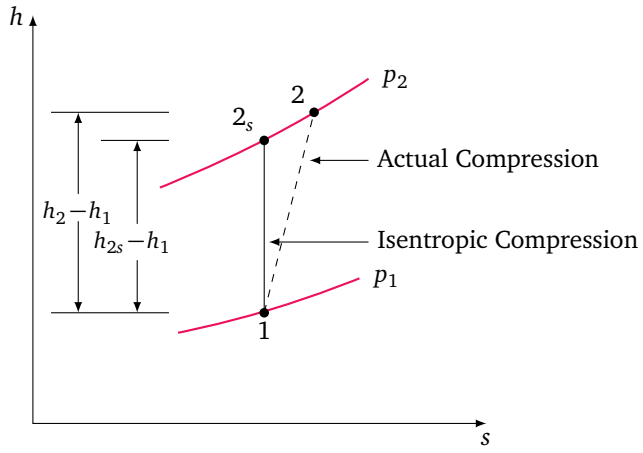

Figure 2.5: Deviation from isentropic compression to normal compression [16]

2.1.2 Fundamentals of Psychrometrics

The study of psychrometrics is used to describe the thermodynamic and thermal properties of gas-vapor mixtures. More specifically, the psychrometrics of air concerning air-water vapor mixtures is important in aspects of heating, ventilation and air conditioning and the determination of human comfort. The fundamentals of psychrometrics become important in understanding what happens to the moist air volume inside the cabin, and how it may be affected by different recirculation strategies.

Air existing in our atmosphere usually contains water vapor. When considering air conditioning applications (under 50°C), it is often convenient and practical to treat both air and water vapor as ideal gases [16]. Under this assumption, atmospheric air can be treated as an ideal gas mixture, and follow Dalton's Law of Additive Pressures shown in Equation 2.9; that is the total pressure of the air is equal to the additive pressures of the dry air and water vapor. It is also interesting to note that when treating water vapor as an ideal gas, the enthalpy of the water vapor may be taken to be equal to the enthalpy of saturated vapor at the same temperature with a negligible

error [16].

$$P = P_a + P_v \tag{2.9}$$

There are several main parameters that must be defined in order to adequately describe the psychrometrics of moist air. These include but are not limited to: absolute and relative humidity, dry-bulb temperature, wet-bulb temperature, dew point, specific volume and specific enthalpy. The amount of water vapor in the air can be expressed by both the absolute and relative humidity. The absolutely humidity 'ω' represents the actual ratio of water vapor per unit mass of dry air shown in Equation 2.10 [16–18].

$$\omega = \frac{m_v}{m_a} \tag{2.10}$$

The amount of water vapor can also be expressed according to the relative humidity (%), which can be defined as the ratio of how much water vapor the air holds relative to the maximum amount of water vapor the air can hold at the same temperature. This can be shown mathematically in Equation 2.11, by dividing the partial pressure of the water vapor by the saturated vapor pressure of water at the same temperature [16–18].

$$\phi = \frac{P_v}{P_g} \tag{2.11}$$

The dry-bulb temperature is the standard temperature of atmospheric air that is used in describing the weather using a normal thermometer. The wet-bulb temperature, however, is measured using a thermometer whose bulb is covered by a cotton wick that has been saturated in water. Air has to be passed over the wick to get the water temperature close to the adiabatic saturation temperature at the existing atmospheric pressure. As unsaturated air is passed over the wick, some of the water in the wick will evaporate, dropping the temperature of the thermometer. The rate of evaporation from the wet-bulb thermometer depends on the humidity of the air as

evaporation is slower when the air is already full of water vapour. For this reason, the difference in the temperatures indicated by the two thermometers gives a measure of atmospheric humidity. The dew point temperature can be described at the temperature at which condensation begins to form, when air is cooled at constant pressure. At this point, the air is 100% saturated and cannot hold any more water vapor, causing condensation to occur. This situation becomes prominent with the fogging of windshields in automobiles. Other properties such as volume and enthalpy are specified per kilogram of dry air as specific volume and specific enthalpy since the amount of dry air remains constant.

The use of a psychrometric chart, whose principal features are showcased in Figure 2.6 [16], is a useful tool for describing the psychrometric parameters of moist air. The dry bulb temperature can be seen along the horizontal axis, while the specific humidity can be seen along the vertical axis. The curved line towards the left of the chart represents the 100% saturation line, where the relative humidity of the air is equal to 100%. Other constant relative humidity lines follow the same general shape. One can easily obtain the dew point temperature by traveling along a horizontal (constant ω) until the 100% saturation line is reached. Lines of constant specific volume slope steeply downward on the psychrometric chart, while lines of constant wet bulb temperature and specific enthalpy run less steep and almost parallel to each other. By knowing any two parameters on the psychrometric chart, the remaining psychrometric parameters can be determined, making it a useful tool for air conditioning applications.

Air conditioning processes can also be easily described with the use of a psychrometric chart. Sensible heating and cooling processes can be visualized by traveling in a horizontal line on the psychrometric chart (constant specific humidity meaning no water vapor added or removed). Adding water vapor or humidifying can

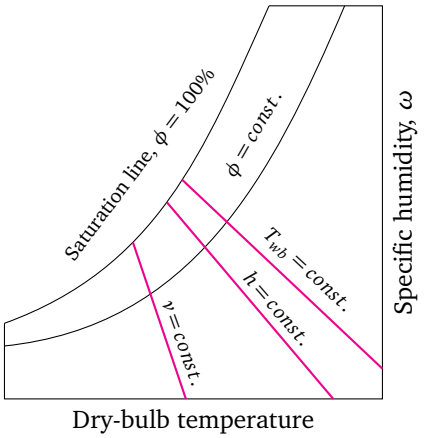

Figure 2.6: The psychrometric chart [16]

be described by traveling vertically upward on the psychrometric chart while removing water vapor or dehumidifying can be seen by traveling vertically downward. Furthermore heating and humidifying can be described by traveling in a north-east direction, heating a dehumidifying can be described by traveling in a south-east direction, cooling and humidifying can be described by traveling in a north-west direction and finally cooling and dehumidifying can be described by traveling in a south-west direction.

2.1.3 Human Thermal Comfort

Thermal comfort may be defined as a state of being satisfied with the thermal environment and associated surroundings. Providing thermal comfort for all individuals can be difficult, as it has a tendency to be a subjective parameter; meaning the thermal comfort needs of one individual may not necessarily satisfy the thermal comfort needs of another. The climate control system in a vehicle makes every effort to maintain the thermal comfort of every occupant, under all possible ambient conditions. The following section will discuss the fundamentals of human comfort and the factors that affect it.

The human body needs to maintain an internal temperature of roughly 37°C, and is in thermal equilibrium when the heat production of the body equals the heat loss to the surroundings [16, 19]. The values of heat production and heat loss can vary due to the metabolic rate of the individual, the amount of heat storage and the rates of radiation, conduction and convection to the surroundings through the skin and respiration [16, 19]. An individual may feel the most comfortable when the body temperature is in a very narrow range, and the body is able to regulate this temperature with minimal effort [19].

There are several factors both environmental and personal which contribute most to a human's perception of thermal comfort. Several sources [16, 19] have listed the following as the most contributing environmental factors that affect thermal comfort: dry-bulb temperature, relative humidity, mean radiant temperature, and local air movement. Other personal factors such as a person's clothing and metabolism can also have a significant effect on thermal comfort.

Dry-bulb Temperature and Mean Radiant Temperature

In general, humans are most sensitive to variability in the dry-bulb temperature, as it affects the evaporative and convective heat losses of the body [16, 19]. If the body temperature increases above or falls below a certain set-point, physiological processes will occur such as sweating or shivering in order to control the heat balance of the body and regulate an acceptable internal temperature. Table 2.1 shows the acceptable temperature ranges, along with relative humidity limits for suitable thermal comfort according to ASHRAE Standards [20]. The mean radiant temperature is the uniform temperature of an imaginary enclosure in which radiant heat from the human body equals the radiant heat transfer in the actual non-uniform enclosure [19]. It is calculated as the area weighted mean temperature of all the objects surrounding the body. It can also be calculated using measured values of the temperature of the

Table 2.1: Temperature/Humidity Ranges for Comfort [19, 20]

Conditions	Relative Humidity	Acceptable Operating Temperatures	
		°C	°F
Summer (Light Clothing)	If 30%, then	24.5-28	76-82
	If 60%, then	23-25.5	74-78
Winter (Warm Clothing)	If 30%, then	20.5-25.5	69-78
	If 60%, then	20-24	68-75

surrounding walls and their angular position relative to the individual. The mean radian temperature has the ability to affect the radiant heat loss from the body, meaning thermal comfort can be affected by the temperature of surrounding walls, regardless of the air temperature of the surroundings.

Relative Humidity

As previously described in Section 2.1.2, relative humidity is the ratio of the partial pressure of the water vapor in the air to the saturated vapor pressure of water at the same temperature [16–18]. As the amount of water vapor air can hold decreases as the temperature decreases, the relative humidity of the air will increase with a decrease in temperature and vice-versa. Although human sensitivity to variations in relative humidity is much lower than to variations in temperature, controlling it is important to provide adequate thermal comfort. Table 2.1 shows the relative humidity ranges and temperature ranges that provide acceptable thermal comfort in both winter and summer conditions. Humans generally feel comfortable with a relative humidity ranging from 30/40-60%, provided the temperature is also in an acceptable range [16, 19–21]. Relative humidity values under 30% have been shown to cause eye and throat irritation, and drying of the mucous membranes and nasal passages [19, 21], while relative humidity values above 60% can cause reduced evaporative cooling of the body, mold growth in buildings and other moisture related problems [19, 21].

A study done by Tsutsumi et al. [22], looked at the effects of the car cabin environment on passenger comfort and fatigue. The study had subjects report their sensations and general fatigue under different driving simulating conditions. The study found that the rate of complaints related to fatigue increased under high humidity conditions (>60%), which could represent the possibility of difficulty concentrating. It also showed that indoor humidity and local air velocity have a negative impact on subjective eye dryness sensation and visual fatigue, which could also result in further distractions due to discomfort while driving.

Local Air Movement

Local air movement also has the ability to affect thermal comfort in humans, mainly by influencing the amount of convective heat loss from the skin. This parameter can more specifically apply to the blower fans inside the passenger compartment in a vehicle cabin. ASHRAE Standard 55 considers two recommendations for allowable local air velocities to maintain thermal comfort: minimizing the risk of draft, and to provide adequate occupant cooling [20]. These two cases represent where local air velocity could be needed (increased convective cooling), or unwanted (undesired local convective cooling). In order to eliminate draft, limits on local air velocity are in place as a function of the air temperature and turbulence intensity when the individual does not have localized control over the mean air velocity. Lower air temperatures and higher turbulence intensities have been shown to increase the severity of the draft [20], as they affect the amount of heat loss from the skin. In the case of air velocity to provide increased convective cooling, ASHRAE Standard 55 allows the lower limit of air velocity to be higher if the occupant has direct control over these velocities [20]. In the case of a vehicle cabin, the occupants have direct control over the blower air speed, allowing the limit of air velocity to be higher.

Personal Factors

Personal factors such as metabolism and clothing insulation have the ability to greatly affect human comfort levels [16, 19]. The metabolism of the human body will affect the heat generation rate inside the body, therefore requiring different energy balancing loads. The body's metabolism generally decreases with age; thus an older individual may feel thermal discomfort at the same conditions a younger individual may feel comfortable. A rise in activity level will also produce increased metabolic heat generation inside the body, therefore requiring more heat loss to the environment to feel comfortable as compared to a resting individual [16, 19]. Some typical heat generation values for different activities are 40 W/m^2, 60-115 W/m^2 and 175-235 W/m^2 for sleeping, driving and exercising respectively [19]. The clothing an individual wears affects the body's heat loss and comfort due to the insulation provide by the clothing [16, 19]. Clothing insulation values can be described by its clo value, with 1.0 clo being equivalent to 0.155 m^2K/W. Typical clo values for summer clothing are in the range of 0.35-0.6, while clo values for heavy winter clothing can range from 0.8-1.2 clo or higher. The preference of clothing further increases the subjectivity for optimal thermal comfort making it difficult to always satisfy 100% of occupants.

2.2 Particle and Carbon Dioxide Pollution

Before looking to implement a flap strategy to control particle pollution and carbon dioxide pollution in the vehicle cabin, it is essential to understand the pollutants in question and also the potential health risks of both short term and long term exposure. Furthermore, it is also important to look at any standards placed on these pollutants in order make the mitigation strategy most effective. By investigating the health risks imposed by the pollutants, we can truly understand any benefits gained from the strategy.

2.2.1 Risks of Particle Pollution

Particle pollution, specifically ultra-fine particle pollution, which can enter the cabin through the HVAC system when in oustide air (OSA) mode, can be harmful to occupants inside the cabin [2, 3, 9–11, 23]. Due to the higher concentration of particulate matter on roadways, the risk for occupants traveling on a busy roadway may be even more severe [2, 3, 9–11, 23]. For a daily hour commute exposure, the cabin environment can contribute 10-50% of a person's daily exposure to ultra-fine particles, enforcing the need to reduce occupant exposure to fine particle pollution [2]. The cabin air-filter looks to mitigate the particle pollution entering the cabin, but is not always 100% effective. Ultra-fine particle exposure has been linked to various health effects such as respiratory and cardiovascular effects for short-term and long-term exposures [14, 15, 24]. The use of recirculation (RC) mode inside the cabin provides a temporary barrier to any particulate matter that may enter the cabin while in OSA mode. A study by Y. Zhu [3] looked at analyzing the effects of particulate matter entering the cabin when using RC mode and OSA mode. The study found a maximum protection of around 85% for ultrafine particle pollution when in RC mode with the fan on. By utilizing the benefits of RC mode, either fractional or full, the particle concentrations entering the cabin can be reduced.

2.2.2 Risks of Carbon Dioxide Exposure

At standard temperature and pressure, carbon dioxide is a colourless, odourless gas that exists in our atmosphere at roughly 390 ppm, representing about 0.04% of the atmospheric air. In addition, it is also the most common by-product of living organisms, with the average adult male exhaling carbon dioxide at a rate of 220 mL/min at rest and up to 1650 mL/min during moderate exercise, with a concentration ranging from 38,000-57,000 ppm [15]. There are a multitude of

resources detailing the effects of both acute exposure and also prolonged, low-level exposure to carbon dioxide. In this investigation, prolonged low-level exposure may be the more logical scenario for concentrations inside the vehicle cabin.

Carbon dioxide acts as both a depressant and a stimulant on the central nervous system. At concentrations of 17% and above, convulsions, unconsciousness and even death can occur in seconds; and at a concentration about 10% this same result can occur in anywhere from 10-20 minutes [14, 15, 24]. The threshold of hearing can be reduced with concentrations in the range of 3-8%, and increased respiration levels have been noted at concentrations as low as 1% and above [14, 15, 24]. Furthermore, carbon dioxide has the ability to act as an asphyxiant due to its ability to displace oxygen, greatly contributing to the danger of high carbon dioxide concentrations [14, 15, 24]. Table 2.2 [24] details some of the effects of acute carbon dioxide exposure at different concentrations and exposure times. While prolonged low level exposure (<3%) is not immediately life threatening, and shows non-threatening effects in healthy young adults, it may have consequences for sensitive populations. Some of these sensitive populations include: infants and children, medicated individuals, and individuals performing complex tasks (requiring psychomotor coordination, visual perception, attention, and rapid response) [14]. It is possible that even at lower concentrations of 1-3%, the effects of carbon dioxide exposure have the ability to influence driving ability, which could be classified under the category of a complex task.

2.2.3 Occupational Standards for Carbon Dioxide Levels

There are several established occupational exposure limits around the world that are listed in Table 2.3 [15, 25, 26]. It is clear that these standards are very similar to establish a time weighted average of 5000 ppm as well as a ceiling limit of 30 000 ppm. By reducing short term exposures of carbon dioxide pollution below 3%, and

Table 2.2: Acute Health Effects of Carbon Dioxide [24]

Carbon Dioxide Concentration (%)	Exposure Time	Associated Effects
2	Several Hours	Headache, dyspnea upon mild exertion
3	1 Hour	Mild headache, sweating, and dyspnea at rest, hearing threshold reduces
4-5	Few Minutes	Headache, dizziness, increased blood pressure, uncomfortable dyspnea
	1-2 Minutes	Hearing and visual disturbances
6	<16 Minutes	Headache, dyspnea
	Several Hours	Tremors
7-10	Few Minutes-Hour	Headache, increased heart rate, shortness of breath, dizziness, sweating, rapid breathing, near unconciousness
10-15	Several Minutes	Dizziness, drowsiness, severe muscle twitching, unconciousness
17-30	Within 1 Minute	Loss of controlled and purposeful activity, unconsciousness, convulsions, coma, death

establishing a time weighted average of 0.5%, symptoms and effects relating to carbon dioxide exposure can be reduced.

Table 2.3: Occupational Exposure Limits for Carbon Dioxide [15, 25, 26]

	8-hour TWA	15-min STEL
OSHA PEL	5,000 ppm	N/A
NIOSH REL	5,000 ppm	30,000 ppm
AGGIH TLV	5,000 ppm	30,000 ppm
UK WEL	5,000 ppm	15,000 ppm
NIOSH ISDLH: 40,000 ppm		

2.2.4 ASHRAE Standard for Carbon Dioxide Levels

Since the environment in a workplace can be drastically different than the environment inside a vehicle cabin, occupational limits on carbon dioxide may not be the most appropriate boundaries for acceptable cabin air quality. The American Society of Heating, Refrigerating and Air-Conditioning Engineers is a global society which focuses on building systems, energy efficiency, indoor air quality, refrigeration

and sustainability, who operate through the development of research, standards writing, and publishing to ensure sustainable technology for today's world. ASHRAE Standard 62 presents a wide range of information concerning ventilation for acceptable indoor air quality. Although this standard does not include any specific information pertaining to air quality inside a vehicle cabin, this standard can provide adequate relevance when considering the vehicle cabin as a conditioned space. ASHRAE standard 62, provides the carbon dioxide limit that satisfies human comfort levels in a conditioned space. This ASHRAE limit is specified as 700 ppm, on a continuous basis, over the ambient concentrations in the atmosphere [27]. This 700 ppm guideline is based on the use of indoor carbon dioxide concentration as an indicator of human bioeffluent concentrations, and it is important to note that this 700 ppm limitation is not related to any health effects from the carbon dioxide itself, but only to an odor sensitivity caused by human bioeffluents [27].

ASHRAE also includes a detailed summary of how this 700 ppm guideline was calculated. Using a mass balance equation, the outdoor air flow rate needed to maintain the steady-state carbon dioxide concentration below a certain limit can be calculated. Further information included in the ASHRAE standard, shows that an outdoor air flow rate of 7.5 L/s per person will dilute odors from human bioeffluents to levels that will satisfy a large majority of un-adapted persons to a space [27]. If the ventilation rate is kept to 7.5 L/s per person, the resulting carbon dioxide concentration relative to the outdoor air can be calculated as shown in Equation 2.12 and Equation 2.13.

$$V_o = N/(C_s - C_o) \tag{2.12}$$

$$\begin{aligned}(C_s - C_o) &= N/V_o \\ &= 0.31/(7.5 \times \tfrac{60sec}{min}) \\ &= 0.00689\text{litres of CO2 per litre of air} \\ &\approx 700ppm\end{aligned} \tag{2.13}$$

Several studies have used the following guideline when considering controlling carbon dioxide emissions inside a vehicle cabin [2, 8, 9]. Due to the relevance of this guideline to human comfort levels, and the widespread use in related studies and literature, it will be considered appropriate for use in controlling carbon dioxide levels inside the vehicle cabin.

2.3 Vehicle Air Exchange Rates

The air exchange rate (AER) is a measure of how many times the air is replaced in a designated space during one hour. Inside a vehicle cabin, the air exchange rate is the main factor that establishes the build-up of pollutants inside the cabin, as well as the ratio of outside concentrations to inside concentrations [1, 2, 7–11, 23, 28–30]. Several studies have strived to quantify the air exchange rate in vehicles, with the majority doing so in order to predict in-cabin particle pollution concentrations. The following section will discuss previous studies to quantify the air exchange rates inside vehicle cabins based on different vehicle parameters.

Fletcher and Saunders [28] was one of the first to study infiltration rates of a gas into a vehicle cabin. During this study, five vehicles were tested using a tracer gas method (SF6). Experiments for determining the air exchange rate were conducted using a stationary vehicle with different wind speeds and directions and as well in a moving vehicle at constant speeds between 35 and 75 mph. This study found that the air exchange rate in a moving vehicle at a given speed was greater than the air exchange

rate in a stationary vehicle with the wind passing at the same speed. Further results from this study derived an empirical equation shown in Equation 2.14 for calculating the air exchange rate based on vehicle speed for the case of passive ventilation (RC mode off and vents open).

$$AER = 0.6 \cdot V^{1.25} \tag{2.14}$$

Ott et al. [30] studied air exchange rates in vehicles in order to model in-vehicle pollutant concentrations from second-hand smoke. Using a tracer gas method (SF6), this study made more than 100 air exchange rate measurements on four different vehicles under moving and stationary conditions. This study found that vehicle speed, window position, ventilation system and air conditioner setting had a significant effect on the air exchange rate inside the vehicle cabin. Reported air exchange rates with the windows closed were in the range of 1.9 to 40 h^{-1} with speeds ranging from 32-116 km/h. Further important aspects revealed that by opening a single window 3 inches, the air exchange rate increased 8-16 times. This study was also able to correlate its results to the empirical model derived by Fletcher and Saunders from Equation 2.14 for passive ventilation.

Knibbs at al. [29] is the second largest study to date concerning air exchange rates in vehicle cabins. This study used a tracer gas approach to study the air exchange rate in six vehicles, ranging in age up to 18 years, at three vehicle speeds under four strictly different ventilation settings. Conducting more than 200 measurements, this study found air exchange rates ranging from 1 to 33 h^{-1} at a vehicle speed of 60km/h and ranging from 3 to 47 h^{-1} at a vehicle speed of 110 km/h. Results obtained correlated with other studies previously mentioned, and were used to create linear regression models for each vehicle at each ventilation setting. These measurements not only showed the variation of air exchange rate with vehicle speed, but also the differences between OSA and RC mode, and the large variability from one vehicle to another.

For the automotive HVAC system, there are a large number of fan speed, vent position, and air intake position combinations which will affect the air exchange rate [10, 11, 23]. Since it is impractical to measure the air exchange rate in a substantially large number of vehicles, with a large number of parameter combinations, predictive models are necessary in order to estimate the value [10]. Studies done by Hudda et al. [11, 23] are the largest to date that relate to the prediction of air exchange rates inside vehicle cabins. These studies used CO_2 as a tracer gas to perform air exchange rate measurements on a total of 132 vehicles (between both studies). A total of 453 different combinations (308 RC Mode and 145 OSA Mode) were used on 73 vehicles under different vehicle speeds and fan settings. Vehicles were chosen from a wide variety of sub categories (sub-compact, compact, mid-size, etc.), in order to properly represent their proportions in the U.S. fleet, and create a model that encompasses a wide range of cabin sizes. These measurements were then used in order to create a generalized estimating equation (GEE) of the air exchange rate in both RC and OSA modes.

The study incorporated a large amount of independent variables such as: ventilation fan strength, vehicle age, mileage, cabin volume, manufacturer, and the product of coefficient of drag and frontal area, with only the most influential variables being used into the GEE model. When the vehicle was operated under RC mode conditions, vehicle age, speed and volume were among the most influential factors along with the vehicle manufacturer [11, 23]. Fan setting was observed to slightly increase the air exchange rate, but was not significant [11, 23]. The final GEE model for RC mode is shown in Equation 3.5 [11]. Units involved in these equations are expressed in mph for vehicle speed, $cubic\ feet$ for vehicle volume, and $years$ for vehicle age. When the vehicle was operated under OSA mode conditions, fan strength showed the most variability, followed by the vehicle speed along with vehicle cabin

volume. The final GEE model for OSA mode is shown in Equation 3.6 [11]. Again, units involved in these equations are expressed in mph for vehicle speed, $cubic\ feet$ for vehicle volume, and $years$ for vehicle age. A more in-depth discussion of the influential parameters, and their effects on the air exchange rate will be discussed further in Section 3.2. The predictive models derived by Hudda et al. had a relatively good fit with experimental data (R^2 of 0.68 for RC and 0.79 for OSA) and were cross-validated to a different data set to obtain a cross-validated R^2 value of 0.60 and 0.73 for RC and OSA modes respectively. Given the widespread vehicle-to-vehicle differences for air exchange rates, especially in RC mode, this model has produced an adequate predictive equation for estimating the air exchange rates for different vehicles.

2.4 HVAC Mode Control Strategies

The author has reviewed two major studies that specifically look at different mode control strategies for the suppression of carbon dioxide inside the vehicle cabin [8, 9]. These mode control strategies were adopted into this thesis research for a strategy comparison. The first study uses an on-off type and timed control that only can address full RC or full OSA modes. The second study looks at implementing a fractional control strategy, in order to have any fraction of recirculated air from 0 to 100%. The following section will focus on these previous studies to investigate different mode control strategies for mitigating carbon dioxide build-up inside the vehicle cabin, and their results. These two studies feature experimental results of different recirculation strategies as feasibility tests to verify the concept of the strategies. This thesis research looks to take a further step by the simulation of carbon dioxide build-up and the comparison of these different recirculation strategies via a computational simulation model.

2.4.1 On-Off and Timed Recirculation Control

A study done by Gursuran Mathur [8], looked at the carbon dioxide build-up inside a vehicle cabin, and used an on-off type recirculation flap strategy to control this build-up. Mathur suggested that this strategy be timed (switch to OSA mode every 10 minutes) or controlled by limiting values provided the use of a carbon dioxide sensor. The objectives of this study were the following: to measure peak cabin carbon dioxide concentrations for increasing amounts of occupants at city and highway driving conditions, and to also investigate the effects of applying an on-off type control under the same conditions. Experiments were conducted using a model year 2003 vehicle, under specific driving routes where carbon dioxide concentrations were monitored in real time. Results for city driving conditions (20-25mph) measured peak concentrations of 1200 and 4025 ppm for 1 and 4 passengers respectively. Further results for highway driving conditions (65-70mph) measured peak concentrations of 1020 and 2800 for 1 and 4 passengers respectively, concluding that at lower vehicle speeds there will be higher peak concentrations due to lower amounts of body leakage. When applying the recirculation control to the above city and highway driving tests, Mathur followed ASHRAE Standard 62 for the upper threshold, and around 500 ppm for the lower threshold. The control resulted in cycling of the blower mode door in approximately 6 minutes for one occupant and a reduced time of 2 minutes for four occupants during city driving. Under highway driving conditions the cycling time was approximately 9 minutes for one occupant and 3 minutes with four occupants. As an example of their results, carbon dioxide concentrations for four occupants in city traffic can be shown in Figure 2.7 [8].

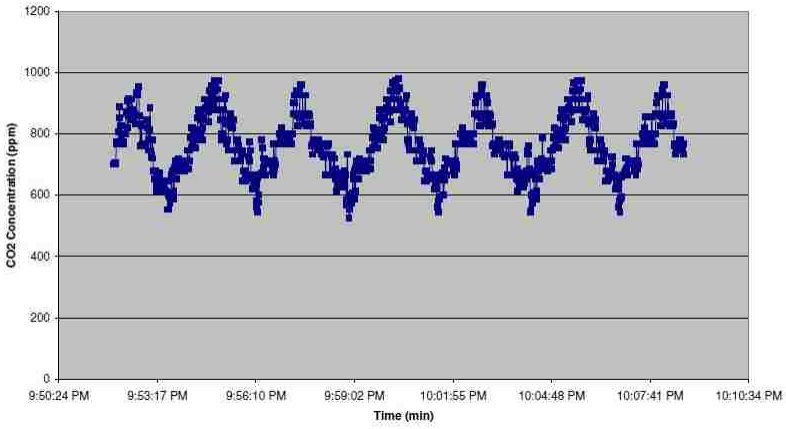

Figure 2.7: On-off control strategy experimental results for 4 occupants in city traffic [8]

2.4.2 Fractional Recirculation Control

A study done by Michael L. Grady and Heejung Jung [9] also investigated carbon dioxide buildup, water buildup and particle concentrations inside vehicle cabins. Instead of using an on-off type recirculation control strategy for controlling carbon dioxide, this study proposed a new fractional recirculation strategy. The study first looked to characterize the influence of different parameters (vehicle speeds, passenger number, ventilation fan speed, and ventilation mode setting) on the equilibrium carbon dioxide concentrations inside the cabin. Three constant vehicle speeds of 15, 40, and 70 mph were tested using a standard size Hyundai-Kia Motors SUV. The 15 mph tests were used to characterize the influences of passenger number, ventilation fan speed and ventilation mode setting on the equilibrium concentration, while the 40 and 70 mph tests were used to characterize the influence of vehicle speed. The study verified that at higher ventilation and vehicle speeds, the carbon dioxide equilibrium concentrations were lower due to an increased amount of body leakage.

Secondly, the study attempted to implement a fractional recirculation control strategy in a feasibility study that could be used as a first-step towards automatic fractional control. The original HVAC control unit was replaced with a

pre-programmed unit which could position the recirculation door at any angle, allowing any fraction of recirculation from 0-100%. Feasibility tests were done at vehicle speeds of 15 mph and different ventilation fan speed settings. The recirculation door control was done manually, by providing DC power to an actuator which controlled the position of the recirculation door, in order to keep carbon dioxide levels to a constant level of 2000 ppm. Figure 2.8 [9] shows the results of different amount of recirculation required for different ventilation settings.

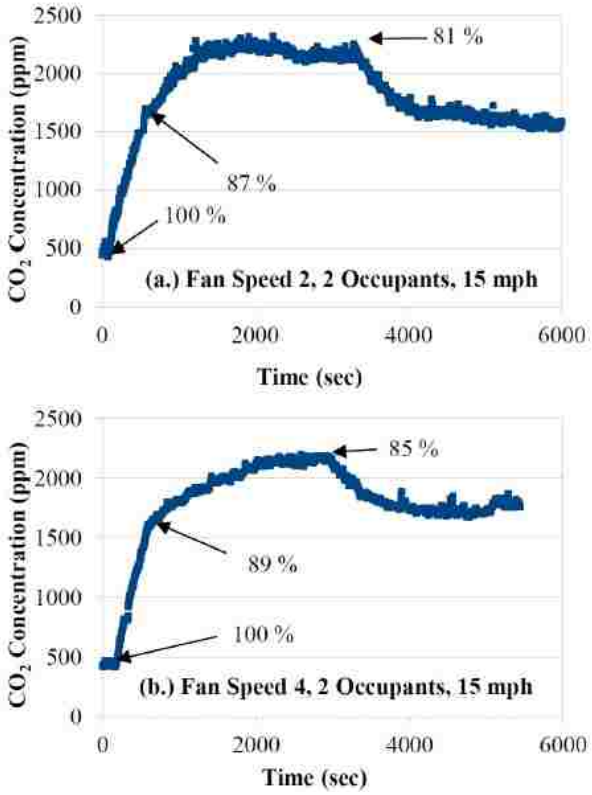

Figure 2.8: Feasibility test to control carbon dioxide at a target level of 2000 ppm [9]

The study concluded that cabin particle concentrations were reduced 20% with the use of recirculated air, while carbon dioxide and water inside the cabin increased drastically. The study also concluded that an open loop control for carbon dioxide suppression is possible, given that the characteristics of the cabin air system are

known. The balance of carbon dioxide build-up was influenced by five main parameters: vehicle speed, ventilation fan speed, fraction of recirculation, cabin volume and number of passengers, and body leakage rates are vehicle dependent which much be fully understood for the vehicle in question [9]. These conclusions have also been stated by many of the previous studies mentioned above [7–11, 23].

Chapter 3
Methodology

To reiterate the objectives listed in Chapter 1, the following section will detail the methodology involved in the creation of a lumped parameter model designed to offer a generalization of a large number of vehicle makes and manufacturers, and provide a simple prediction of the CO_2 build-up inside the vehicle cabin. A sensitivity analysis will be included to describe the effects that different parameters have on the carbon dioxide build-up inside the cabin. Further methods will detail the modeling of various recirculation strategies to control the cabin dioxide build-up inside the cabin, and the selection of any model parameters involved in the simulation of various control strategies. The various control strategies will then be analyzed and compared based on the carbon dioxide concentrations inside the cabin, compressor load savings of the air conditioning system, and any implications on the thermal environment inside the cabin.

3.1 Lumped Parameter System and Environment Modeling using AMEsim

3.1.1 CO_2 Build-up Model

The vehicle cabin of today should be considered to be an airtight space except for a distinctive inlet and outlet to allow air flow. Air enters the vehicle cabin through the HVAC system and exits through a body vent usually located near the bottom of the luggage compartment at the rear of the cabin. In order to maintain a pressure balance inside the cabin, air flow into the cabin must equal airflow exiting the cabin. Air may also infiltrate and exfiltrate the vehicle as leakages through seals and other areas that are not completely air tight. Jung H. [2] and Hudda et al. [10, 11] have both detailed a CO_2 mass balance approach to predicting the build-up of carbon dioxide in the vehicle cabin. The change in cabin carbon dioxide concentration is equal to the mass

flow of carbon dioxide entering the cabin via the HVAC system and human production, minus the mass flow of carbon dioxide exiting the cabin. Q_i and Q_o represent the volumetric air flow rate in and out of cabin, and to maintain a pressure balance, $Q_i = Q_o = Q_l$. As a human body inhales air, oxygen is absorbed into the bloodstream through the lungs, and delivered by the heart throughout the body. As the cells use oxygen, carbon dioxide is produced and absorbed back into the bloodstream and returned back to the lungs by the heart, where it is removed via exhalation. Any carbon dioxide that is inhaled into the body is returned back into the atmosphere or control volume by exhalation, which allows for the omission of an inhalation term in the governing differential equation. Figure 3.1 [2] and Equation 3.1 [2] detail the schematic of CO_2 buildup and the differential equation governing CO_2 build-up inside the vehicle cabin proposed by Jung H.

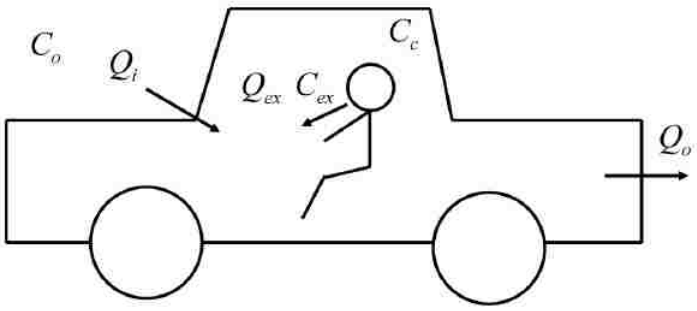

Figure 3.1: Schematic of vehicle cabin air system proposed by Jung H. [2]

$$V_c \cdot \frac{dC_c}{dt} = n \cdot C_{ex} \cdot Q_{ex} + C_o \cdot Q_l - C_c \cdot Q_l \tag{3.1}$$

Another study done by Hudda et al. [10, 11] proposed a similar equation considering the air exchange rate in the cabin, rather the vehicle body leakage shown in Equation 3.2 [10, 11]. In this equation S is the source mass flow rate inside the cabin via the passengers (similar to the $n \cdot C_{ex} \cdot Q_{ex}$ value in the Jung model). Both

equations are essentially the same, where the body leakage is equal to the air exchange rate multiplied by the cabin volume.

$$\frac{dC_c}{dt} = \frac{S}{V_c} + (C_o - C_c) \cdot AER \tag{3.2}$$

The final mass balance equation used in the CO_2 build-up model is a mixture of both the equations presented by Jung H. and Hudda et al. Since a reasonable amount of information was available on estimating the vehicle air exchange rate based on different parameters, an air exchange method was preferred, resulting in the final schematic shown in Figure 3.2 and the mass balance equation shown in Equation 3.3.

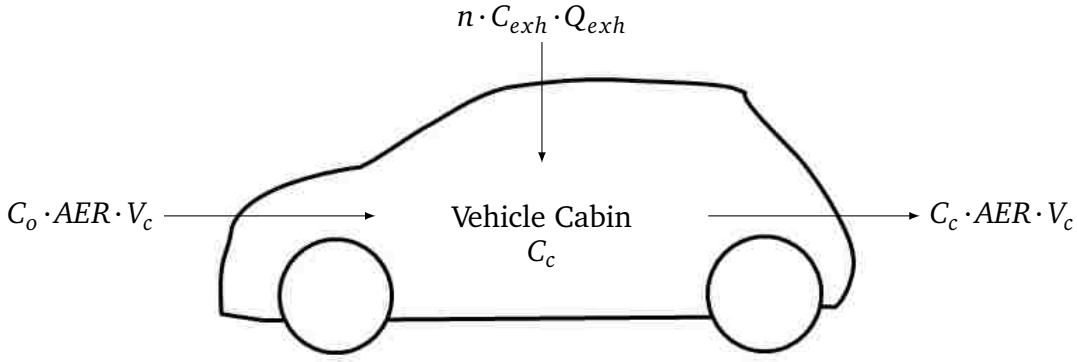

Figure 3.2: Final Model Schematic

$$V_c \cdot \frac{dC_c}{dt} = n \cdot C_{ex} \cdot Q_{ex} + (C_o - C_c) \cdot AER \cdot V_c \tag{3.3}$$

The solution of this differential equation results in the predicted CO_2 concentrations inside the cabin. All parameters in this equation are held constant except for the air exchange rate, which will vary according to several parameters: vehicle speed, HVAC mode, fan speed and cabin volume. Since one of the proposed solutions to control CO_2 build-up will involve a fractional recirculation strategy [9], it was important to create a prediction equation which could account for any fraction of recirculation from

0-100% shown in Equation 3.4. The assumption for the resultant air exchange rate is that it is proportional to the amount of outside air and recirculated air entering the vehicle. For example, for 50% recirculated air, the resultant air exchange rate (AER_D) is equal to 50% of the air exchange rate in OSA mode ($AER_{OA} \cdot (1-0.5)$) plus 50% of the air exchange rate in RC mode ($AER_{RC} \cdot 0.5$). Air exchange rates in both modes can be obtained through equations presented by Hudda et al. [11] shown in Section 3.1. As little information is available on the prediction of air exchange rates inside a vehicle, Equations 3.5 and 3.6 were integrated into the carbon dioxide build-up model to provide an estimate of the air exchange rate at different operating points during the cycle.

$$V_c \cdot \frac{dC_c}{dt} = n \cdot C_{ex} \cdot Q_{ex} + (C_o - C_c) \cdot AER_D \cdot V_c \tag{3.4a}$$

where:

$$AER_D = AER_{RC} \cdot FR + AER_{OA} \cdot (1-FR) \tag{3.4b}$$

The differential equation governing the build-up of carbon dioxide was translated into AMEsim using the Signal Library, creating a representative block diagram model for the differential equation (similar to that of Simulink). Using appropriate gains, signal additions and subtractions, the model could accurately represent Equation 3.3, with the ability to modify specific parameters (cabin volume, number of occupants and associated parameters, air exchange rate, outdoor carbon dioxide concentration, and fraction of recirculated air). The ability to modify specific parameters is critical for understanding how each parameter can affect the severity of carbon dioxide build-up inside the vehicle cabin, which will be investigated further in this section. For simplicity, the model acknowledges the human production of carbon dioxide as point sources, and does not consider the volume reduction of the cabin due to the occupants

inside. The volume of the cabin will affect the time constant in the governing equation of carbon dioxide build-up and thus the time it takes for an equilibrium value to occur. Further discussion on the cabin volume, its sensitivity to carbon dioxide build-up and the consequences of not considering any cabin volume reduction will be discussed in Section 3.2. Furthermore, the human production of carbon dioxide is considered the only source of carbon dioxide inside the cabin, and any carbon dioxide content stemming from the exhaust that may leak into the cabin is not considered. Prediction Equation 3.5 and Equation 3.6 derived by Hudda et al. [11] were used in order to evaluate the vehicle air exchange rate depending on the fraction of recirculation from 0-100%, the vehicle speed, age, cabin volume, and blower strength whose definition will be discussed further below. The creation of this carbon dioxide build-up lumped parameter model, represented as a block diagram in Figure 3.3, offers a simulation tool that can evaluate the carbon dioxide concentration under a multitude of vehicle conditions and multiple HVAC modes encompassing full RC mode, full OSA mode, and fractional RC mode.

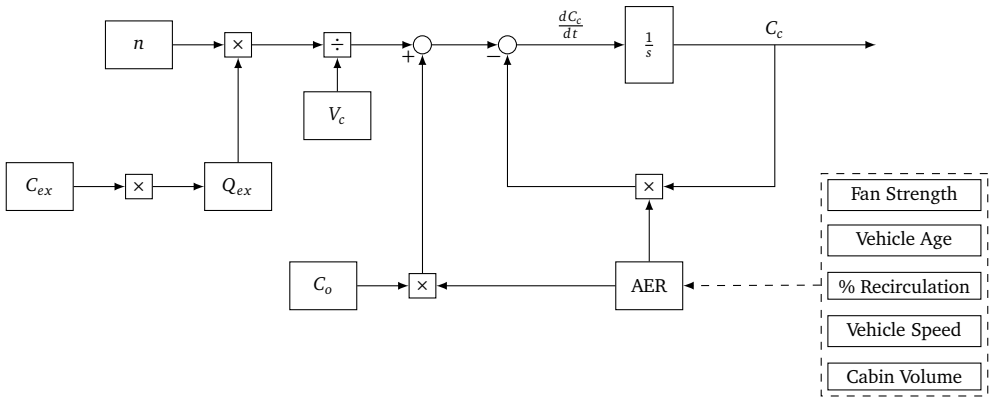

Figure 3.3: Representative Block Diagram of Carbon Dioxide Build-up Model

$$\ln(AER) = 2.27 + (0.019 \times speed) + (0.015 \times age + 3.3 \times 10^{-3} age^2) + (-0.023 \times vol + 6.6 \times 10^{-5} vol^2) + Manuf\ Adjustment \quad (3.5a)$$

$$\ln(AER) = 2.27 - 0.51 + (0.015 \times age + 3.3 \times 10^{-3} age^2) + (-0.023 \times vol + 6.6 \times 10^{-5} vol^2) + Manuf\ Adjustment \quad (3.5b)$$

$$\ln(AER) = 4.20 + \left[(1.88 \times fan\ strength) + (-0.92 \times fan\ strength^2)\right] + (0.0048 \times speed) + (-0.0073 \times vol) \quad (3.6a)$$

$$\ln(AER) = 4.20 + \left[(0.4 \times fan\ strength) + (0.13 \times fan\ strength^2)\right] - 0.32 + (-0.0073 \times vol) \quad (3.6b)$$

3.1.2 Model AER Comparison and Validation

In order to validate the use of the predictive equations for air exchange rates into the carbon dioxide build-up model, it was necessary to compare the air exchange rates under both RC and OSA conditions to other experimental values of air exchange rates found in literature. These values would have to correlate over a wide range of vehicle operating conditions and sizes in order to be deemed appropriate for use in the carbon dioxide build-up model. Three different literature comparisons were made as discussed in Chapter 2 which can evaluate the model in terms of air exchange rates for RC and OSA mode, as well as carbon dioxide build-up.

Table 3.1 and Table 3.2 show air exchange rate comparisons between predictive equations developed by Hudda et. al [11], and experimental results obtained by Knibbs L. [29] for both OSA and RC modes respectively. As can be seen in Table 3.1, the predictive equations show a good correlation with experimental results from Knibbs for the OSA mode condition at a medium to high blower speed, velocities of 60 and 115 km/h and for different vehicle models and ages. Table 3.2 however, showcases the vast differences between the same vehicles while in RC mode. It is evident that in some

cases the air exchange rates using the predictive equations are much larger than the air exchange rates seen in the study done by Knibbs and vice versa. This comparison coincides with a statement made by multiple sources [10,11,23] about the variability of AER between vehicles and models in RC mode. The predictive equations were based on a wide variety of vehicle models, which could explain the variation from experimental measurements for specific models made by Knibbs.

Table 3.1: Model Air Exchange Rate Comparison in Outside Air Mode

Vehicle	Volume m^3	Age years	Speed km/h	AER (Knibbs) m^3/h	AER (Model) m^3/h
Toyota HiLux	3.33	7	60	265	274
			115	320	300
Volkwagen Golf	3.88	7	60	310	280
			115	325	327
Mitsubishi Magna	3.72	14	60	275	274
			115	335	325

Table 3.2: Model Air Exchange Rate Comparison in Recirculation Mode

Vehicle	Volume m^3	Age years	Speed km/h	AER (Knibbs) h^{-1}	AER (Model) h^{-1}
Toyota HiLux	3.33	7	0	0.7	2.2
			60	4.8	4.5
			100	6.9	8.1
Volkwagen Golf	3.88	7	0	0.1	0.8
			60	1.3	3.5
			100	3.1	6.4
Mitsubishi Magna	3.72	14	0	1.1	1.7
			60	13.6	5.3
			100	22	9.6

Table 3.3 details the switching frequency for the recirculation door flap during an on-off type strategy investigated by Mathur [8] and compared with the CO_2 build-up model that uses the predictive equations for the air exchange rate. Both strategies utilized the same upper and lower carbon dioxide limits, and were compared at different speeds (city and highway) and with varying number of passengers. The comparison

shows good correlation between the two switching frequencies, validating that both the differential equation modeling the build-up of carbon dioxide in addition to the air exchange rate in both OSA and RC modes agree with experimental results obtained by Mathur.

Table 3.3: Switching Frequency Comparison for On-Off Recirculation Control

Vehicle Speed	Volume	Occupants	Switching Frequency (Mathur)	Switching Frequency (Model)
City (36 km/h)	Segment B Vehicle	1	6 Minutes	6.2 Minutes
		4	2 Minutes	2 Minutes
Highway (108 km/h)	Segment B Vehicle	1	9 Minutes	8 Minutes
		4	3 Minutes	2.5 Minutes

Studies mentioned above, in addition to others mentioned in Section 2.3 showed good correlation between each other, even when considering the limited number of equivalent cases for comparison. To the satisfaction of the author, the comparisons shown above along with considerations made in literature discussing the variation of the air exchange rate in RC mode among different vehicles, adequately validates the use of prediction equations for air exchange rates during RC mode, OSA mode and for vehicles ranging in different models and years.

3.1.3 Cabin and HVAC System Modeling

In order to evaluate the associated compressor load reductions for different recirculation strategies, it was necessary to include a vehicle cabin and HVAC system model and integrate it into the carbon dioxide build-up model. Since the objective of this thesis work was to study and compare the relative effects of different recirculation strategies, a standard AMEsim reference AC loop system was used and modified to allow RC and OSA modes. Saving time by not completely modeling the HVAC and cabin systems from scratch, allowed more time for focusing on the carbon dioxide build-up model and appropriate recirculation strategies. The following section will

detail the AC loop and cabin models. Any changes made to form the final HVAC system and the integration with the carbon dioxide model to create the final lumped parameter system will also be discussed.

There are several advantages associated with the creation of a lumped parameter model. In general, a lumped parameter system simplifies spatially distributed physical systems into a network consisting of discrete items that approximate the behaviour of the distributed system. The lumped parameter model does not consider spatial variations in the solution and is an approximation of the real system, however, the solution is much easier to solve, reducing costly computational time with low data requirements. To the author's knowledge, the lumped parameter system developed provides an acceptable approximation in the interest of CO_2 build-up inside the vehicle cabin and other implications sought after in this thesis research.

Figure 3.4 shows the reference AC loop that was selected from the AMEsim reference library, complete with condenser, evaporator, thermal expansion valve, and compressor. The model allows inputs for vehicle speed, outside air temperature and relative humidity, compressor rpm, and many other internal details of individual components, in order to predict the temperature and relative humidity in the cabin, as well as the associated compressor load of the driving cycle. The majority of the individual component parameters remained unchanged from the reference AC system (condenser, evaporator, and thermal expansion valve), as the main goal was to compare different recirculation strategies and the associated carbon dioxide build-up on a simple vehicle HVAC system.

Several modifications were made to the AMEsim reference system in order to better represent a real case HVAC system. These changes involved the compressor type and control, the addition of a heater core and flap, specific controls for both the blower mass flow rate and heater flap in order to regulate the desired cabin temperature, and

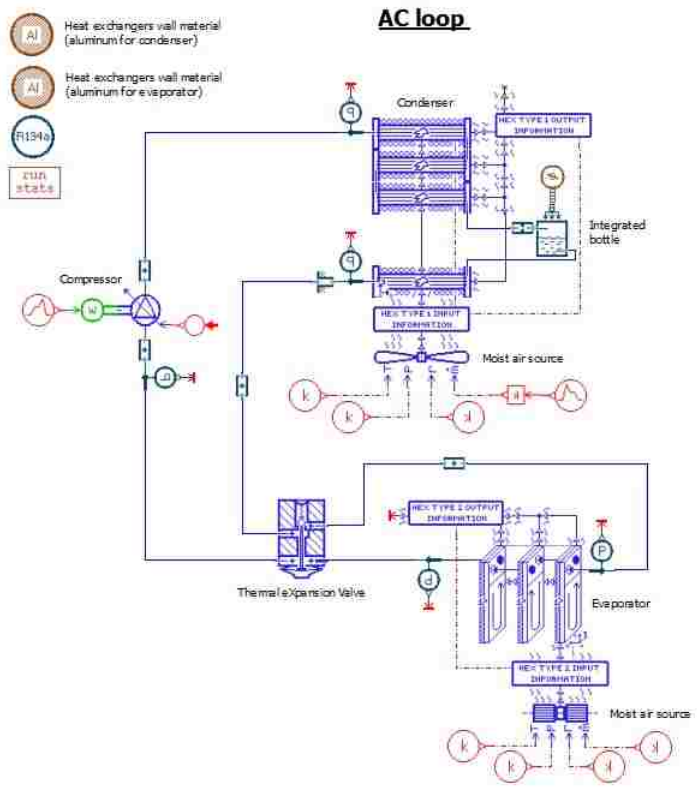

Figure 3.4: AMEsim reference AC loop

finally the ability to allow cabin air recirculation. The externally controlled variable displacement compressor that was initially used in the reference AC loop was changed to an internally controlled variable displacement compressor with parameters that matched a typical internally controlled variable displacement compressor for a typical B-segment/sub-compact vehicle (Ford Fiesta, Fiat Punto, Volkswagen Polo, etc.). In this way, the compressor size and performance corresponded with the vehicle volume size. Specifics of the compressor parameters are not important for understanding the main concepts in this thesis work, and are therefore not presented. A representative volume chamber was used to simulate the presence of a heater core in the system model. This chamber was given a constant heat flux of 1000 W in order to permit the

re-heating of air before entering the cabin. The blower mass flow rate and heater flap would be used to regulate the cabin temperature instead of the externally controlled compressor found in the reference system. Two proportional-integral controllers were used for the blower mass flow rate and heater flap control in order to regulate the cabin temperature. Due to time constraints, it is important to note that the controllers were not fully optimized, but only to the point of achieving adequate functionality of the system.

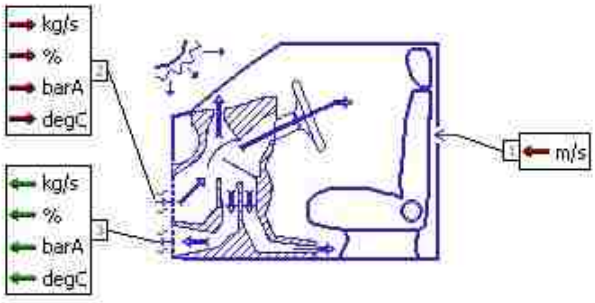

Figure 3.5: AMEsim cabin sub-model

The cabin sub-model added to the AMEsim reference AC loop, shown in Figure 3.5, provided an adequate solution to evaluate the air inside the cabin and any associated thermal balances of the moist air volume. The sub-model includes an inlet port for vehicle velocity in order to evaluate the external convective heat transfer, an inlet moist air port to evaluate the temperature, pressure, mass flow rate and relative humidity of the air entering the cabin, and lastly an outlet moist air port to evaluate the properties of the air inside the cabin for regulation purposes. The simple cabin sub-model assumes near perfect mixing of air upon entering the cabin, and takes the passenger moisture production as point sources (no cabin volume reduction due to human occupancy). This condition also complies with the carbon dioxide production from passengers as point sources stated earlier. The final cabin and HVAC model used for the simulations

is shown in Figure 3.7. The implementation of various recirculation control strategies into the carbon dioxide build-up model and AMEsim environment will be discussed further on in Section 3.3.

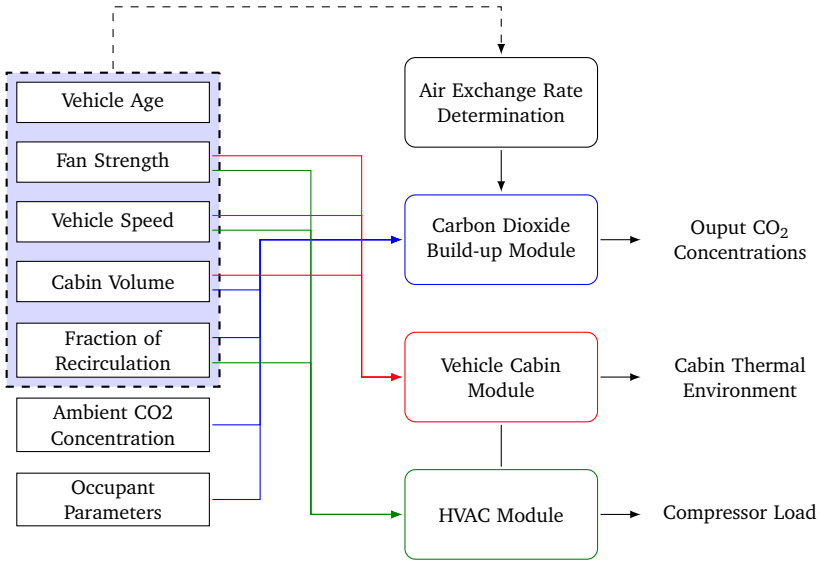

Figure 3.6: Block representation of final lumped parameter model

In order to connect the HVAC model to the carbon dioxide build-up model, the vehicle speed, blower mass flow rate and appropriate value for the fraction of recirculation from both models had to be linked together. Simple signal relays through AMEsim were used for the vehicle speed and fraction of recirculation. In order to correlate with the carbon dioxide build-up model, the blower mass flow rate was translated into a fraction of the maximum blower mass flow rate that represented the blower strength. These three connections created the final lumped parameter model, allowing the two models to be properly linked together and simulated in tandem. A block representation of the final lumped parameter system can be seen in Figure 3.6. The carbon dioxide model can be linked to any existing AC loop in AMEsim using these three connections, making it a widespread tool for evaluating the compressor load and carbon dioxide build-up of a particular recirculation strategy.

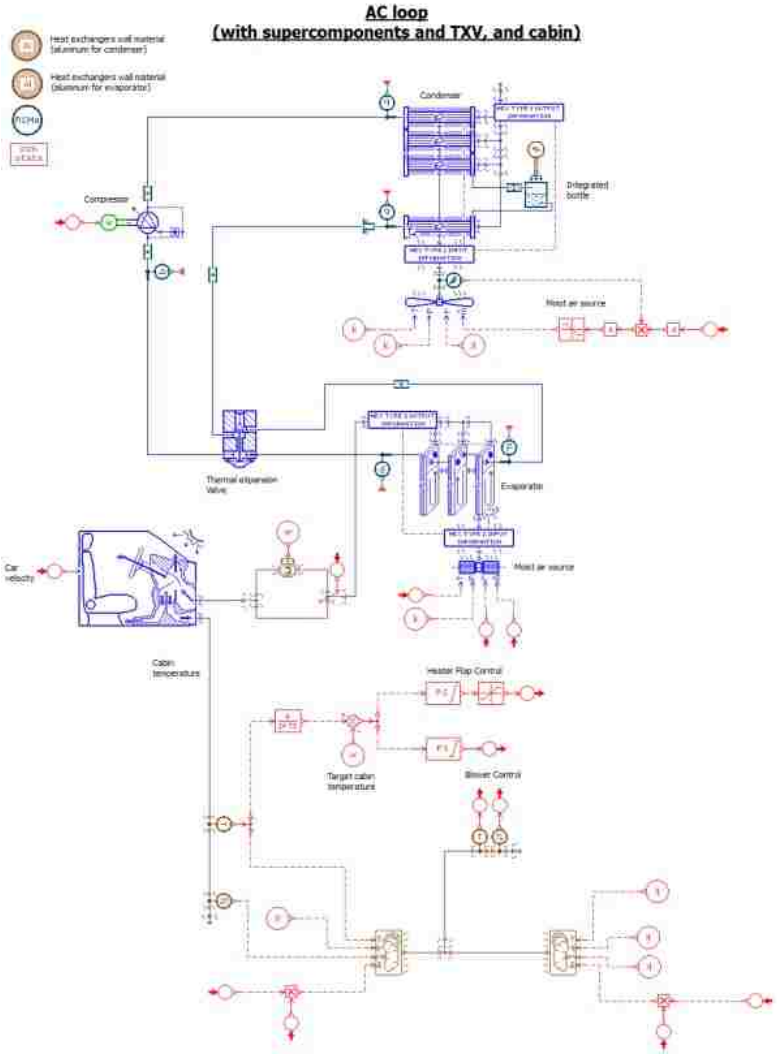

Figure 3.7: AMEsim final HVAC and cabin model

3.2 CO_2 Model Sensitivity Analysis

To further understand how the CO_2 concentration model functions, it was important to perform a sensitivity analysis to investigate how different parameters will affect the build-up of carbon dioxide inside the vehicle cabin. The parameters in question are those discussed in Section 2.3 and suggested by multiple sources [2, 7–11, 23] as the main parameters affecting the air exchange rate inside the vehicle, in addition to occupant dependent parameters. The following section will address each parameter, its effect on the air exchange rate inside the vehicle and on the carbon dioxide build-up inside the cabin. During the sensitivity analysis only one parameter will vary, while the other parameters remain constant. Future work involving the sensitivity analysis would involve varying multiple parameters simultaneously to examine any futher important sensitivity ramifications. It is important to note that the accuracy of the sensitivity analysis and build-up of CO_2 is highly dependent on the accuracy of the predictive equations used to calculate the AER discussed previously. For consistency during the sensitivity analysis, the following will be taken as baseline parameters:

- 40 km/h Vehicle Speed
- 2.5m^3 Cabin Volume (B-Segment/Sub-compact)
- 1 Occupant
- Full Blower Velocity
- 6.5 L/min Occupant Exhalation Rate at 47,000 ppm CO_2 Concentration

3.2.1 Vehicle Occupants

The occupants are the sources of carbon dioxide production inside the cabin. Being the only sources of carbon dioxide, the number of occupants plays a large role in the build-up of carbon dioxide concentrations [2, 3, 7–11, 23]. Figure 3.8 shows the build-up of carbon dioxide in RC mode with occupants ranging from 1 to 4 persons. Since RC mode experienced a much larger sensitivity to the number passangers in the vehicle compared to OSA mode, sensitivity results for OSA mode is not shown. It is important to note the equilibrium concentrations for 1 and 4 occupants differ by almost 7000 ppm (0.7%), and that the initial rate of build-up can be estimated as 108 ppm/min and 433 ppm/min for 1 and 4 occupants respectively. Under this driving condition, the carbon dioxide concentrations can be shown to approach 1% volume in a time frame of 2 hours. Considering the effects of CO_2 at this concentration and the effect of O_2 displacement by carbon dioxide, this particular, but unrealistic scenario could result in undesired symptoms to the vehicle occupants [14, 15]. Further occupant parameters that can increase the severity of carbon dioxide build-up in addition to the number of occupants inside the vehicle will be discussed further below.

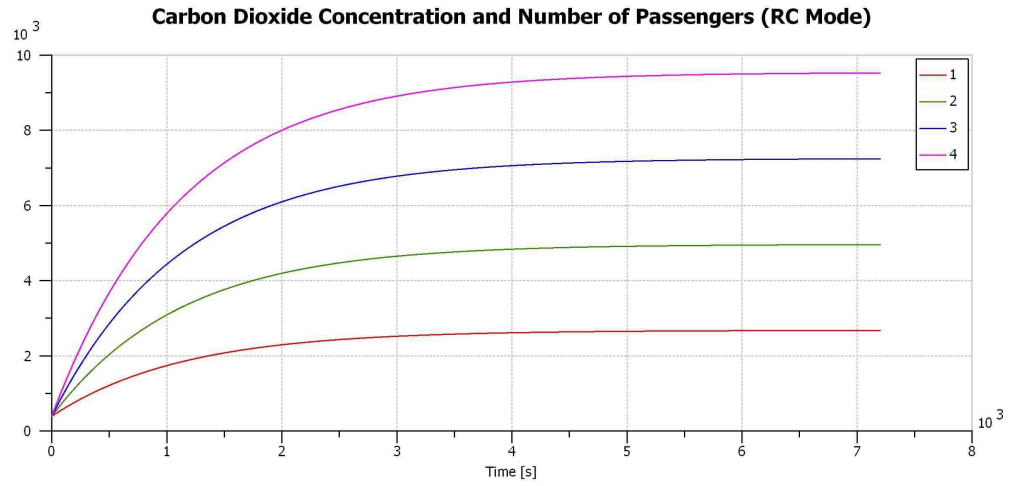

Figure 3.8: Carbon dioxide concentration (ppm) with increasing number of occupants

3.2.2 Cabin Volume

The cabin space is the control volume in which the carbon dioxide build-up occurs. Considering the role that the cabin volume takes as part of the time constant in the solution to the differential equation of carbon dioxide buildup, the cabin volume will affect how quickly cabin concentrations reach an equilibrium value. In addition, it will also cause a slight difference in the equilibrium concentration, due to its role in the calculation of the air exchange rate. A smaller cabin will reach an equilibrium value much more rapidly than a larger cabin. This sensitivity parameter was important, since the lumped parameter model does not consider the volume reduction of the cabin due to human occupancy. Using values of 70kg and 1050 kg/m^3 for the weight and density of an average human [31], we can estimate the volume of a human to be 0.067 m^3. This being said, we can estimate a minimum volume reduction of 0.067m^3 for 1 occupant and 0.268m^3 for 4 occupants. Figure 3.9 shows this effect with cabin volumes ranging from 2 to 3.5m^3 in RC mode. These cabin volumes range from a minicompact vehicle (A-Segment) to a large vehicle (E-Segment).

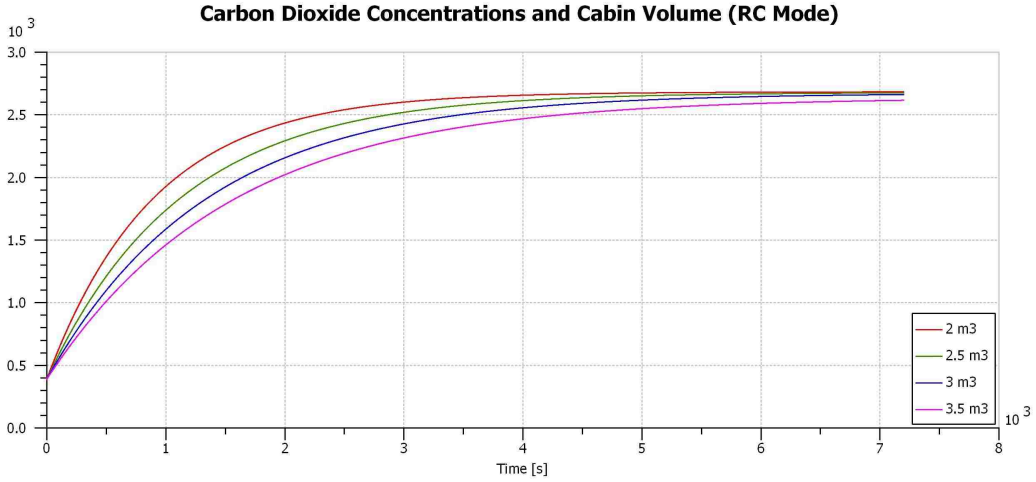

Figure 3.9: Carbon dioxide concentration (ppm) and cabin volume in RC mode

Due to the considerably larger amounts of body leakage in OSA mode, the volume

of the cabin has a much smaller effect on the resulting air exchange rates and thus the carbon dioxide concentrations inside the vehicle cabin. These larger exchange rates make it difficult to notice the decrease in time to equilibrium for the smaller cabin volumes, but amplify the slight variation in equilibrium concentrations not able to be seen completely in RC mode. Figure 3.10 shows the different equilibrium concentrations for cabin volumes ranging from 2-3.5m^3 in OSA mode. A relatively small difference of 10 ppm exists.

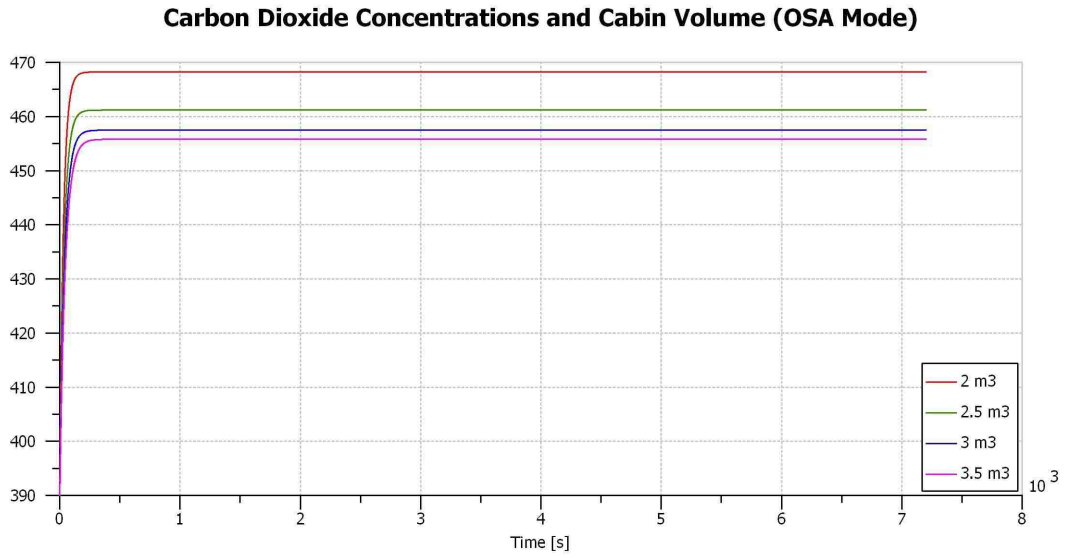

Figure 3.10: Carbon dioxide concentration (ppm) and cabin volume in OSA mode

3.2.3 Vehicle Speed

The speed of a vehicle has a large impact on the air exchange rate, and thus any pollutant concentration build-up inside the cabin. Higher vehicle speeds cause an increase in the air exchange rate or body leakage due to larger pressure differentials between the inside of the cabin and the exterior of the vehicle [2, 7–11, 23]. The higher pressure differentials caused by greater vehicle velocities can be shown to reduce the equilibrium concentrations inside the vehicle cabin, often refered to as pressure-driven ventilation [2, 7–11, 23]. Figure 3.11 shows the predicted decrease in

equilibrium carbon dioxide concentrations (ppm) in RC mode from zero speed to 120 km/h and the resultant increase of the air exchange rate by pressure-driven ventilation caused by higher vehicle speeds. Since the results are more prominent in the case of RC mode (much lower air exchange rates), results for OSA mode are not shown, even though some sensitivity was observed).

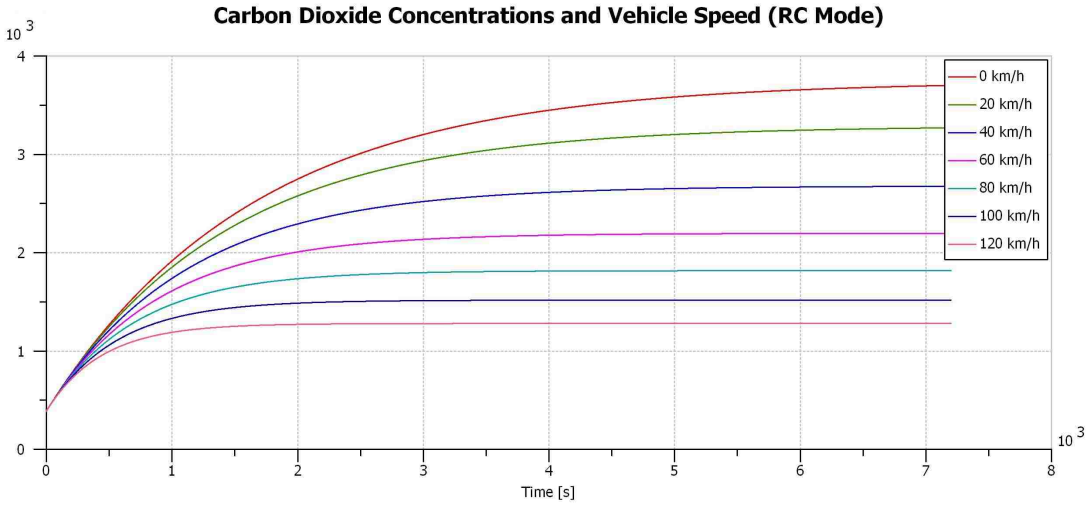

Figure 3.11: Carbon dioxide concentration (ppm) and vehicle speed in RC mode

3.2.4 Blower Strength

The blower fan speed has a similar effect to that of vehicle speed in terms of increasing the air exchange rate inside the vehicle cabin. Instead of a pressure-driven increase in the air exchange rate caused by vehicle velocity, the blower fan causes an increase in the air exchange rate due to mechanically-driven ventilation via the air outlet vent near the rear of the vehicle. A higher blower velocity will in turn cause a higher air exchange rate compared to a lower blower velocity [2, 7–11, 23]. The carbon dioxide build-up model uses the parameter fan strength, as presented by Hudda et al. [11] in order to account for the vehicle variation in the number of options for the fan setting. The ratio is thus the selected fan setting divided by the total number of fan settings available. In the case of continuous modulation, the fan

strength was calculated as the fan mass flow rate divided by the maximum possible fan mass flow rate. The predictive equations used for the calculation of the air exchange rate [11] interestingly found a large correlation between fan strength and air exchange rate in OSA mode, but did not notice a significantly large difference in the air exchange rate with varying fan strength in RC mode. The study by Hudda et al. concluded not to have the fan strength as one of the influencing parameters in RC mode, and is therefore not presented in the carbon dioxide build-up model studied in this thesis research. Figure 3.12 shows the variation in carbon dioxide concentrations caused by different fan strengths from 0-1, shown in OSA mode.

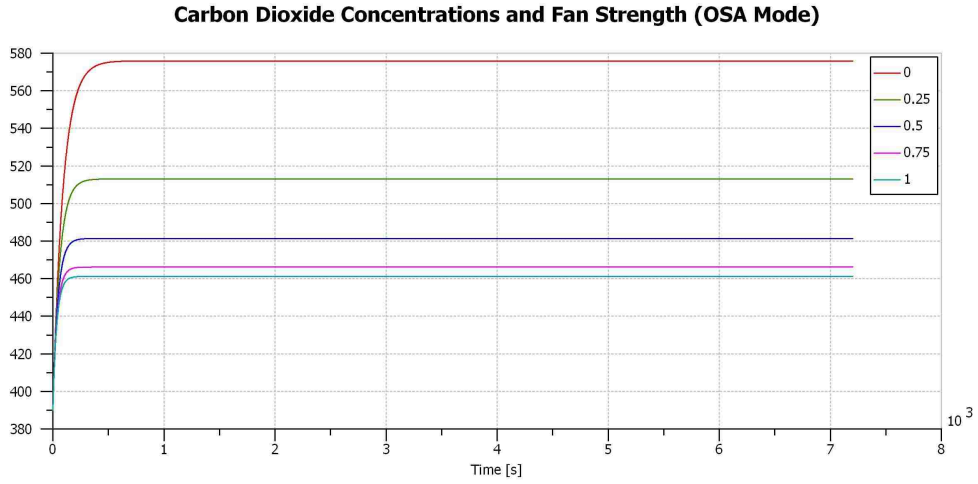

Figure 3.12: Carbon dioxide concentration (ppm) and blower strength in OSA mode

3.2.5 Fraction of Recirculation

The fraction of recirculation will affect the air exchange rate based on the derived equation shown in Section 3.1.1. The resulting air exchange rate when fractional recirculation is employed will be the proportional addition of the air exchange rate in RC mode and the air exchange rate in OSA mode. Figure 3.13 shows in-cabin equilibrium concentrations for fractions of recirculated air ranging from 0-100%. Due to the order of magnitude or greater difference between air exchange rates in RC and

OSA modes, it can be shown that by introducing as little as 5% outside air into the cabin, the equilibrium concentration can be reduced by almost 1500 ppm in this specific driving condition and parameter set point. As stated by Mathur [8] it is for this reason that employing fractional recirculation is an effective way to mitigate high carbon dioxide concentrations while maximizing the amount of recirculated air.

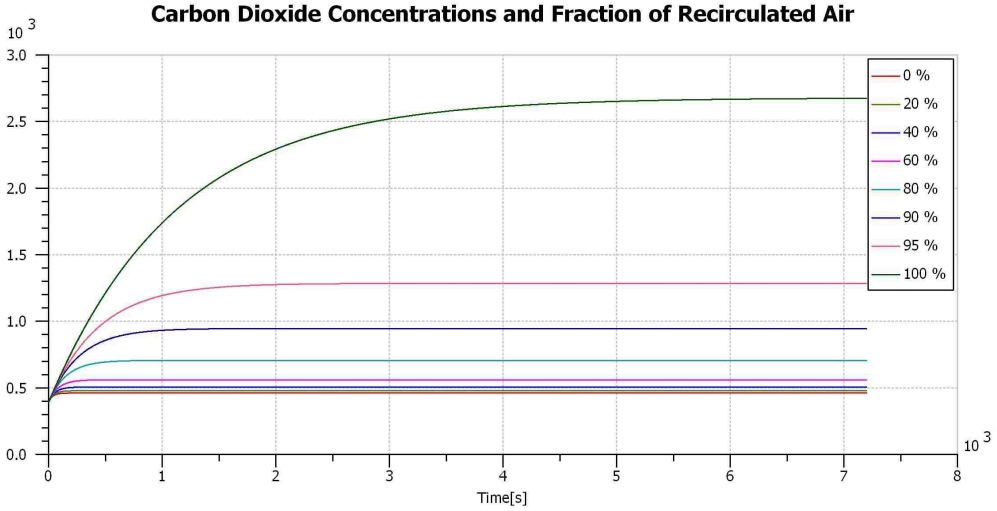

Figure 3.13: Carbon dioxide concentration (ppm) and fraction of recirculated air

3.2.6 Vehicle Age

The age of a vehicle has a pronounced effect on the air exchange rate and thus carbon dioxide concentrations, specifically when RC mode is engaged. The study done by Hudda et al. [11] looked at a wide range of age groups for the vehicles tested, and found a relationship between the age of the vehicle and the air exchange rate only in RC mode (no significant effect in OSA mode was observed). As a vehicle ages, seals around the vehicle body will begin to wear, causing the vehicle to become more susceptible to increased body leakage and greater air exchange rates. The increased leakage caused by the wearing of the seals may be attributed to the pressure-driven ventilation, seen more in RC mode, compared to the mechanically-driven ventilation seen in OSA mode when the fans are engaged. Figure 3.14 shows the equilibrium carbon dioxide concentrations

for a vehicle age ranging from 1-15 years, operating at the baseline conditions given above. As can be seen, there is almost a 1500 ppm difference between 1 year old vehicle compared to a 15 year old vehicle. This result can conclude that a newer vehicle can be more susceptible to larger carbon dioxide concentrations inside the cabin while in RC mode.

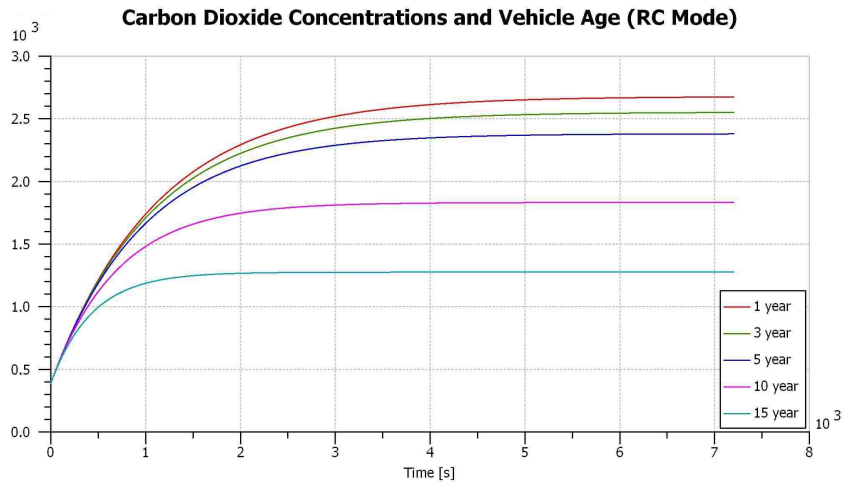

Figure 3.14: Carbon dioxide concentration (ppm) and vehicle age in RC mode

3.2.7 Occupant Parameters

Being the only source of carbon dioxide, occupants and their associated parameters can have a significant effect on the severity of carbon dioxide build-up inside the cabin. Given the ranges of both exhalation flow rates (5-7 L/min) and carbon dioxide concentrations (38,000-56,000 ppm) for a normal healthy individual [15], an array of carbon dioxide equilibrium concentrations can be found by varying the two parameters. The upper limit of these ranges can be extended even further if the individual has a higher metabolic rate (during or after physical activity) [15], but this case is not presented as the likelihood of this occurring inside a vehicle is considerably low. Figure 3.15 and Figure 3.16 show the equilibrium concentration ranges of carbon dioxide for varying occupant exhalation flow rates and carbon dioxide concentrations

respectively. The simulation parameters were set at baseline values listed above, with one occupant inside the vehicle. The in-vehicle equilibrium concentrations increase more than 500 ppm from the minimum to maximum exhalation flow rate, and almost 1000 ppm from the lowest to the highest carbon dioxide concentration found in human exhalation. With these effects being a product of the number of people inside the cabin, resulting in-vehicle concentrations can increase significantly.

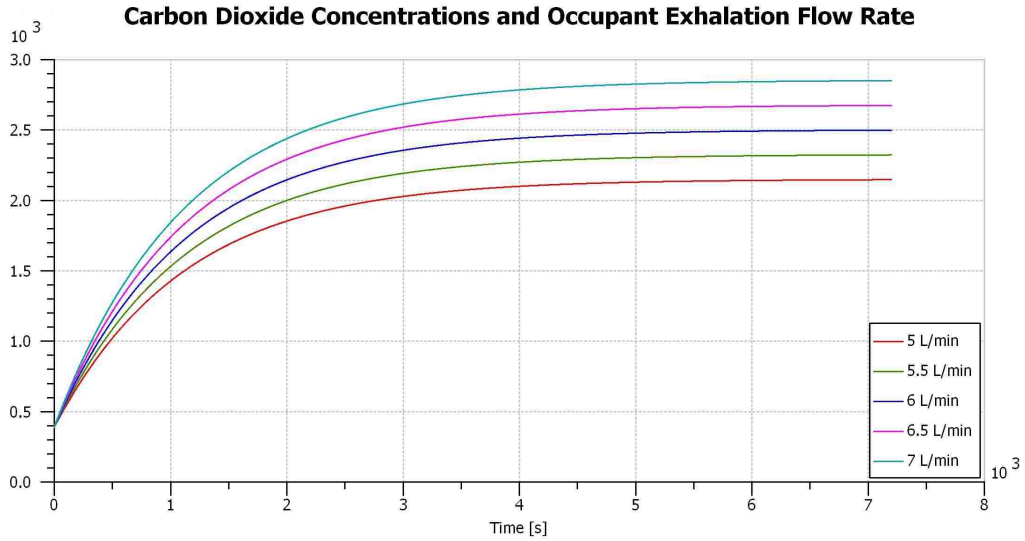

Figure 3.15: Carbon dioxide concentration (ppm) and occupant exhalation flow rate

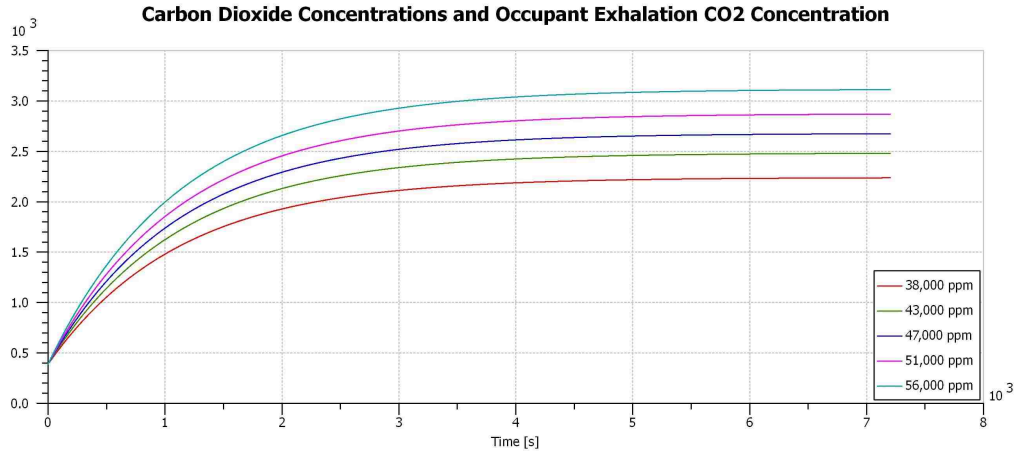

Figure 3.16: Carbon dioxide concentration (ppm) and occupant exhalation concentration of carbon dioxide

3.3 Modeling Mode Control Strategies

The scope of this thesis research encompassed three different recirculation control strategies for comparison and evaluation: on-off recirculation control, timed recirculation control, and fractional recirculation control as referenced in Chapter 2. All three of these control strategies have been discussed and/or studied by previous literature in Section 2.4 as practical approaches for controlling the carbon dioxide build-up inside the cabin. The following section will detail the methodology for the implementation and modeling of these control strategies inside the AMEsim environment.

3.3.1 On-off Recirculation Mode Control

The first control strategy implemented was an on-off type recirculation control, that would be used with a CO_2 sensor. The most common type of CO_2 sensor used in practice is a non-dispersive infrared (NDIR) sensor. As the air diffuses into a tube, gas molecules that are the same size as an infrared source wavelength absorb the infrared light, allowing other wavelengths to pass through. An infrared detector reads the amount of light that is not absorbed by a wavelength filter (wavelength absorbed by CO_2), and calculates the difference between the light emitted by the infrared source. The difference is proportional to the amount of CO_2 molecules in the air inside the tube. In order to implement an on-off recirculation control strategy, a "trigger" function was used in the AMEsim environment. This trigger has the ability to switch the recirculation door to full RC mode until an upper limit of carbon dioxide concentration is reached, and to switch the recirculation door to full OSA mode until an appropriate lower limit of carbon dioxide is reached. The upper limit of carbon dioxide concentration was set to be 1090 ppm, in accordance with ASHRAE Standard 62. The lower limit was determined based on switching frequency, which could cause

reliability issues if too large, and also the lowest concentration that could be achieved in OSA mode. The lower limit changes according to the number of occupants inside the cabin, due to the higher equilibrium concentrations experienced with increasing the number of occupants. To satisfy these requirements, a lower limit value for 1 occupant was established at 400 ppm and 800 ppm for 4 occupants. If the number of occupants in the vehicle falls between 1 and 4, the lower limit value would be linearly interpolated between these two values. The final carbon dioxide concentration model with integrated on-off recirculation control can be seen in Figure 3.17. The on-off recirculation strategy did not include an additional control for relative humidity inside the cabin. In this way, the implications of this strategy on the relative humidity inside the cabin will be shown.

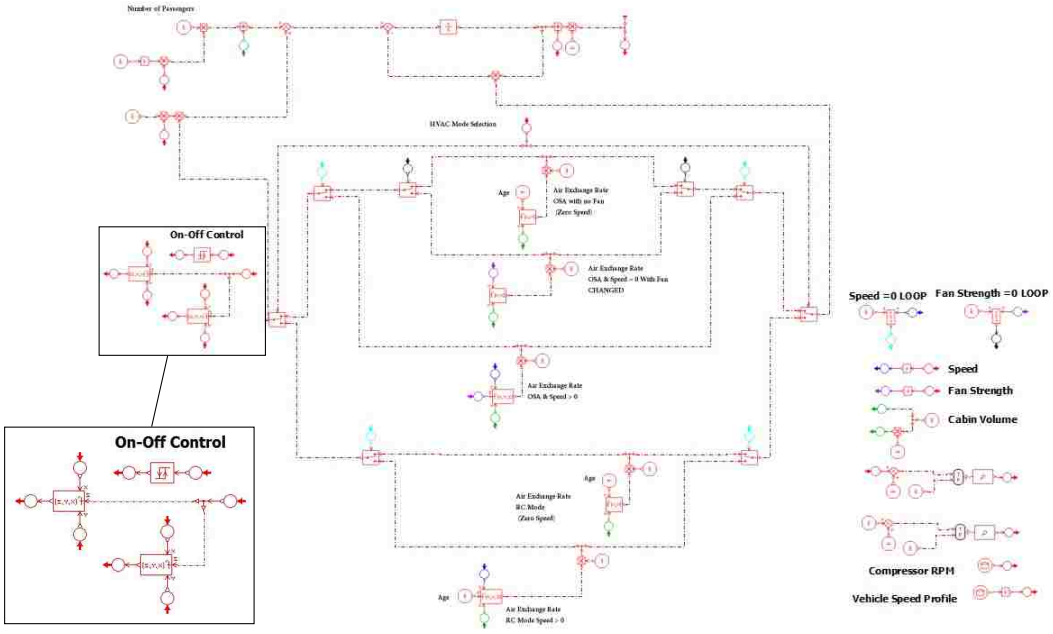

Figure 3.17: Carbon dioxide build-up model with integrated on-off recirculation control

3.3.2 Timed Recirculation Mode Control

Timed strategy control was implemented in the AMEsim environment by creating pre-determined signals that would be relayed to the air recirculation door. This

strategy would operate without the use of a CO_2 sensor. In the case of timed control, the recirculation door position had three options: 100% RC, 50% RC and 100% OSA. In order to encompass a wide range of timed strategies for analysis, four different timed controls were established. To the author's knowledge, the time strategies chosen offer a strategy in which a large amount of recirculation is used, a strategy which features a frequent switch from RC to OSA mode (any faster could cause mechanical reliability issues), and sufficient strategies to cover links in between.

- 15 minutes of recirculation followed by 1 minute of 50% outside air
- 10 minutes of recirculation followed by 1 minute of 100% outside air
- 7 minutes of recirculation followed by 2 minutes of 100% outside air
- 3 minutes of recirculation followed by 1 minute of 100% outside air

By encompassing a wide range of timed strategies, the effect of time spent in RC, and OSA modes on the compressor load and carbon dioxide build-up in the cabin can be determined. The final carbon dioxide build-up model with the integrated timed recirculation control is shown in Figure 3.18.

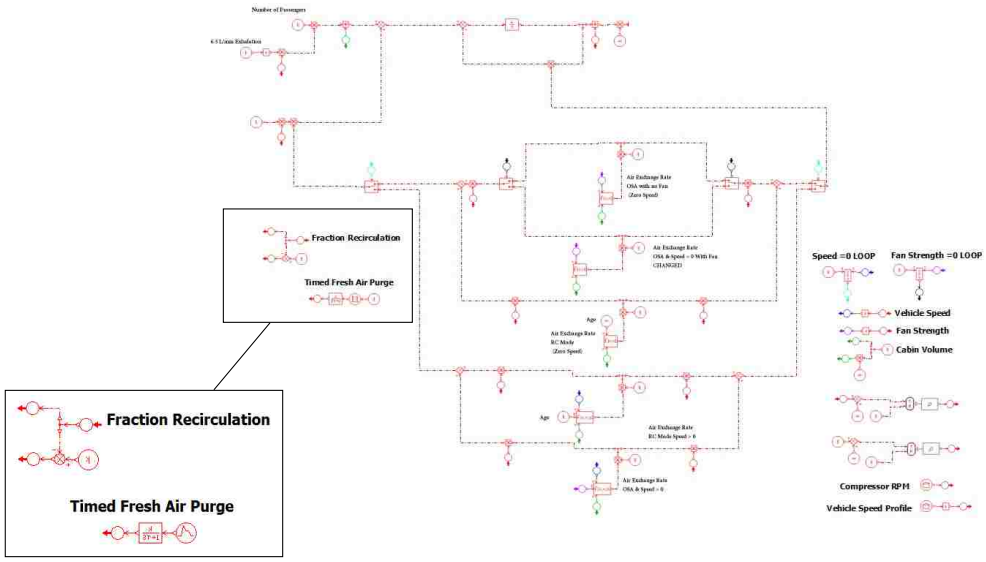

Figure 3.18: Carbon dioxide build-up model with integrated timed recirculation control

3.3.3 Fractional Recirculation Mode Control

The last recirculation strategy that was to be simulated involved fractional air recirculation with an integrated control for relative humidity inside the cabin. The fractional control, as discussed by Michael L. Grady and Heejung Jung [9], was realized through the use of a proportional integral controller evaluating the in-cabin carbon dioxide concentration by means of a a CO_2 sensor, and transmitting a signal to the recirculation door flap. The controller was tuned in order to achieve adequate functionality of a constant carbon dioxide concentration at the threshold limit. In order to insure the initial overshoot did not exceed the maximum limit of CO_2 as per ASHRAE Standard 62, the controller was tuned with the worst case build-up of carbon dioxide inside the cabin. Figure 3.19 shows the controller response for 4 people in the cabin and a constant vehicle speed of 0 km/h while in RC mode, and the fraction of recirculation for the controller response can be seen in Figure 3.20.

A smooth response as seen in Figure 3.19 is ideal to ensure the mechanical integrity of the recirculation door flap. Other controller responses for various speeds

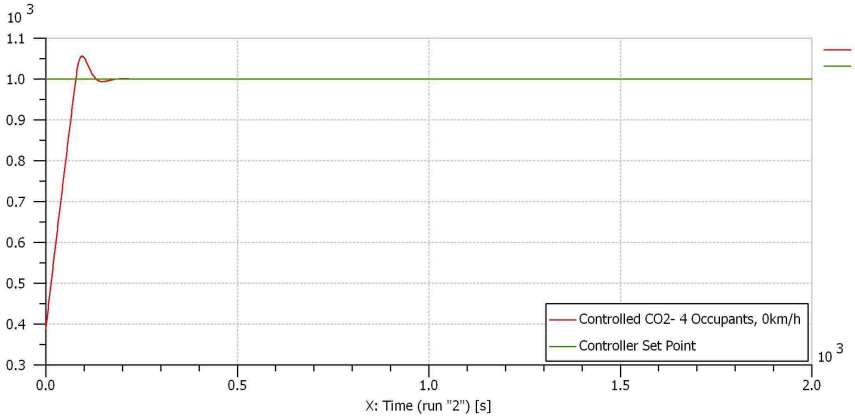

Figure 3.19: Carbon dioxide concentration (ppm) for controller tuning

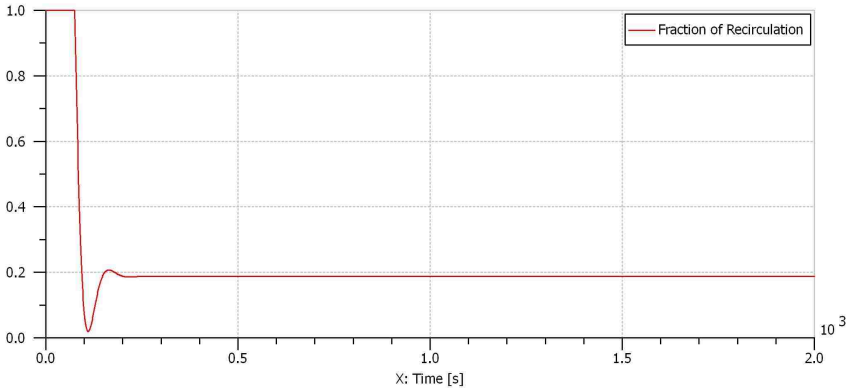

Figure 3.20: Fraction of recirculation for controller tuning

can also be seen in Figure 3.21. By utilizing Equations 3.5 and 3.6, the air exchange rate could be calculated based on the fraction of recirculation, and thus the carbon dioxide concentration build-up during the cycle. Carbon Dioxide concentrations were limited to ASHRAE Standard 62; 700 ppm over the ambient concentration on a continuous basis as discussed in Section 2.2.4. The carbon dioxide build-up model with implemented fractional recirculation and relative humidity control is shown in Figure 3.22.

Prolonged use of recirculated air mode causes air to be continuously passed

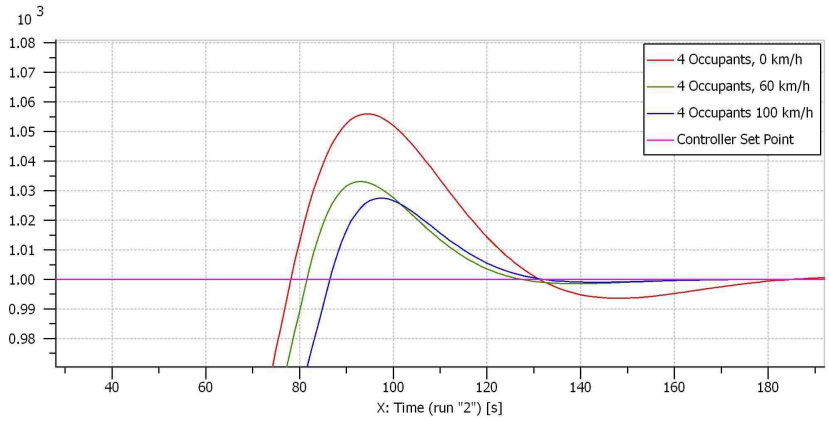

Figure 3.21: Controller response for various constant driving velocity scenarios

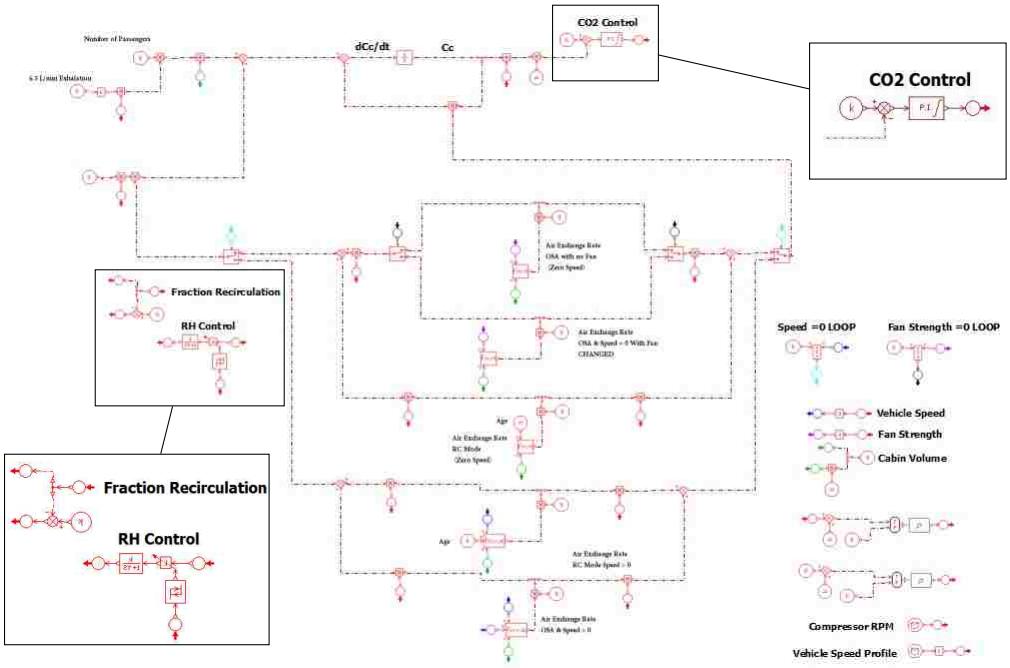

Figure 3.22: Carbon dioxide build-up model with fractional recirculation and relative humidity control

through the air conditioning evaporator, consequently reducing the relative humidity in the cabin if moisture production from passengers is not significant. As the air flows through the evaporator, the moisture in the air will be removed via condensation on the much cooler evaporator fins, and is permitted to run off into the condensate pan

and drain underneath the vehicle. Since the air inside the cabin is continuously recirculated, this condensation/moisture removal will lead to reduction of the relative humidity inside the cabin. As stated above in Section 2.1.3, passenger comfort is best achieved within a relative humidity range of 30-60%, and so this particular strategy aims to control relative humidity between these values. The relative humidity control was achieved in AMEsim with the use of a trigger function. If the relative humidity levels in the cabin drop below 30%, the compressor shuts off, the recirculation door flap is set to a 100% fresh air position, and the relative humidity is allowed to rise. Once the relative humidity reached a permissible upper value (50-60%), the compressor is re-engaged and the control strategy is permitted to continue.

3.4 Simulation Parameters

The goal of this thesis work was to simulate the carbon dioxide build-up of different driving cycles under different ambient conditions, and compare the relative effects of different CO_2 control strategies. Additionally, the implications of these control strategies on the relative humidity in the cabin, and compressor load savings were to be investigated.

In order to encompass a wide range of driving cycles, four specific cycles were selected: New European Driving Cycle (NEDC), Worldwide Harmonized Light Vehicles Test Procedure (WLTP), Federal Test Procedure-75 (FTP75), and US06 Supplemental Federal Test Procedure. The four driving cycles selected consist of two driving cycles from United States standards and two cycles from European standards. The NEDC is used to represent the typical driving profile and vehicle usage in Europe, and is used for emission certification and fuel economy calculations. The cycle consists of four repeated urban driving cycles followed by a higher speed, and more aggressive extra-urban driving cycle. The WLTP is a driving cycle currently being developed to

replace the NEDC cycle for better representing a real-world driving case and to be used as a standard on a global scale. The WLTP is split into three classes based on the vehicle's power to weight ratio. The Class 3 cycle, which was chosen for the simulations, features 4 speed sections: low, medium, high and extra high. The FTP75 driving cycle is used for emission certification and fuel economy determination in the United States. The FTP75 cycle features a cold-start phase, a stabilization phase and lastly a hot-start phase. For the purposes of using the FTP75 cycle in the simulations, the hot soak before the hot-start phase was eliminated from the cycle, and was proceeded using a continuous approach (non-stop cycle). The US06 driving cycle, also used in the United States, was created to address the limitations of the FTP75 cycle. The US06 cycle represents a more aggressive, driving behavior featuring more rapid speed fluctuations, higher accelerations and higher speeds than the FTP75 cycle.

Despite that during normal emission certification and fuel economy testing, these four cycles do not normally proceed with the air conditioning operating, they offer standards to compare different recirculation strategies seen in this thesis research. Table 3.4 details the distance travelled, duration, and average speed for all four driving cycles chosen for the simulations.

Table 3.4: Driving Cycle Characteristics

Driving Cycle	Distance Traveled km	Duration s	Average Speed km/h
NEDC	11.02	1180	33.6
WLTP	23.30	1800	46.5
FTP75	17.77	1874	34.1
US06	12.80	600	77.9

Table 3.5 details the driving cycles and ambient conditions that were used for the simulation of different recirculation control strategies. The different NEDC cycles provide strategy comparisons at different ambient temperatures and relative

humidities, in order to investigate the effect of increasing ambient temperature on the compressor load reduction, as well as the implications concerning the relative humidity during the cycle. The WLTP, FTP75, and US06 cycles provide comparisons for different driving cycles; more specifically the different average speeds of the respective driving cycles can provide an evaluation of the severity of carbon dioxide build-up of a low speed cycle versus a high speed cycle.

Table 3.5: Simulation Parameters

Simulation Number	Drive Cycle	Ambient Temperature °C	Ambient Relative Humidity %	Temperature Set Point °C
1	NEDC 1	15	70	22
2	NEDC 2	28	50	22
3	NEDC 3	35	60	22
4	NEDC	22	50	19
5	WLTP	22	50	19
6	FTP75	22	50	19
7	US06	22	50	19

The compressor rpm needed for the AMEsim compressor sub-model was pre-processed using the AMEsim model shown in Figure 3.23. Essentially, this model uses Equation 3.7 to calculate the engine rpm over the cycle, and multiplies that value by the belt ratio in order to arrive at the correct compressor rpm. Pre-processing of the compressor rpm for each driving cycle was done to reduce computational time of the simulations.

$$\text{Engine RPM} = \frac{V\left[\frac{km}{hr}\right]\cdot 60}{2\pi\cdot R_0\left[m\right]\cdot 3.6}\cdot\tau_{gear}\cdot\tau_{final} \tag{3.7}$$

Other values that needed to be specified for the simulation model included the occupant parameters of carbon dioxide exhalation, ambient carbon dioxide concentration, vehicle volume, vehicle age, maximum blower mass flow rate, manufacturing adjustment for the air exchange rate prediction equations and other vehicle cabin parameters. Once these values were determined and specified, the

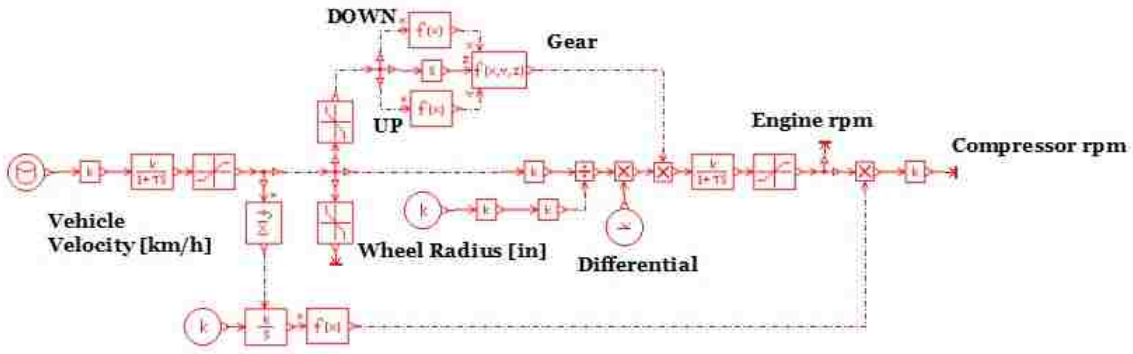

Figure 3.23: AMEsim model used to determine compressor rpm

simulations could begin and an analysis of the different recirculation strategies could be undertaken. Table 3.6 details further input values for the parameters discussed above. With reference to Section 2.2.2, an average adult exhales carbon dioxide at concentrations ranging from 38,000-56,000 ppm, and at a rate of 220 mL/min at rest to 1650 mL/min during exercise. Values chosen for the simulation fell midway between the concentration range at 47,000 ppm, and slightly higher than the resting flow rate of 220 mL/min at 300mL/min due to the increased metabolic rate during driving [19]. This concentration corresponded to a human exhalation flow rate of approximately 6.5 L/min. The age of the vehicle was selected to be 1 year, due to the more severe carbon dioxide concentration build-up in newer vehicles, particularly in RC mode. All other vehicle related parameters listed, including the maximum blower mass flow rate, compressor to engine belt ratio, wheel radius, and cabin volume are well-matched with a sub-compact/segment B vehicle. In order to utilize the prediction Equations 3.5 and 3.6, a manufacturer adjustment for the RC mode air exchange rate had to be specified. Given the maximum value of -0.39 (Japanese manufactured) representing the highest air exchange rate for a given speed, volume and age, and the minimum value of -0.71 (German manufactured), representing the lowest air

exchange rate for a given speed, volume and age, a value midway between the two limits (-0.55) was selected. Since the comparison of different recirculation strategies is a generalized comparison and not related to a specific vehicle make and model, a value of -0.55 will establish an average air exchange rate between different vehicle manufacturers.

Table 3.6: Additional Simulation Parameters

Parameter	Unit	Value
Occupants Exhalation Flow Rate	L/min	6.5
Occupant Exhalation Carbon Dioxide Concentration	ppm	47,000
Ambient Carbon Dioxide Concentration	ppm	390
Vehicle Volume	m^3	2.4
Vehicle Age	years	1
Wheel Radius	in	13
Compressor to Engine Belt Ratio	-	1.174
Manufacturing Adjustment	-	-0.55
Maximum Blower Mass Flow Rate	kg/s	0.111

Table 3.7 details the input parameters for the cabin sub-model used in the simulations. Initial conditions inside the cabin were set equal to the ambient conditions in question. Passenger water production was important for the estimation of the relative humidity inside the cabin. Humans produce moisture through two mechanisms: respiration and transpiration. Respiration refers to any moisture released via human exhalation, while transpiration refers to any moisture release through the skin. Based on values suggested by several sources cited by Anton TenWolde and Crystal Pilon [32], the total contribution of human moisture production due to respiration and transpiration ranges from 30-70 g/hr. Although slightly lower than values referenced by ASHRAE [33] human moisture production was estimated to be 50 g/hr per person based on an average value between the lower and upper limits. All simulation parameters were kept constant when simulating different recirculation strategies in order to allow a relative comparison between all strategies studied.

Table 3.7: Vehicle Cabin Parameter Settings

Parameter	Units	Value
Cabin Volume	m^3	2.4
Initial Relative Humidity	%	Ambient
Initial Temperature	°C	Ambient
Wall Thermal Capacity	J/°C	7000
Internal Aerodynamic Coefficient	-	20
External Temperature	°C	Ambient
External Relative Humidity	%	Ambient
External Pressure	barA	1.013
Solar Flux	W/m^2	700
Solar Flux Absorption Coefficient	-	0.45
Passenger Water Production	g/hr	50

The driving cycles will be first simulated with the two compressor load limit cases that establish the minimum compressor load (cycle in RC mode) and the maximum compressor load (cycle in OSA mode). The compressor load at all points during the cycle is evaluated using Equation 2.4 and multiplying by the refrigerant mass flow rate. Furthermore, the AMEsim compressor submodel allows an immediate calculation of the compressor load without the evaluation of Equation 2.4. An average value of the compressor load over the cycle could be obtained by taking the integral over the cycle and dividing it by the cycle time shown in Equation 3.8.

$$\text{Average Compressor Load} = \frac{1}{t}\int_0^t \dot{W}_c(t)\,\mathrm{d}t \tag{3.8}$$

The simulation cases are then run according to each specified recirculation strategy: timed recirculation control, on-off recirculation control and fractional recirculation control, and varying the number occupants. Simulations are to be run with 1 and 4 occupants in the cabin, representing the minimum and maximum carbon dioxide production from passengers. The average compressor load is evaluated for each simulation case, and compared to the baseline minimum and maximum

compressor values for the drive cycle. For comparison purposes, the recirculation strategies were evaluated based on the percent decrease from the maximum compressor load (OSA mode) shown in Equation 3.9.

$$\%\ \text{Decrease from OSA} = \frac{W_{c,Max} - W_{c,Strategy}}{W_{c,Max}} \cdot 100\% \tag{3.9}$$

For strategies that did not have a particular control in place for peak carbon dioxide concentrations (Timed Control), average carbon dioxide concentrations over the cycle can be calculated as follows:

$$\text{Average } CO_2 \text{ Concentration} = \frac{1}{t}\int_0^t C_c(t)\mathrm{d}t \tag{3.10}$$

By utilizing the average concentration over the cycle, the carbon dioxide build-up severity between different timed strategies and strategies that control carbon dioxide peak levels can be compared. More importantly, a comparison between the time weighted average concentration and time weighted average concentrations stated in occupational exposure limits discussed in Section 2.2.2 can also be made. Furthermore, an analysis on the implications of the specific strategy on the relative humidity inside the cabin will be performed for strategies not having a specific relative humidity control in place (timed and on-off control). Specifically, the analysis will consider whether or not the relative humidity falls out of the range requirements for human comfort discussed in Section 2.1.3.

Chapter 4
Results and Discussion

The following section will discuss the results obtained for all three various recirculation control strategies based on the different simulations discussed in Section 3.4. The following section will also analyze the results and implications of the control strategies, including detailed comparisons between them. All control strategies simulated will be assessed based on the following four characteristics:

- Compressor load reduction (percent decrease from the maximum compressor load obtained during the cycle)
- Peak and average carbon dioxide levels calculated over the cycle, and any implications of these levels
- Any positive or negative implications the recirculation strategy has on the thermal environment inside the cabin
- Any constraints that may develop due to the control, and mechanical operation of the recirculation door flap

4.1 On-off Recirculation Control

The on-off recirculation control strategy with the use of a carbon dioxide sensor, offers a simplistic system that has the ability to control carbon dioxide emissions inside the cabin without the need to precisely determine the recirculation door flap position. With two door positions, the off-on control strategy has only full RC and full OSA modes available. Since the strategy offers an oscillation between an upper and lower limit of carbon dioxide, it can be stated that the average concentrations during all simulated driving cycles will lie in between the upper and lower limit, and below 1100 ppm; complying with ASHRAE Standard 62 for acceptable carbon dioxide levels.

As the upper limit of carbon dioxide is also controlled, peak concentrations of carbon dioxide inside the cabin during all driving cycle cases will also fall below this limit.

Table 4.1 and Table 4.2 shows several results for the different driving cycles discussed in Section 3.4 for 1 and 4 occupants respectively simulated at 22°C and 50% RH. It can be seen that the percent decrease from OSA mode is around 32-33% for all cycles tested at this specific ambient level with 1 occupant inside the vehicle. However, with 4 occupants inside the cabin a significant reduction in the percent decrease from OSA mode can be seen from 32-33% down to 8-9%. Due to the added production of carbon dioxide from the additional occupants, the concentration in the cabin will reach the upper limit more frequently, causing an increase in the RC mode to OSA mode oscillation. This can be further realized by the average cycle times shown in Table 4.1 and Table 4.2. Average cycle times for 1 occupant are more than double the average cycle times for 4 occupants. Differences in average cycle times between driving cycles can be attributed to the different average speeds of the respective driving cycles. A driving cycle with a higher average speed (US06) will be expected to have a higher average cycle length than a lower speed cycle (NEDC) due to the higher air exchange rates, and slower carbon dioxide build up experienced at higher vehicle speeds.

Table 4.1: Various Cycle Compressor Load Results with On-Off Control for 1 Occupant: 22°C, 50% RH

Driving Cycle	Minimum Compressor Load kW	Maximum Compressor Load kW	Compressor Load On-Off Control kW	% Decrease from OSA	Avgerage Switching Time
US06	0.1923	0.3136	0.2112	33%	10
NEDC	0.2227	0.3851	0.2574	33%	7.5
FTP75	0.2019	0.3585	0.2452	32%	7.8
WLTP	0.2014	0.3533	0.2365	33%	8.5

The results for the NEDC cycles at various ambient temperature and relative

Table 4.2: Various Cycle Compressor Load Results with On-Off Control for 4 Occupants: 22°C, 50% RH

Driving Cycle	Minimum Compressor Load kW	Maximum Compressor Load kW	Compressor Load On-Off Control kW	% Decrease from OSA	Avgerage Switching Time
US06	0.1923	0.3136	0.2858	9%	4
NEDC	0.2227	0.3851	0.3497	9%	2.5
FTP75	0.2019	0.3585	0.3283	8%	2.9
WLTP	0.2014	0.3533	0.3225	9%	3.5

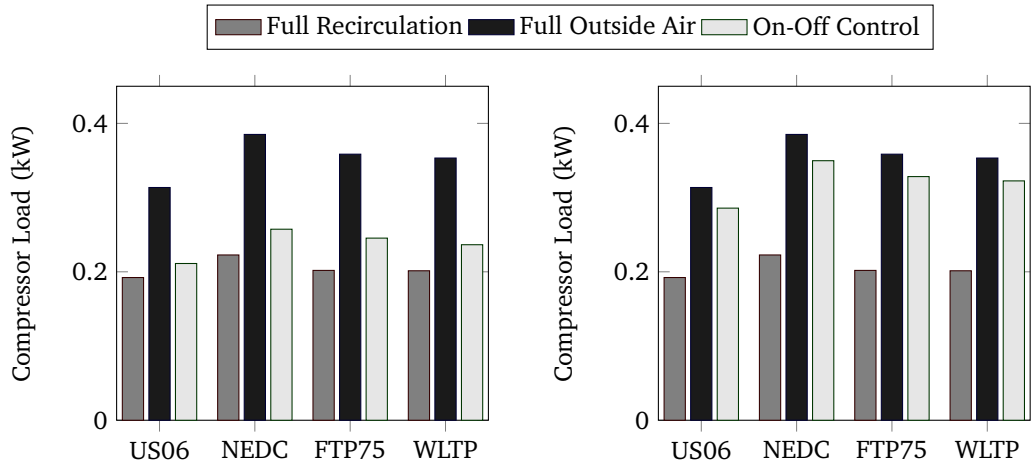

(a) 1 Occupant

(b) 4 Occupants

Figure 4.1: Compressor Load with On-off Recirculation Control With 1 and 4 Occupants

humidities can be seen in Table 4.3 and Table 4.4 for 1 and 4 occupants respectively. These simulations allow the implications and effectiveness of the recirculation strategies across multiple ambient temperatures and humidities to be investigated. Again, the results show a substantial decrease in the compressor load savings for 4 occupants compared to 1 occupants due to the increased production of carbon dioxide from passengers. At higher ambient temperatures (28°C and 35°C) the compressor load savings are much higher compared to the lower temperature NEDC cycle shown in Table 4.3 and Table 4.4. Using RC mode allows the air conditioning system to be in a lower power to cool state. As the energy needed to cool high ambient outside air is

much higher than the energy need to cool lower temperature recirculated cabin air, compressor load savings will show an increasing trend as the ambient temperature rises. It can be also stated that as the high ambient temperature approaches the set cabin temperature, the use of RC mode will have a reduced benefit on the compressor load savings. The NEDC conducted at 15°C and 70% RH shows a negative percent decrease from OSA due to the set point temperature in the cabin being higher than the ambient temperature. Using RC mode in this scenario creates a larger compressor load due to the air conditioning system having to cool air that is higher than the ambient condition outside (Energy required to heat the air is always constant and continuous). Realistically in this scenario, the air conditioning system would normally not be used.

Table 4.3: NEDC Compressor Load Results with On-Off Control for 1 Occupant

Driving Cycle	Minimum Compressor Load kW	Maximum Compressor Load kW	Compressor Load On-Off Control kW	% Decrease from OSA
NEDC 1: 15°C, 70% RH	0.1284	0.1089	0.1237	-14%
NEDC 2: 28°C, 50% RH	0.3080	0.8465	0.4101	52%
NEDC 3: 35°C, 60% RH	0.4575	2.3324	0.7704	67%

Table 4.4: NEDC Compressor Load Results with On-Off Control for 4 Occupants

Driving Cycle	Minimum Compressor Load kW	Maximum Compressor Load kW	Compressor Load On-Off Control kW	% Decrease from OSA
NEDC 1: 15°C, 70% RH	0.1284	0.1089	0.1117	-2.6%
NEDC 2: 28°C, 50% RH	0.3080	0.8465	0.6785	24.6%
NEDC 3: 35°C, 60% RH	0.4575	2.3324	1.7588	20%

Looking more in depth into the results of the NEDC cycle at 28°C and 50% relative humidity, Figure 4.3 and Figure 4.4 show the variation of carbon dioxide and relative humidity over the time of the entire NEDC cycle. In addition to the carbon dioxide concentrations, Figure 4.3 also shows the variation in cycle times for 1 and 4

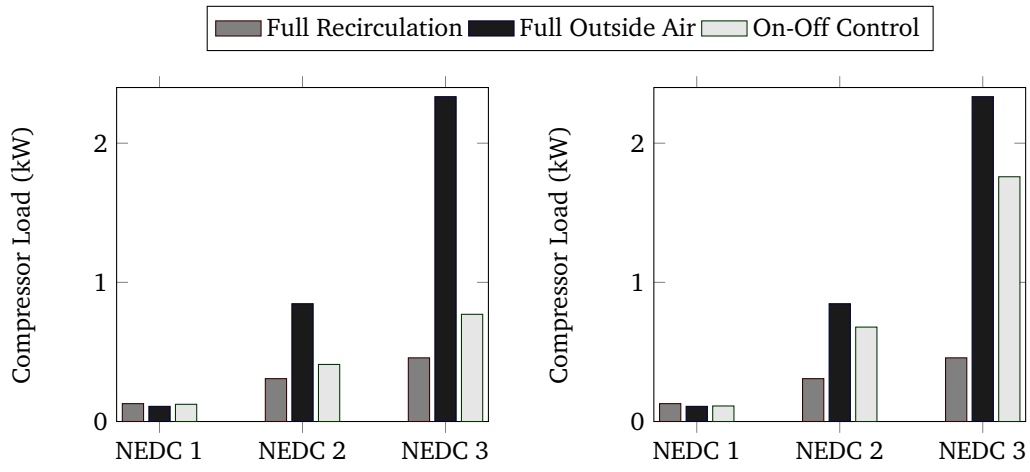

(a) 1 Occupant

(b) 4 Occupants

Figure 4.2: NEDC Compressor Load with On-off Recirculation Control With 1 and 4 Occupants

occupants. The upper limit is controlled by the use of a CO_2 sensor, and the lower limit by minimum concentration able to be reached based on the number of occupants; complying with ASHRAE Standard 62. The relative humidity over the cycle can be seen in Figure 4.4, mostly falling between the limits of human comfort at 30-60%, with an exception coming near the end of the cycle with 1 occupant. Human comfort issues may arise toward the end of this cycle as the relative humidity drops below 30%. When 1 occupant is inside the cabin, the moisture removal from the evaporator overshadows the moisture production of the occupant, causing a reduction in relative humidity towards the lower limit. On the contrary, with 4 occupants inside the cabin, the moisture production from passengers outweighs the moisture removal from the A/C evaporator causing the relative humidity to rise towards the upper limit of 60%.

Figures 4.5 and 4.6 show the detailed results for FTP75 at 22°C and 50% relative humidity featuring carbon dioxide concentrations and cabin relative humidity inside the cabin respectively. The carbon dioxide can be seen to be successfully controlled between the upper and lower limits, while the relative humidity for both 1 and 4

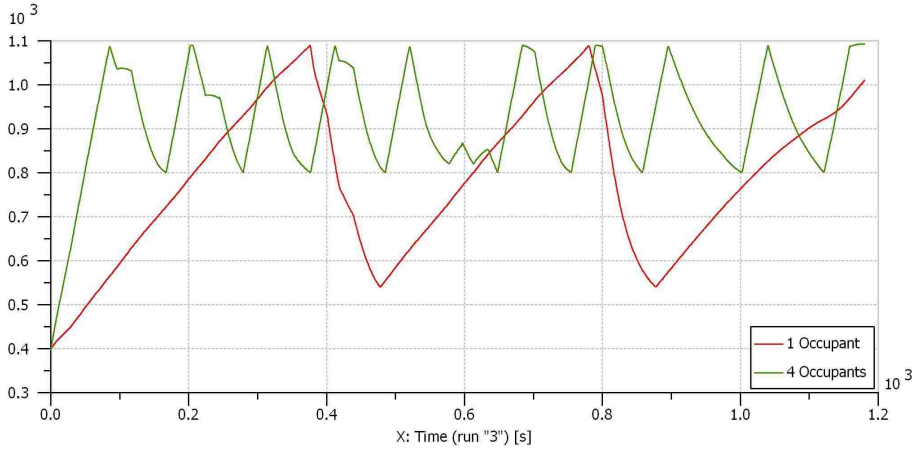

Figure 4.3: Cabin CO_2 Concentrations (ppm) for On-off Control: NEDC Cycle- 28°C, 50% RH

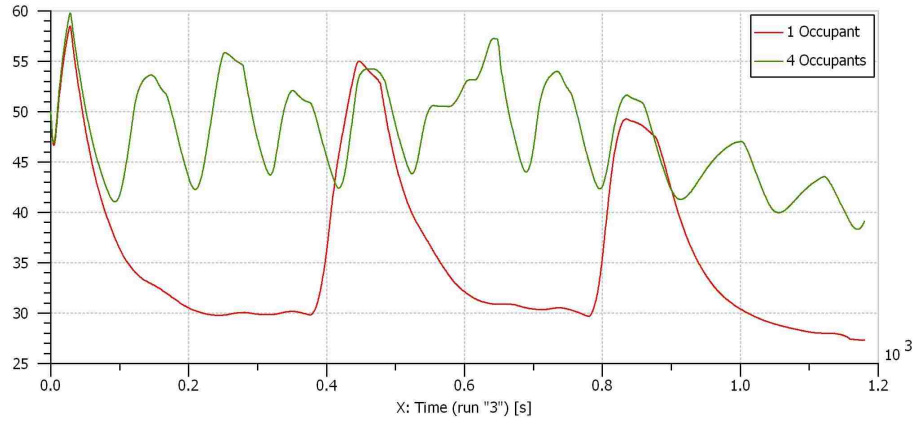

Figure 4.4: Cabin Relative Humidity (%) for On-off Control: NEDC Cycle- 28°C, 50% RH

occupant scenarios falls between 30-60%, as for all simulations conducted at 22°C and 50% RH. As can be seen with 1 occupant, the relative humidity in the cabin falls much lower towards the lower comfort limit due to the limited production of water vapor and the dehumidifying action of the air conditioning evaporator.

In order to look at possible thermal environment implications of the control strategy, the most severe temperature scenario featured in the simulations must be analyzed. Any fluctuations in cabin temperature will be emphasized during the most

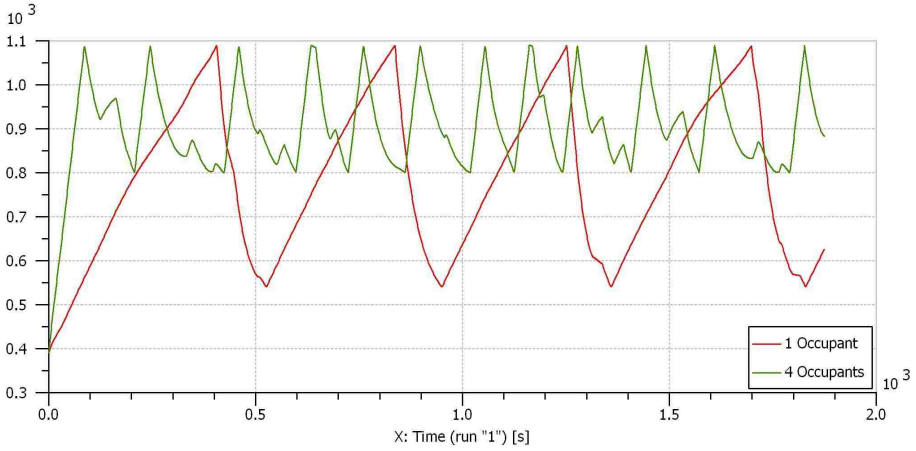

Figure 4.5: Cabin CO_2 Concentrations (ppm) for On-off Control: FTP75 Cycle- 22°C, 50% RH

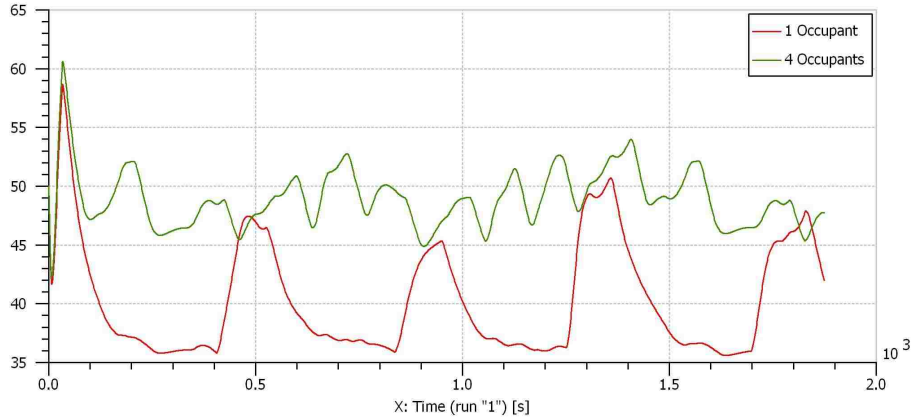

Figure 4.6: Cabin Relative Humidity (%) for On-off Control: FTP75 Cycle- 22°C, 50% RH

severe temperature case, as the air conditioning compressor will be working at its full potential in order to maintain the set cabin temperature. Figure 4.7 shows the temperature variation in the cabin under the NEDC driving cycle at 35°C and 60% relative humidity for 1 and 4 occupants. Looking to this figure, the fluctuations in temperature for 4 occupants can be seen to be much more frequent than the fluctuations in temperature for 1 occupant. The fluctuations in temperature can be attributed to the switch from RC mode to OSA mode. When the switch from RC to

OSA mode is made, the air conditioning compressor transitions from a low power to cool scenario (cooling lower temperature recirculated air) to a high power to cool scenario (cooling high temperature ambient air). At a very high 35°C ambient temperature, the reference air conditioning system cannot maintain the set cabin temperature causing the temperature in the cabin to rise. As the air conditioning system transitions back towards a lower power to cool scenario in RC mode, the temperature in the cabin will begin to fall back towards the set cabin temperature. Although the carbon dioxide concentrations are controlled for both 1 and 4 occupants, these two scenarios feature situations where the rise in cabin temperature may cause human discomfort. As the fluctuations are more frequent for 4 occupants, human discomfort may be more pronounced. All other driving cycle scenarios were able to maintain the set cabin temperature of 22°C without any large temperature fluctuations.

All of the driving cycle cases conducted at 22°C and 50% RH maintained cabin relative humidity between 30-60% throughout the entire duration of the cycle. The cabin relative humidity for 1 occupant scenarios were found to drop much lower than the 4 occupant scenarios due to the limited production of water vapor from 1 occupant, and the ability of the air conditioning evaporator to act as a dehumidifier. All NEDC cycles that were conducted at various ambient temperatures and humidities (15°C, 28°C and 35°C) showed relative humidity concerns with 1 occupant inside the cabin. Relative humidies fell below the lower limit of 30%, which has the potential to cause human discomfort.

The on-off recirculation control strategy manages to successfully control carbon dioxide concentrations in the cabin according to ASHRAE Standard 62; however relative humidity and temperature variations due to the strategy have been shown to potentially cause human comfort issues under certain scenarios. The compressor load

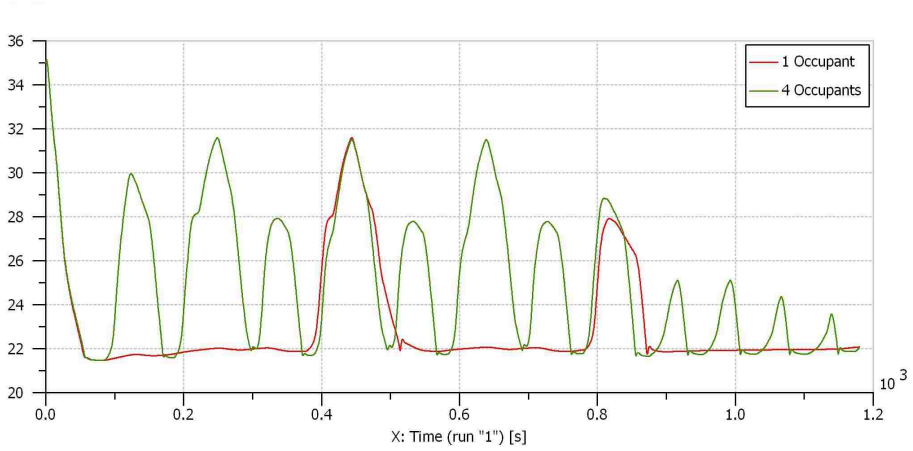

Figure 4.7: Cabin Temperature (°C) for On-off Control: NEDC Cycle- 35°C, 60% RH

savings are noticeably reduced under the 4 occupant situation due to the increased carbon dioxide production when compared to 1 occupant. What is also evident is the time lag that occurs between cabin temperature and CO_2 concentrations during a change from RC mode to OSA mode. The rate of change of CO_2 concentrations in the cabin is more dependant on vehicle parameters such as speed, and fan strength than the temperature, thus a time lag occurs. Mechanical constraints during the operation of this specific control strategy depend on the switching frequency of the recirculation flap door. The mechanism of the recirculation flap door with the on-off control strategy must ensure no further wear or durability issues arise compared to a flap system without the strategy. With cycle times ranging from 1 minute when driving a low speed with a full cabin, to 10 minutes when driving at high speed with an empty cabin shown in Figure 4.8, the mechanism of the recirculation flap door must ensure durability, and reliability throughout the lifetime of the vehicle.

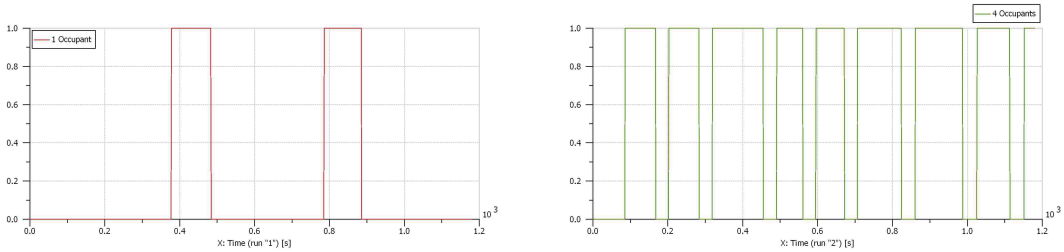

Figure 4.8: On-off Recirculation Flap Door Response for 1 & 4 Occupants: NEDC Cycle- 28°C, 50% RH

4.2 Timed Recirculation Control

The timed strategy represents the only control strategy in this thesis work that does not need the inclusion of a CO_2 sensor in order to operate. Both the fractional and on-off strategies discussed utilize communication with a CO_2 sensor in order to determine the position of the recirculation flap door. Without the inclusion of a CO_2 sensor, the timed strategy becomes comparably the easiest strategy to implement inside an actual vehicle. The timed recirculation strategy features three possible door positions: 100% RC, 50% RC and 100% OSA. The following section will detail the results of all four timed control strategies simulated, including information on compressor load reduction, carbon dioxide concentrations during the cycles, and any thermal environment and mechanical implications of the control strategies.

4.2.1 15 Minutes of Recirculation & 1 Minute of 50% Outside Air

Tables 4.5 and 4.6 show compressor load reductions and carbon dioxide concentrations for various driving cycles at 22°C and 50% relative humidity for 1 occupant and 4 occupants respectively, using the first timed recirculation control strategy. With the use of the timed control strategy, the percentage decrease from the maximum compressor load can be seen to be 39-43%. Since the timed control strategies do not use a CO_2 sensor to operate, the compressor load savings do not depend on the CO_2 production from the passengers, unlike the on-off and fractional

control strategies. The consequences of this indicate that the compressor load savings do not change according to the number of occupants shown in Tables 4.5 and 4.6. This can be a clear advantage over other strategies in which the compressor load savings depend on the number of occupants.

The difference, however, for the timed control strategies between 1 and 4 occupant scenarios are the average carbon dioxide concentrations of the cycle shown in Tables 4.5 and 4.6. Average concentrations can be seen to be as high as 1448 ppm over the FTP75 cycle for 1 occupant and 4620 ppm for 4 occupants. Comparing these average concentrations to limits established by ASHRAE and OSHA, it can be seen that this timed control strategy does not conform to ASHRAE Standard 62, and is on pace to be higher than the OSHA established limits of a 5000 ppm time weighted average for an 8 hour day. Concentrations are dependent on the air exchange rate over the cycle which will be higher at greater vehicle velocities. For this reason, we can see a higher average speed cycle (US06) having a lower average concentration than a lower speed cycle (NEDC). Average concentrations are also dependent on the increasing nature of the average over the cycle, and then number of fresh air purges. The NEDC cycle, for example, has a lower average vehicle velocity compared to the FTP75 cycle. It would be expected for the FTP75 cycle to have lower carbon dioxide concentrations than the NEDC cycle however the opposite is the case. The increasing nature of the average concentration and the location of the fresh air purge for both cycles cause the FTP75 cycle to have a higher average carbon dioxide concentration. Peak concentrations seen in the cycle were significantly above ASHRAE Standard 62, and will be shown in detail later in the section.

Tables 4.7 and 4.8 show NEDC cycle results for various ambient temperatures and relative humidities which include the compressor load savings and the average carbon dioxide concentrations over the cycle. Similarly to Tables 4.5 and 4.6, the compressor

Table 4.5: Various Cycle Compressor Load Results with Timed Control 1 for 1 Occupant:: 22°C, 50% RH

Driving Cycle	Minimum Compressor Load kW	Maximum Compressor Load kW	Compressor Load Timed Control kW	% Decrease from OSA	Avg. CO_2 Concentration
US06	0.1923	0.3136	0.1923	39%	858 ppm
NEDC	0.2227	0.3851	0.2272	41%	1220 ppm
FTP75	0.2019	0.3585	0.2053	43%	1448 ppm
WLTP	0.2014	0.3533	0.2043	42%	1350 ppm

Table 4.6: Various Cycle Compressor Load Results with Timed Control 1 for 4 Occupants: 22°C, 50% RH

Driving Cycle	Minimum Compressor Load kW	Maximum Compressor Load kW	Compressor Load Timed Control kW	% Decrease from OSA	Avg. CO_2 Concentration
US06	0.1923	0.3136	0.1923	39%	2270 ppm
NEDC	0.2227	0.3851	0.2272	41%	3700 ppm
FTP75	0.2019	0.3585	0.2053	43%	4620 ppm
WLTP	0.2014	0.3533	0.2043	42%	4237 ppm

load savings can be seen to be the same for both 1 occupant and 4 occupant scenarios. The increased compressor load savings at higher ambient temperatures can be seen, due to the power to cool reduction which increases as a result of increasing ambient temperature. Similarly with the driving cycle cases at 22°C and 50% relative humidity, the average carbon dioxide concentrations are significantly higher for the 4 occupant scenarios with values around 3700 ppm. As the average will continuously rise due to the nature of carbon dioxide build-up and the small amount of fresh air purges in the strategy, repeating the driving cycle would result in unacceptably high average carbon dioxide concentrations; leading to poor air quality that could be potentially hazardous to occupants in the vehicle.

Figures 4.9 and 4.10 show details of carbon dioxide concentrations and relative humidity during the NEDC cycle simulated at 28°C and 50% relative humidity. Figure 4.9 shows peak concentrations reaching close to 6000 ppm, and concentrations

Table 4.7: NEDC Compressor Load Results with Timed Control 1 for 1 Occupant

Driving Cycle	Minimum Compressor Load kW	Maximum Compressor Load kW	Compressor Load Timed Control kW	% Decrease from OSA	Avg. CO_2 Concentration
NEDC 1: 15°C, 70% RH	0.1284	0.1089	0.1283	-18%	1226 ppm
NEDC 2: 28°C, 50% RH	0.3080	0.8465	0.3168	63%	1200 ppm
NEDC 3: 35°C, 60% RH	0.4575	2.3324	0.5000	79%	1123 ppm

Table 4.8: NEDC Compressor Load Results with Timed Control 1 for 4 Occupants

Driving Cycle	Minimum Compressor Load kW	Maximum Compressor Load kW	Compressor Load Timed Control kW	% Decrease from OSA	Avg. CO_2 Concentration
NEDC 1: 15°C, 70% RH	0.1284	0.1089	0.1283	-18%	3728 ppm
NEDC 2: 28°C, 50% RH	0.3080	0.8465	0.3168	63%	3718 ppm
NEDC 3: 35°C, 60% RH	0.4575	2.3324	0.5000	79%	3624 ppm

reduced by almost 2000 ppm due to the 1 minute fresh air purge at 50% recirculation for the 4 occupant scenario, and peak concentrations of close to 2000 ppm with a 750 ppm reduction due to the purge for the 1 occupant scenario. This reduction will depend on the air exchange rate during that purge which can be influenced by vehicle speed and fan strength. Relative humidity, shown in Figure 4.10, during the cycle can be seen to be approaching and falling under the lower limit of 30% for 1 occupant, and acceptably between 30-60% for 4 occupants.

Figures 4.11and 4.12 show details of carbon dioxide concentrations and relative humidity during the FTP75 cycle simulated at 22°C and 50% relative humidity. Figure 4.11 showcases the increasing nature of carbon dioxide concentration, which will push the average concentration higher over time. Peak concentrations can be seen to be as high as 7000 ppm for the 4 occupant scenario and 2000 ppm for the 1 occupant scenario. The 1 minute fresh air purge at 50% recirculation can be shown to reduce the carbon dioxide concentrations similar magnitudes for both the 1 occupant

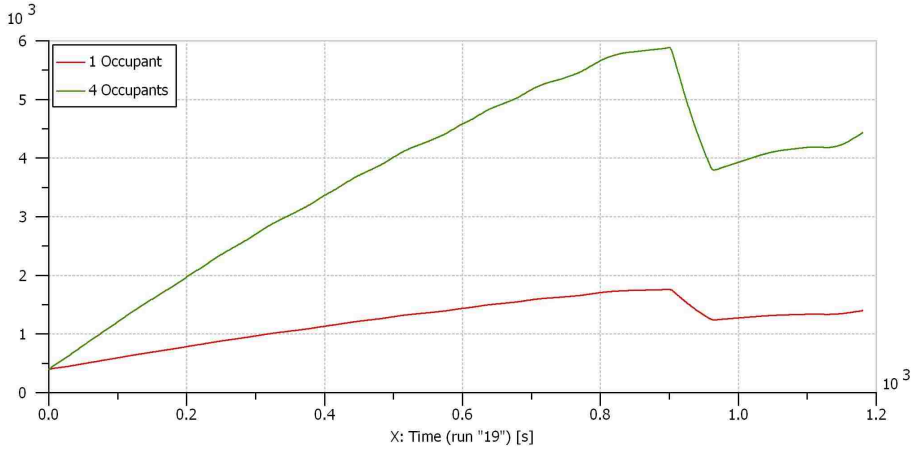

Figure 4.9: Cabin CO_2 Concentrations (ppm) for Timed Control 1: NEDC Cycle- 28°C, 50% RH

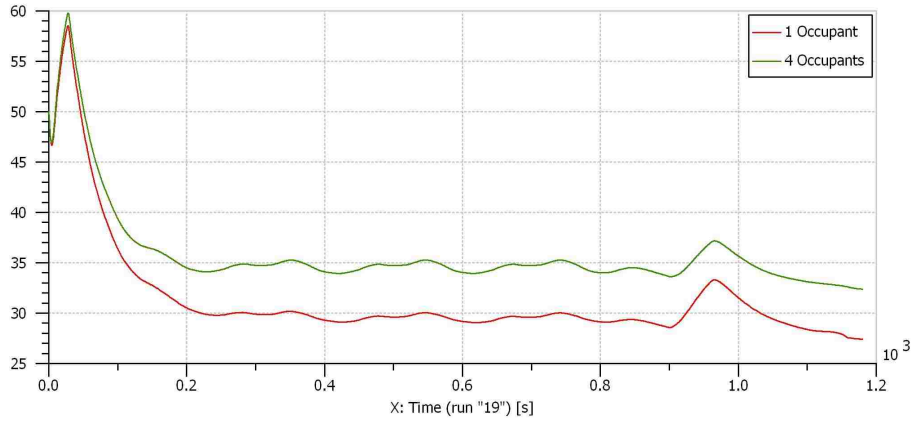

Figure 4.10: Cabin Relative Humidity (%) for Timed Control 1: NEDC Cycle- 28°C, 50% RH

and 4 occupant scenarios. Relative humidity during the cycle, shown in Figure 4.12, can be seen to be between the acceptable limits for human comfort (30-60%). This particular strategy can be shown to have no negative repercussions on the relative humidity in the cabin at 22°C and 50% relative humidity during this specific driving cycle.

The temperature implications of the strategy can be seen in the most severe case during the NEDC cycle at 35°C and 60% relative humidity in Figure 4.13. Large

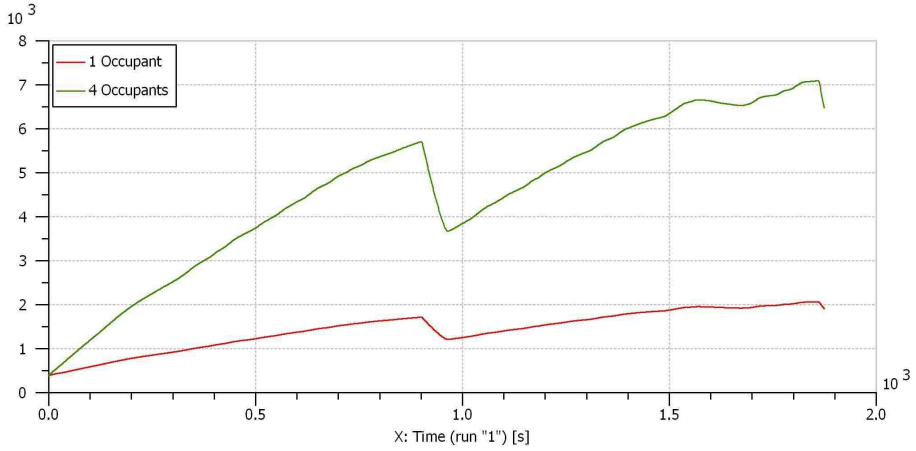

Figure 4.11: Cabin CO_2 Concentrations (ppm) for Timed Control 1: FTP75 Cycle- 22°C, 50% RH

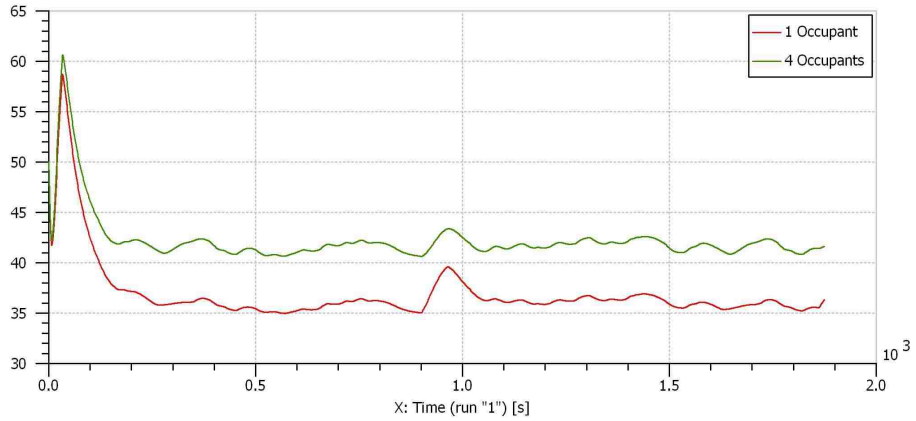

Figure 4.12: Cabin Relative Humidity (%) for Timed Control 1: FTP75 Cycle- 22°C, 50% RH

temperature fluctuations can be caused by the air conditioning system transitioning from a low power to cool state to a high power to cool state, as seen with the on-off control strategy and the switch from RC mode to OSA mode. Since the majority of the cycle is spent in full RC mode, and the fresh air purge still uses 50% RC, the air conditioning system remains in a low power to cool state throughout the entire cycle. No large cabin temperature fluctuations can be seen, and the air conditioning system is able to maintain a cabin temperature of 22°C, even operating with a high ambient

temperature of 35°C. From a cabin temperature standpoint, the timed strategy is more favorable compared to the on-off strategy, which featured multiple high fluctuations in cabin temperature.

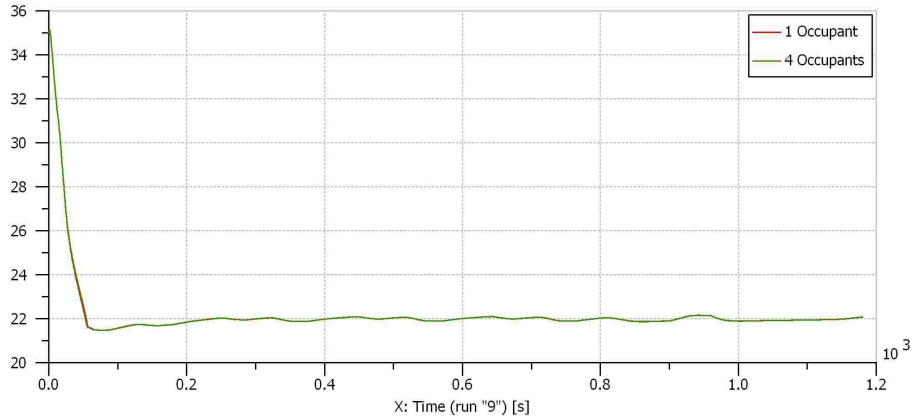

Figure 4.13: Cabin Temperature (°C) for Timed Control 1: NEDC Cycle- 35°C, 60% RH

All of the driving cycle cases conducted at 22°C and 50% RH maintained cabin relative humidity between 30-60% throughout the entire duration of the cycle. The relative humidity in the cabin remained higher for 4 occupants than for 1 occupant due to increased water vapor production of more passengers. NEDC cycles conducted at 15°C, 28°C and 35°C showed cabin relative humidity dropping below 30% for long time periods during the 1 occupant scenarios. Similarly to the on-off strategy, during the 1 occupant scenarios water vapor removal via the air conditioning evaporator mode outweighed the water vapor production of the passenger in RC mode, resulting in a drop in cabin relative humidity.

Since this timed control strategy features seldom fluctuations from RC to OSA modes, the mechanical durability and reliability of the recirculation flap door should not be compromised (compared to lower cycle time and frequency of on-off strategy). The strategy proves to maintain a high level of recirculation throughout the majority of the cycle. The results above indicate that this particular timed control strategy has

the advantage of improved compressor load reductions over the on-off strategy, due to the large amount of time spent in RC mode, and its lack of dependence on the number of occupants. A disadvantage, however, proves to be the higher carbon dioxide concentrations experienced at both the 1 occupant and 4 occupant scenarios. These high carbon dioxide concentrations are well above the limits established in ASHRAE Standard 62, and have the potential to rise above occupational health and safely limits established by OSHA.

4.2.2 10 Minutes of Recirculation & 1 Minute of 100% Outside Air

The second timed strategy aims to increase the frequency of fresh air purges by reducing recirculation cycle time to 10 minutes, and to allow the fresh air purges to operate at 100% OSA mode. Tables 4.9 and 4.10 show compressor load reductions and carbon dioxide concentrations for various driving cycles at 22°C and 50% relative humidity for 1 occupant and 4 occupants respectively using the second timed recirculation control strategy. Due to the reduction in RC mode cycle time, the compressor load savings for both 1 and 4 occupant scenarios were reduced to 39-40%, a 1-3% reduction from the previous timed control strategy. This reduction in compressor load savings is accompanied by a decrease in average carbon dioxide concentrations shown in Tables 4.9 and 4.10 compared to the first time control strategy. Depending on the length of the driving cycle, some cycles now have two fresh air purges at 100% OSA mode, which can be shown to decrease the average concentrations of the cycle. These average concentrations are within the limit established by ASHRAE for 1 occupant in the vehicle cabin, but remain close to 3000 ppm for the 4 occupant scenario. It is evident that the 4 occupant scenario may cause air quality issues resulting from an unacceptably high carbon dioxide concentration. The rising nature of these average concentrations over time could potentially cause 4

occupant concentrations to be comparable to OSHA limits for occupational health and safety.

Table 4.9: Various Cycle Compressor Load Results with Timed Control 2 for 1 Occupant: 22°C, 50% RH

Driving Cycle	Minimum Compressor Load kW	Maximum Compressor Load kW	Compressor Load Timed Control kW	% Decrease from OSA	Avg. CO_2 Concentration
US06	0.1923	0.3136	0.1923	39%	858 ppm
NEDC	0.2227	0.3851	0.2346	39%	1041 ppm
FTP75	0.2019	0.3585	0.2158	40%	1132 ppm
WLTP	0.2014	0.3533	0.2137	40%	1052 ppm

Table 4.10: Various Cycle Compressor Load Results with Timed Control 2 for 4 Occupants: 22°C, 50% RH

Driving Cycle	Minimum Compressor Load kW	Maximum Compressor Load kW	Compressor Load Timed Control kW	% Decrease from OSA	Avg. CO_2 Concentration
US06	0.1923	0.3136	0.1923	39%	2270 ppm
NEDC	0.2227	0.3851	0.2346	39%	3001 ppm
FTP75	0.2019	0.3585	0.2158	40%	3363 ppm
WLTP	0.2014	0.3533	0.2137	40%	3042 ppm

Tables 4.11 and 4.12 show compressor load reductions and average carbon dioxide concentrations during NEDC cycles at various ambient temperatures and relative humidities for both 1 occupant and 4 occupant scenarios. Similarly to the tables above, the second timed strategy showcases a slight decrease on the compressor load reduction, and lower average carbon dioxide concentrations than the first timed control strategy. Reductions in compressor load savings can be seen to be 63% to 59% for the NEDC simulated at 28°C and 70% RH, and 79% to 76% for the NEDC cycle simulated at 35°C and 60% RH. The NEDC cycle conducted at 15°C and 70% RH features an increase in savings due to the negative implications of using recirculation at that specific ambient temperature and set cabin temperature. The fresh air purges

at 100% OSA allow a greater decrease in the carbon dioxide concentrations, but cause an increase in compressor load due to the switch from a low power to cool state to a high power to cool state. Concentrations for 4 occupant scenarios are still well above limits established by ASHRAE, and pose a potential hazard compared to OSHA standards, if the cycle continued over time.

Table 4.11: NEDC Compressor Load Results with Timed Control 2 for 1 Occupant

Driving Cycle	Minimum Compressor Load kW	Maximum Compressor Load kW	Compressor Load Timed Control kW	% Decrease from OSA	Avg. CO_2 Concentration
NEDC 1: 15°C, 70% RH	0.1284	0.1089	0.1270	-17%	1089 ppm
NEDC 2: 28°C, 50% RH	0.3080	0.8465	0.3542	59%	1032 ppm
NEDC 3: 35°C, 60% RH	0.4575	2.3324	0.5707	76%	1111 ppm

Table 4.12: NEDC Compressor Load Results with Timed Control 2 for 4 Occupants

Driving Cycle	Minimum Compressor Load kW	Maximum Compressor Load kW	Compressor Load Timed Control kW	% Decrease from OSA	Avg. CO_2 Concentration
NEDC 1: 15°C, 70% RH	0.1284	0.1089	0.1270	-17%	2989 ppm
NEDC 2: 28°C, 50% RH	0.3080	0.8465	0.3542	59%	2937 ppm
NEDC 3: 35°C, 60% RH	0.4575	2.3324	0.5707	76%	2890 ppm

Figures 4.14 and 4.15 show details of carbon dioxide concentrations and relative humidity during the NEDC cycle simulated at 28°C and 50% relative humidity. Figure 4.14 shows peak concentrations under 5000 ppm for the 4 occupant scenario, a reduction of almost 1000 ppm compared to the previous timed control strategy. The reduction in carbon dioxide concentrations during the fresh air purge for the 4 occupant scenario can be seen to be approaching 3000 ppm; an increase due to the fresh air purge operating at 100% OSA compared to 50% OSA. A slight reduction in peak concentrations can be seen for the 1 occupant scenario. Relative humidity during the cycle can be seen to be approaching and falling under the lower limit of 30% for 1

occupant, and acceptably between 30-60% for 4 occupants.

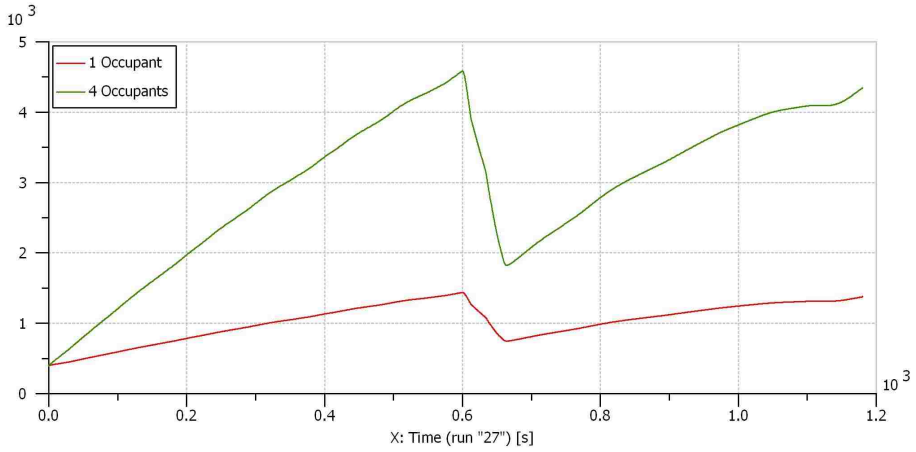

Figure 4.14: Cabin CO_2 Concentrations (ppm) for Timed Control 2: NEDC Cycle- 28°C, 50% RH

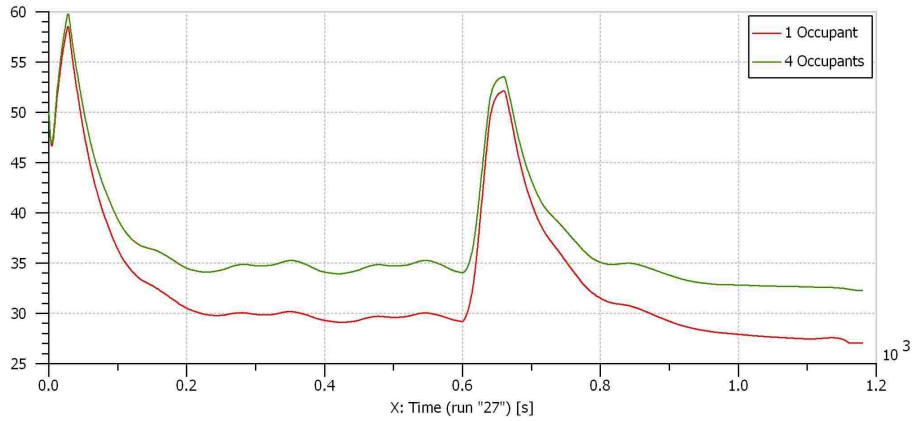

Figure 4.15: Cabin Relative Humidity (%) for Timed Control 2: NEDC Cycle- 28°C, 50% RH

Details of carbon dioxide concentrations and relative humidity during the FTP75 cycle simulated at 22°C and 50% relative humidity can be seen in Figures 4.16 and 4.17. Peak concentrations shown in Figure 4.16 can be seen to be reduced below 5000 ppm for the 4 occupant scenario, compared to peak concentrations of 7000 ppm from timed control strategy number 1. A slight reduction in peak concentrations for the 1 occupant scenario can also be seen. Similarly to the NEDC cycle above, the 1 minute fresh air

purge at 100% OSA shows a large decrease in the carbon dioxide concentrations for the 4 occupant scenario compared to the 1 minute fresh air purge at 50% OSA seen in the last timed strategy. Relative humidity during the cycle, shown in Figure 4.17, can be seen to be between the acceptable limits for human comfort (30-60%) for both 1 occupant and 4 occupant scenarios.

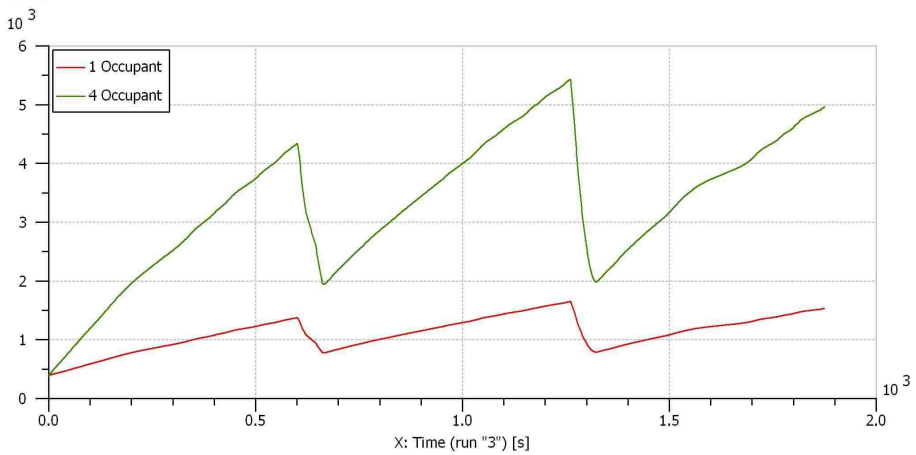

Figure 4.16: Cabin CO_2 Concentrations (ppm) for Timed Control 2: FTP75 Cycle- 22°C, 50% RH

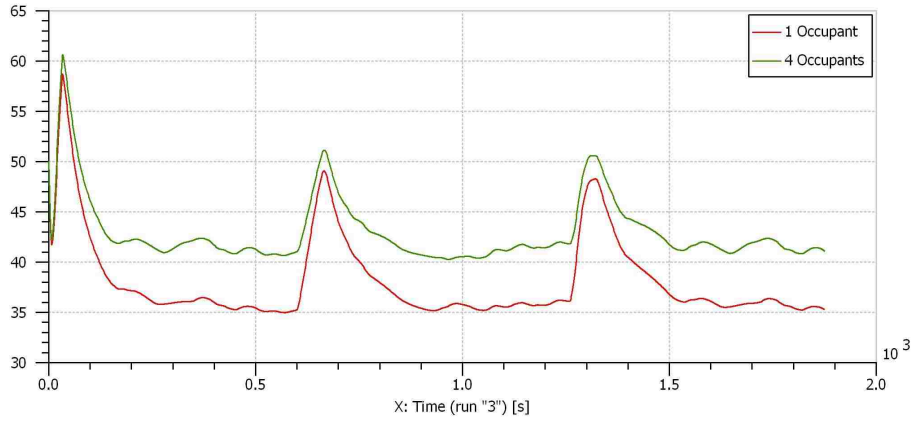

Figure 4.17: Cabin Relative Humidity (%) for Timed Control 2: FTP75 Cycle- 22°C, 50% RH

Figure 4.18 shows the worst case temperature scenario simulated at 35°C and 60% relative humidity over the NEDC cycle. The large temperature peak fluctuation seen

at 600s is the result of the air conditioning system switching from a low power to cool state to a high power to cool state via the switch from RC mode to 100% OSA mode. Since the cycle spends the majority of the time in RC mode, the frequency of any large temperature fluctuation remains low. From a cabin temperature standpoint, this timed control strategy is slightly worse than the last control strategy, but better than the on-off control strategy, which featured multiple, severe temperature fluctuations.

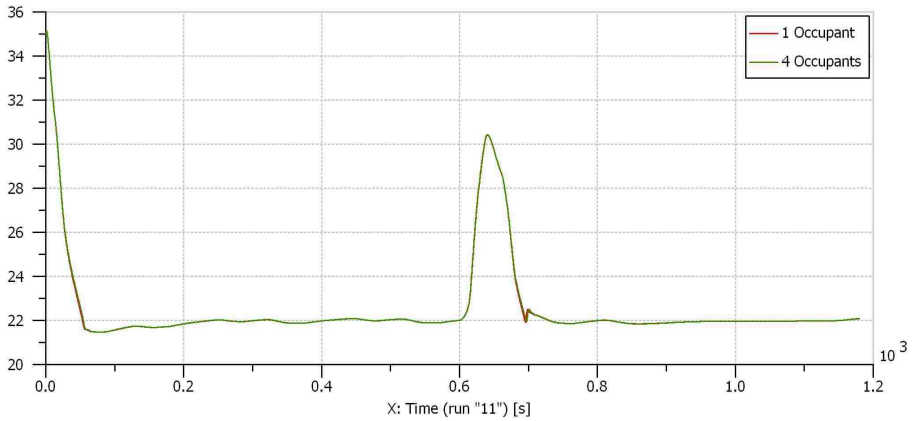

Figure 4.18: Cabin Temperature (°C) for Timed Control 2: NEDC Cycle- 35°C, 60% RH

Similarly to the first timed control strategy, all of the driving cycle cases conducted at 22°C and 50% RH maintained cabin relative humidity between 30-60% throughout the entire duration of the cycle. The relative humidity in the cabin remained higher for 4 occupants than for 1 occupant due to increased water vapor production of more passengers. NEDC cycles simulated at 15°C, 28°C and 35°C showed cabin relative humidity dropping below 30% for long time periods during the 1 occupant scenarios. As mentioned previously, occupant scenarios water vapor removal via the air conditioning evaporator mode outweighed the water vapor production of the passenger in RC mode, resulting in a drop in cabin relative humidity.

The results above offer similar conclusions to the first timed control strategy: the advantage of improved compressor load reductions over the on-off strategy, however

the disadvantage of high carbon dioxide concentrations in the 4 occupant scenario that were well above the limits established by ASHRAE Standard 62. These high concentrations could potentially jeopardise the air quality inside the cabin and in severe cases the safety of occupants if the cycle is repeated multiple times due to the rising average carbon dioxide concentration over time.

4.2.3 7 Minutes of Recirculation & 2 Minutes of 100% Outside Air

The third timed control strategy simulated involved reducing the cycle time in RC mode from 10 to 7 minutes, and increasing the cycle time spent in OSA mode from 1 minute to 2 minutes. Tables 4.13 and 4.14 show the results of compressor load savings and average carbon dioxide concentrations under various driving cycles simulated at 22°C at 50% relative humidity for 1 occupant and 4 occupant scenarios respectively. As expected, due to the further reduction in RC mode cycle time, and the increase in OSA mode cycle time, the compressor load savings have reduced to 30-34% for both scenarios. Accompanied by the reduction in compressor load savings is the reduction in average carbon dioxide concentrations seen for both 1 occupant and 4 occupant scenarios due to the increased time spent in OSA mode. Average concentrations are still above the limits established by ASHRAE for 4 occupant scenarios with averages ranging from 1700-2250 ppm, and within the limits for 1 occupant scenarios.

Table 4.13: Various Cycle Compressor Load Results with Timed Control 3 for 1 Occupant: 22°C, 50% RH

Driving Cycle	Minimum Compressor Load kW	Maximum Compressor Load kW	Compressor Load Timed Control kW	% Decrease from OSA	Avg. CO_2 Concentration
US06	0.1923	0.3136	0.2205	30%	719 ppm
NEDC	0.2227	0.3851	0.2595	33%	817 ppm
FTP75	0.2019	0.3585	0.2358	34%	867 ppm
WLTP	0.2014	0.3533	0.2376	33%	836 ppm

Tables 4.15 and 4.16 show compressor load reductions and average carbon dioxide

Table 4.14: Various Cycle Compressor Load Results with Timed Control 3 for 4 Occupants: 22°C, 50% RH

Driving Cycle	Minimum Compressor Load kW	Maximum Compressor Load kW	Compressor Load Timed Control kW	% Decrease from OSA	Avg. CO_2 Concentration
US06	0.1923	0.3136	0.2205	30%	1713 ppm
NEDC	0.2227	0.3851	0.2595	33%	2110 ppm
FTP75	0.2019	0.3585	0.2358	34%	2264 ppm
WLTP	0.2014	0.3533	0.2376	33%	2184 ppm

concentrations during NEDC cycles at various ambient temperatures and relative humidities for both 1 occupant and 4 occupant scenarios. Similarly to the tables above, the third timed strategy showcases a decrease in the compressor load reduction, and lower average carbon dioxide concentrations than the previous timed control strategies. Compressor load savings can be seen to be reduced to 59% for NEDC simulated at 35°C and 60% RH, and 51% for NEDC simulated at 28°C and 50% RH. At the more severe temperature scenario (35°C), timed spent in OSA mode shows a larger effect on the overall reduction in compressor load, which is why the NEDC cycle simulated at 35°C shows a larger reduction in savings from the previous times strategy compared to the NEDC simulated at 28°C. The longer two minute fresh air purges at 100% OSA allow a greater decrease in the carbon dioxide concentrations, but cause a large increase in compressor load due to the switch from a low power to cool state to a high power to cool state, especially at the high ambient temperature scenario of 35°C. Concentrations for 4 occupant scenarios are still well above limits established by ASHRAE similarly to the cycles discussed above.

Figures 4.19 and 4.20 show details of carbon dioxide concentrations and relative humidity during the NEDC cycle simulated at 28°C and 50% relative humidity. Figure 4.19 shows peak concentrations reduced under 4000 ppm for the 4 occupant scenario, a reduction of more than 1000 ppm compared to the previous timed control

Table 4.15: NEDC Compressor Load Results with Timed Control 3 for 1 Occupant

Driving Cycle	Minimum Compressor Load kW	Maximum Compressor Load kW	Compressor Load Timed Control kW	% Decrease from OSA	Avg. CO_2 Concentration
NEDC 1: 15°C, 70% RH	0.1284	0.1089	0.1250	-15%	985 ppm
NEDC 2: 28°C, 50% RH	0.3080	0.8465	0.4177	51%	811 ppm
NEDC 3: 35°C, 60% RH	0.4575	2.3324	0.9563	59%	817 ppm

Table 4.16: NEDC Compressor Load Results with Timed Control 3 for 4 Occupants

Driving Cycle	Minimum Compressor Load kW	Maximum Compressor Load kW	Compressor Load Timed Control kW	% Decrease from OSA	Avg. CO_2 Concentration
NEDC 1: 15°C, 70% RH	0.1284	0.1089	0.1250	-15%	2263 ppm
NEDC 2: 28°C, 50% RH	0.3080	0.8465	0.4177	51%	2086 ppm
NEDC 3: 35°C, 60% RH	0.4575	2.3324	0.9563	59%	1979 ppm

strategy and 2000 ppm compared to the first timed strategy. Since the fresh air purge occurs more frequently, the peak carbon dioxide concentrations will be reduced. This peak can be seen to slowly increase throughout the cycle, which will increase the average concentration over time. The reduction in carbon dioxide concentrations during the fresh air purge for the 4 occupant scenario can be seen to be similar to the last timed strategy around 3000 ppm. A slight reduction in peak concentrations can be seen for the 1 occupant scenario. Relative humidity during the cycle can be seen to be approaching and falling under the lower limit of 30% for 1 occupant, and acceptably between 30-60% for 4 occupants.

Details of carbon dioxide concentrations and relative humidity during the FTP75 cycle simulated at 22°C and 50% relative humidity can be seen in Figures 4.21 and 4.22. Peak concentrations shown in Figure 4.21 can be seen to be reduced below 4000 ppm for the 4 occupant scenario, compared to peak concentrations of 5500 ppm from timed control strategy number 2 and 7000 ppm from timed strategy number 1. A

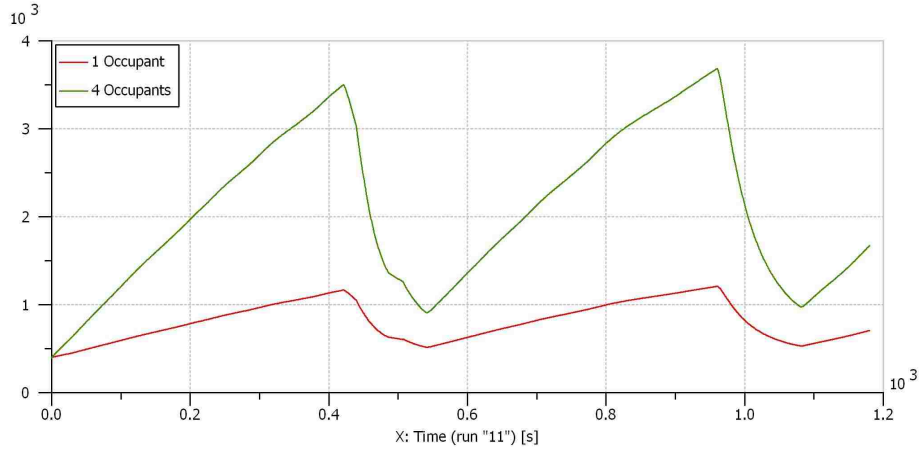

Figure 4.19: Cabin CO_2 Concentrations (ppm) for Timed Control 3: NEDC Cycle- 28°C, 50% RH

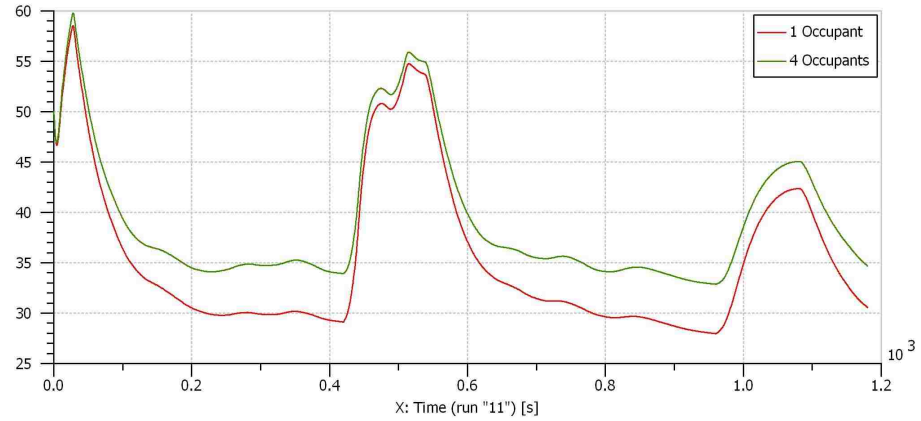

Figure 4.20: Cabin Relative Humidity (%) for Timed Control 3: NEDC Cycle- 28°C, 50% RH

slight reduction in peak concentrations for the 1 occupant scenario can also be seen. Similarly to the NEDC cycle above, the peak concentrations can be shown to be increasing throughout the cycle, which will eventually lead to an increase in the average concentration as the cycle progresses. The 1 minute fresh air purge at 100% OSA shows a large decrease in the carbon dioxide concentrations for the 4 occupant scenario. Relative humidity during the cycle, shown in Figure 4.22, can be seen to be between the acceptable limits for human comfort (30-60%) for both 1 occupant and 4

occupant scenarios.

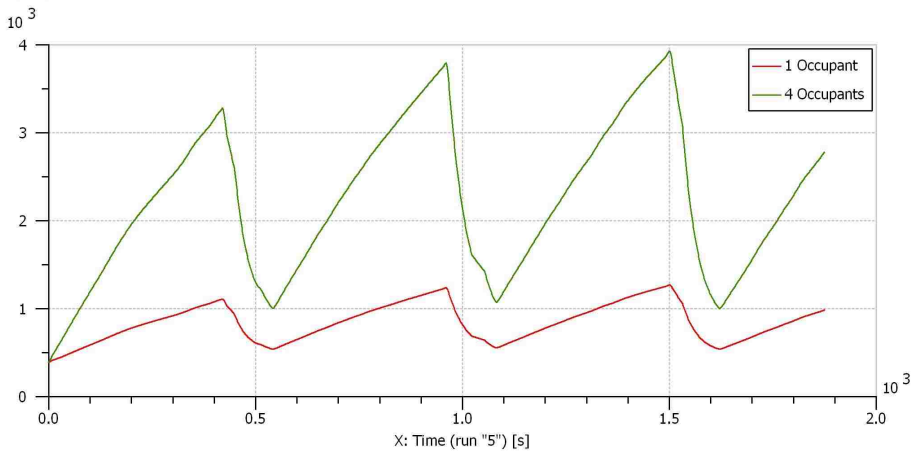

Figure 4.21: Cabin CO_2 Concentrations (ppm) for Timed Control 3: FTP75 Cycle- 22°C, 50% RH

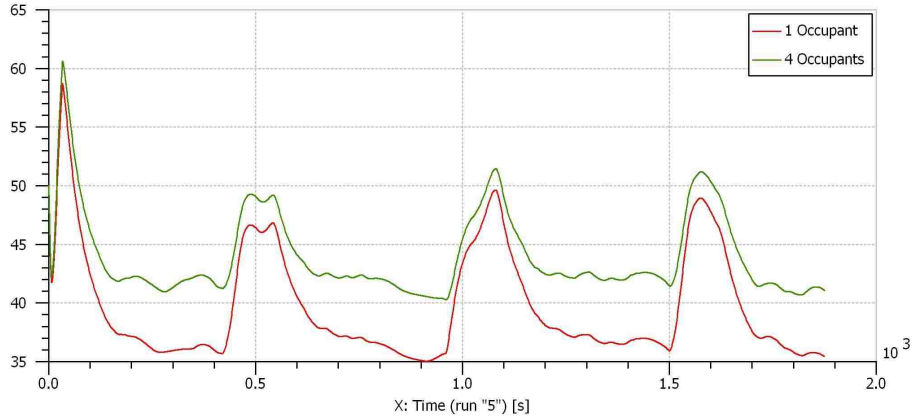

Figure 4.22: Cabin Relative Humidity (%) for Timed Control 3: FTP75 Cycle- 22°C, 50% RH

Figure 4.23 shows the worst case temperature scenario simulated at 35°C and 60% relative humidity over the NEDC cycle. The temperature fluctuation seen at 400s and 1000 s are the result of the air conditioning system switching from a low power to cool state to a high power to cool state via the switch from RC mode to 100% OSA mode. The duration of these fluctuations is also increased from the previous strategy, due to the longer duration of the fresh air purge. Since the cycle still spends the majority of the

time in RC mode, the frequency of any large temperature fluctuation remains low. From a cabin temperature standpoint, this timed control strategy is slightly worse than the previous control strategy due to the longer duration of cabin temperature fluctuations. This timed control strategy still remains more desirable than the on-off strategy because the frequency of any temperature fluctuation remains low in comparison.

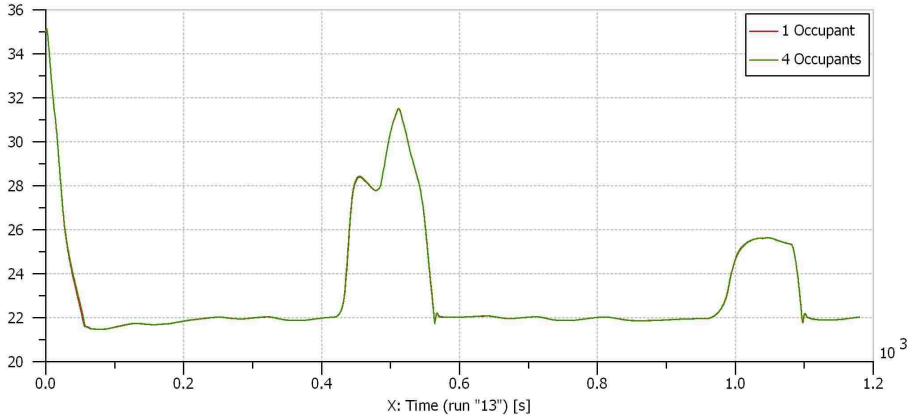

Figure 4.23: Cabin Temperature (°C) for Timed Control 3: NEDC Cycle- 35°C, 60% RH

Similar to the first two timed control strategies, all of the driving cycle cases conducted at 22°C and 50% RH maintained cabin relative humidity between 30-60% throughout the entire duration of the cycle. The relative humidity in the cabin remained higher for 4 occupants than for 1 occupant due to increased water vapor production of more passengers. NEDC cycles simulated at 15°C, 28°C and 35°C showed cabin relative humidity dropping below 30% during the 1 occupant scenarios. As mentioned previously, occupant scenarios water vapor removal via the air conditioning evaporator mode outweighed the water vapor production of the passenger in RC mode, resulting in a drop in cabin relative humidity.

The results above showcase the advantage of improved compressor load savings over the on-off strategy, but reduced compressor load savings over the previous two timed control strategies. The disadvantage of high carbon dioxide concentrations

during the 4 occupant scenarios is still present in the current strategy similarly to the other timed strategies tested. Like the other timed control strategies, these high concentrations could potentially jeopardize the air quality inside the cabin and in severe cases the safety of occupants if the cycle is repeated multiple times due to the rising average carbon dioxide concentration over time.

4.2.4 3.5 Minutes of Recirculation & 1 Minute of 100% Outside Air

The final timed control strategy simulated involved reducing the cycle time in RC mode from 7 to 3.5 minutes, and decreasing the cycle time spent in OSA mode back to 1 minute. This allows the times spent in both RC mode and OSA mode throughout the cycle to be the same, with a varying switch frequency from the last strategy. Tables 4.17 and 4.18 show the results of compressor load savings and average carbon dioxide concentrations under various driving cycles simulated at 22°C at 50% relative humidity for 1 occupant and 4 occupant scenarios respectively. As expected, due to the further reduction in RC mode cycle time, the compressor load savings have slightly reduced to 29-33% for both 1 and 4 occupant scenarios. Accompanied by the reduction in compressor load savings is the reduction in average carbon dioxide concentrations seen for both 1 occupant and 4 occupant scenarios. The increase frequency of the RC to OSA mode switch reduces the build-up of carbon dioxide in the cabin, thus reducing the average concentration over the cycle. Average concentrations are still above the limits established by ASHRAE for 4 occupant scenarios with averages ranging from 1500-2000 ppm, and within the limits for 1 occupant scenarios. It is evident, that in order to reduce average carbon dioxide concentrations for 4 occupant scenarios under ASHRAE standards, the cycle time in RC mode would have to be reduced even further.

Tables 4.19 and 4.20 show compressor load reductions and average carbon dioxide

Table 4.17: Various Cycle Compressor Load Results with Timed Control 4 for 1 Occupant: 22°C, 50% RH

Driving Cycle	Minimum Compressor Load kW	Maximum Compressor Load kW	Compressor Load Timed Control kW	% Decrease from OSA	Avg. CO_2 Concentration
US06	0.1923	0.3136	0.2229	29%	670 ppm
NEDC	0.2227	0.3851	0.2651	31%	765 ppm
FTP75	0.2019	0.3585	0.2394	33%	798 ppm
WLTP	0.2014	0.3533	0.2389	32%	769 ppm

Table 4.18: Various Cycle Compressor Load Results with Timed Control 4 for 4 Occupants: 22°C, 50% RH

Driving Cycle	Minimum Compressor Load kW	Maximum Compressor Load kW	Compressor Load Timed Control kW	% Decrease from OSA	Avg. CO_2 Concentration
US06	0.1923	0.3136	0.2229	29%	1152 ppm
NEDC	0.2227	0.3851	0.2651	31%	1895 ppm
FTP75	0.2019	0.3585	0.2394	33%	2028 ppm
WLTP	0.2014	0.3533	0.2389	32%	1908 ppm

concentrations during NEDC cycles at various ambient temperatures and relative humidities for both 1 occupant and 4 occupant scenarios. What is interesting about these scenarios is the increase in compressor load savings seen for the NEDC simulated at 35°C and 60% RH (59% to 60%), while a reduction in savings is seen for the NEDC simulated at 28°C and 50% RH from the previous strategy (51% to 49%), even though both strategies spend the same amount of time in OSA mode. It is evident that at high ambient temperatures (35°C), the higher frequency switch (4.5 minute cycle) from RC to OSA mode is better for the compressor load savings. Compressor load savings can be seen to be reduced to 49% for NEDC simulated at 28°C and 50% RH, meaning that at lower ambient temperatures, the lower frequency switch (9 minute cycle) from RC to OSA mode is better for the compressor load savings. The longer time cycles (2 minutes) in OSA mode in the previous strategy

shows a negative effect on the compressor load at very high ambient temperatures (35°C). As mentioned previously, the increase frequency of the RC to OSA mode switch reduces the build-up of carbon dioxide in the cabin, thus reducing the average concentration over the cycle. Concentrations for 4 occupant scenarios are still well above limits established by ASHRAE similarly to the cycles discussed above.

Table 4.19: NEDC Compressor Load Results with Timed Control 4 for 4 Occupants

Driving Cycle	Minimum Compressor Load kW	Maximum Compressor Load kW	Compressor Load Timed Control kW	% Decrease from OSA	Avg. CO_2 Concentration
NEDC 1: 15°C, 70% RH	0.1284	0.1089	0.1247	-15%	1950 ppm
NEDC 2: 28°C, 50% RH	0.3080	0.8465	0.4289	49%	1870 ppm
NEDC 3: 35°C, 60% RH	0.4575	2.3324	0.9389	60%	1718 ppm

Table 4.20: NEDC Compressor Load Results with Timed Control 4 for 1 Occupant

Driving Cycle	Minimum Compressor Load kW	Maximum Compressor Load kW	Compressor Load Timed Control kW	% Decrease from OSA	Avg. CO_2 Concentration
NEDC 1: 15°C, 70% RH	0.1284	0.1089	0.1247	-15%	822 ppm
NEDC 2: 28°C, 50% RH	0.3080	0.8465	0.4289	49%	758 ppm
NEDC 3: 35°C, 60% RH	0.4575	2.3324	0.9389	60%	714 ppm

Figures 4.24 and 4.25 show details of carbon dioxide concentrations and relative humidity during the NEDC cycle simulated at 28°C and 50% relative humidity. Figure 4.24 shows peak concentrations reduced under 3000 ppm for the 4 occupant scenario, a reduction of more than 1000 ppm compared to the previous timed control strategy and 3000 ppm compared to the first timed strategy. Since the fresh air purge occurs more frequently, the build-up of carbon dioxide concentrations is less severe, resulting in reduced peak carbon dioxide concentrations. The reduction in carbon dioxide concentrations during the fresh air purge for the 4 occupant scenario can be seen to be similar to the last timed strategy around 3000 ppm. A slight reduction in

peak concentrations can be seen for the 1 occupant scenario. Relative humidity during the cycle can be seen to be approaching and falling under the lower limit of 30% for 1 occupant near the end of the driving cycle, and acceptably between 30-60% for 4 occupants, however large fluctuations in relative humidity do occur.

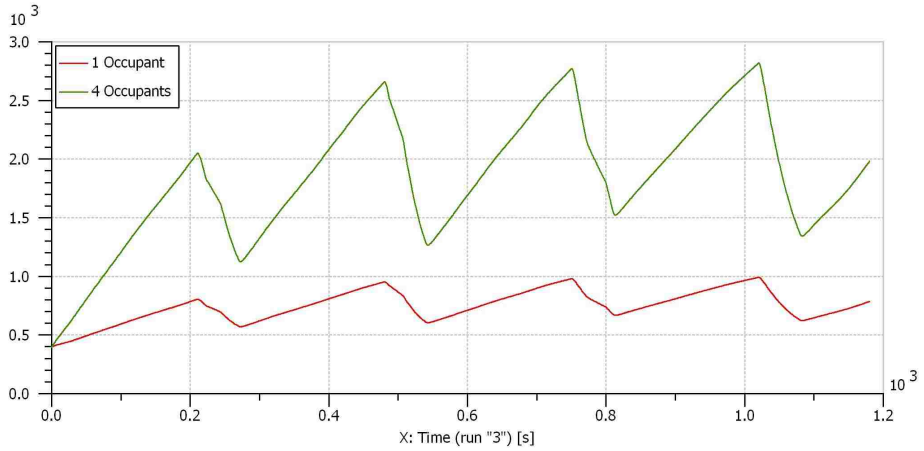

Figure 4.24: Cabin CO_2 Concentrations (ppm) for Timed Control 4: NEDC Cycle- 28°C, 50% RH

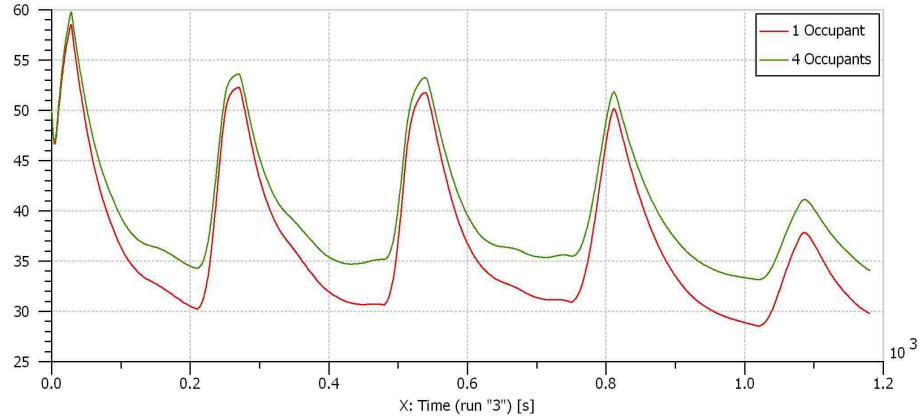

Figure 4.25: Cabin Relative Humidity (%) for Timed Control 4: NEDC Cycle- 28°C, 50% RH

Details of carbon dioxide concentrations and relative humidity during the FTP75 cycle simulated at 22°C and 50% relative humidity can be seen in Figures 4.26 and 4.27. Peak concentrations shown in Fgurei 4.26 can be seen to be reduced below 3000 ppm

for the 4 occupant scenario, compared to peak concentrations of 4000 ppm for timed control strategy number 3, 5500 ppm from timed control strategy number 2 and 7000 ppm from timed strategy number 1. A slight reduction in peak concentrations for the 1 occupant scenario can also be seen. Similarly to the NEDC cycle above, and timed strategy number 2, the 1 minute fresh air purge at 100% OSA shows a large decrease in the carbon dioxide concentrations for the 4 occupant scenario. Relative humidity during the cycle, shown in Figure 4.27, can be seen to be between the acceptable limits for human comfort (30-60%) for both 1 occupant and 4 occupant scenarios.

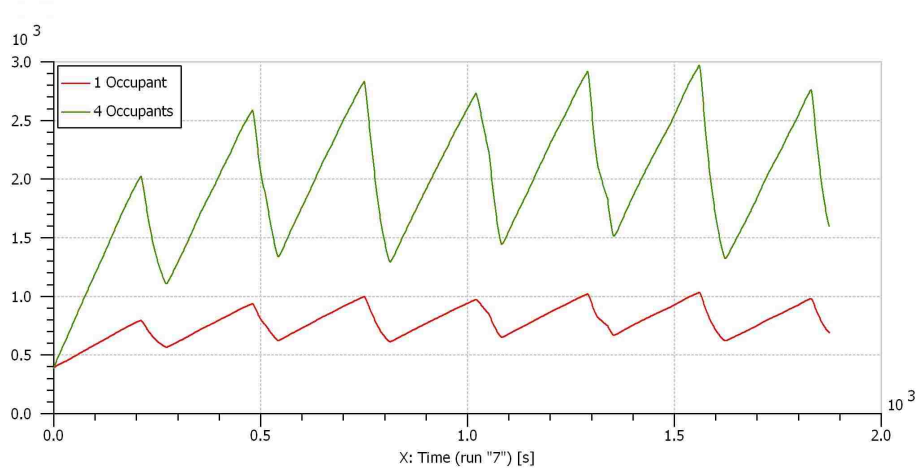

Figure 4.26: Cabin CO_2 Concentrations (ppm) for Timed Control 4: FTP75 Cycle at 22°C, 50% RH

Figure 4.28 showcases the worst case temperature scenario simulated at 35°C and 60% relative humidity over the NEDC cycle. The temperature fluctuations seen throughout the driving cycle are the result of the air conditioning system switching from a low power to cool state to a high power to cool state via the switch from RC mode to 100% OSA mode. The duration of these fluctuations is decreased from the previous strategy, due to the fresh air purge reducing back to 1 minute intervals. Since the cycle still spends the majority of the time in RC mode, the frequency of any large temperature fluctuation remains low. From a cabin temperature standpoint, this timed control strategy is slightly worse than the previous timed control strategy considering

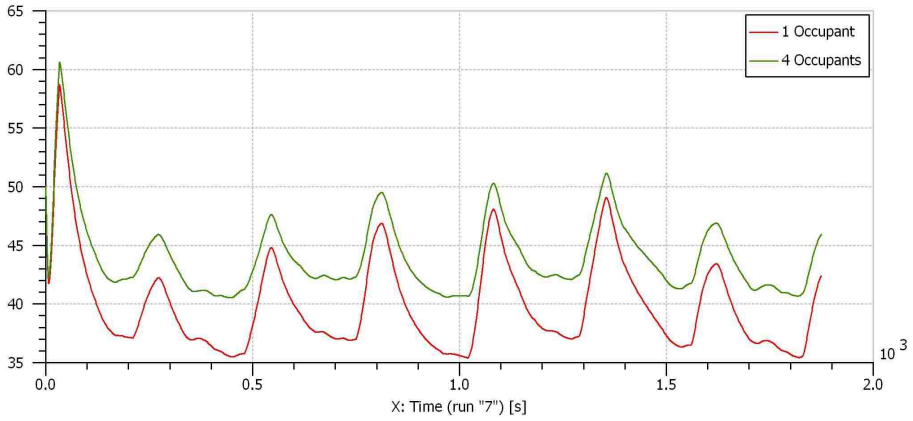

Figure 4.27: Cabin Relative Humidity (%) for Timed Control 4: FTP75 Cycle- 22°C, 50% RH

the number of temperature fluctuations. Furthermore, the duration of these fluctuations are reduced compared to the last control strategy. This timed control strategy still remains more desirable than the on-off strategy because the frequency of any temperature fluctuation remains low in comparison.

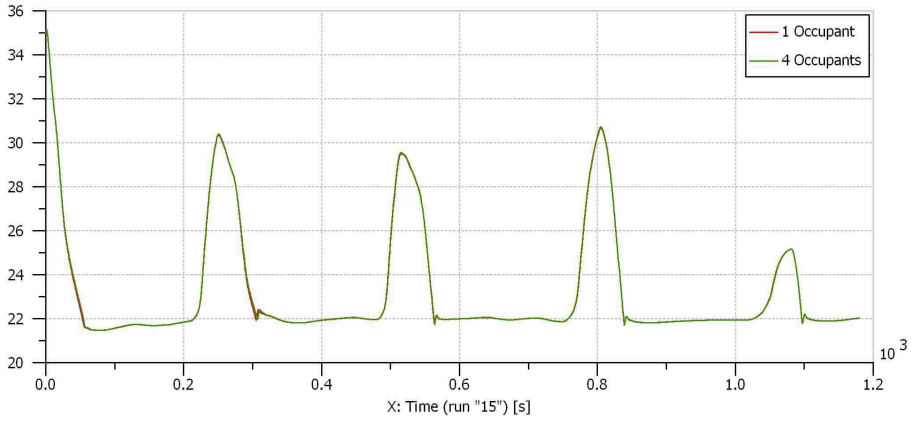

Figure 4.28: Cabin Temperature (°C) for Timed Control 4: NEDC Cycle- 35°C, 60% RH

Similarly to the first three timed control strategies, all of the driving cycle cases conducted at 22°C and 50% RH maintained cabin relative humidity between 30-60% throughout the entire duration of the cycle. The relative humidity in the cabin

remained higher for 4 occupants than for 1 occupant due to increased water vapor production of more passengers. NEDC cycles simulated at 15°C, 28°C and 35°C showed cabin relative humidity dropping below 30% during the 1 occupant scenarios. As mentioned previously, occupant scenarios water vapor removal via the air conditioning evaporator mode outweighed the water vapor production of the passenger in RC mode, resulting in a drop in cabin relative humidity.

The results above detail some main advantages and disadvantages of a timed based strategy. The advantage of improved compressor load savings over the on-off strategy are displayed, but the disadvantage of high carbon dioxide concentrations during all 4 occupant scenarios remains to be an important factor affecting the notoriety of timed based control cycles. Similar to the on-off strategy, a time lag occurs between cabin temperature and CO_2 concentrations during a change from RC mode to OSA mode. Again, the rate of change of CO_2 concentrations in the cabin is more dependant on vehicle parameters such as speed, and fan strength than the temperature, causing a time lag. The above timed control strategies have shown that by increasing the frequency switch from RC to OSA modes, the average carbon dioxide concentration of the cycle could be reduced at the expense of decreasing the compressor load savings. These two factors will remain to be an important trade-off in all control strategies tested, more so in the case of a large number of vehicle occupants. By constantly reducing the switching frequency from RC mode to OSA mode in order to reduce carbon dioxide concentrations, the mechanical operation of the recirculation flap approaches that of the on-off control. Durability and reliability of the recirculation flap must be ensured at high switching frequencies. If the reliability of the recircuation door can be ensured, a higher switching freqency than the last one simulated could be a viable solution for reducing carbon dioxide concentrations within ASHRAE Standard 62 limits. In the event that this cannot happen, it is clear

that an on-off or fractional recirculation strategy may be a more suitable option.

4.3 Fractional Recirculation Control

Fractional recirculation control represents the bridging of benefits related to both on-off and timed recirculation control strategies. By implementing fractional recirculation control, carbon dioxide levels are able to be controlled (as seen using on-off control), while maintaining the highest amount of recirculation possible (a benefit seen in timed recirculation control). A strategy can now exist with the benefits of reduced compressor load, while at the same time maintaining an in-cabin carbon dioxide concentration that does not jeopardize the air quality and safety inside the vehicle cabin. An additional feature of this specific control strategy is the ability to control relative humidity inside the cabin. Low cabin relative humidity becomes a concern with 1 occupant in the cabin as seen with the other control strategies; and so this control strategy uses a relative humidity control function as discussed in Section 3.3.3 in order to maintain cabin relative humidity between human comfort limits.

With the use of a CO_2 sensor along with a signal controller, the fractional control strategy strives to adjust the amount of recirculated air in the cabin to maintain the cabin carbon dioxide concentrations at the upper limit according to ASHRAE Standard 62. The amount of recirculated air will vary between 0 and 100% according to parameters such as vehicle speed and blower velocity in order to maintain the carbon dioxide concentration as close to the upper limit as possible. As the concentration of carbon dioxide in the cabin is kept towards the upper limit level, peak concentrations and average concentrations over the cycle will never rise above this limit; complying to the regulations addressed in ASHRAE Standard 62. Air quality and/or passenger health issue stemming from high carbon dioxide concentrations are mitigated and

always avoided.

Various compressor load results for different driving simulations can be shown in Tables 4.21 and 4.22 for 1 and 4 occupants respectively simulated at 22°C and 50% RH. For 1 occupant inside the cabin, the compressor savings can be seen to be around 37-38% for all driving cycles at 22C and 50% relative humidity. This can be seen to fall in between the compressor load savings of the timed and on-off control strategies. The results for 4 occupants, shown in Table 4.22, show compressor load savings reduced to 12-14% for all cycles. Similarly to the on-off control strategy, the increased production in carbon dioxide from 1 to 4 occupants causes the carbon dioxide limit to be reached at a faster rate. The fractional control strategy must then use less recirculated air when 4 occupants are in the cabin in order to maintain the carbon dioxide concentration at the upper limit compared to 1 occupant in the cabin. As the amount of recirculated air can be directly related to the compressor load savings, it can be expected that the compressor load savings for 4 occupants would be less than for 1 occupant inside the cabin.

Table 4.21: Various Cycle Compressor Load Results with Fractional Control for 1 Occupant: 22°C, 50% RH

Driving Cycle	Minimum Compressor Load kW	Maximum Compressor Load kW	Compressor Load Fractional Control kW	% Decrease from OSA
US06	0.1923	0.3136	0.1966	37%
NEDC	0.2227	0.3851	0.2416	37%
FTP75	0.2019	0.3585	0.2232	38%
WLTP	0.2014	0.3533	0.2203	38%

Tables 4.23 and 4.24 show the various compressor load results for NEDC cycles at different ambient temperatures and relative humidities for 1 and 4 occupants respectively. The compressor load savings can again be seen to fall in between savings for the on-off and timed recirculation control strategies. Similarly to the on-off control

Table 4.22: Various Cycle Compressor Load Results with Fractional Control for 4 Occupants: 22°C, 50% RH

Driving Cycle	Minimum Compressor Load kW	Maximum Compressor Load kW	Compressor Load Fractional Control kW	% Decrease from OSA
US06	0.1923	0.3136	0.2701	14%
NEDC	0.2227	0.3851	0.3371	12%
FTP75	0.2019	0.3585	0.3133	13%
WLTP	0.2014	0.3533	0.2079	13%

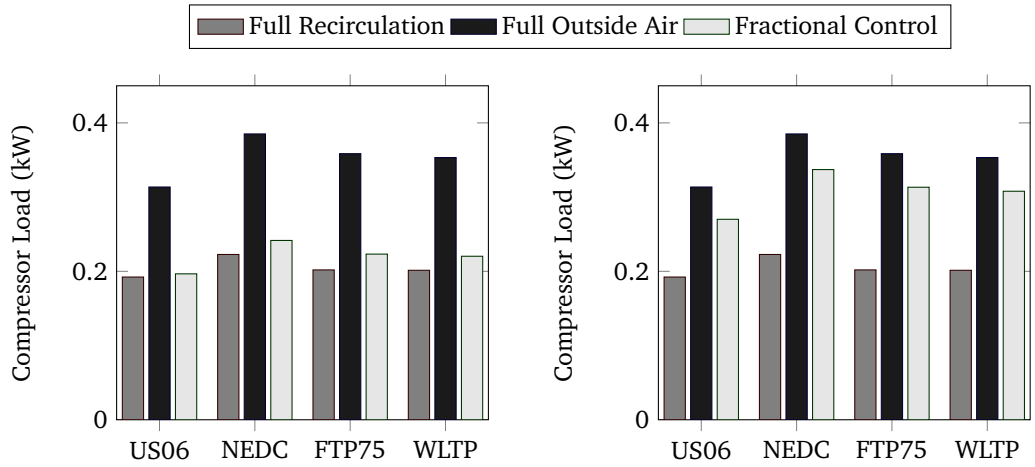

(a) 1 Occupant

(b) 4 Occupants

Figure 4.29: Compressor Load with Fractional Recirculation Control With 1 and 4 Occupants

strategy, a decrease in compressor load savings of more than half can been seen from 1 to 4 occupants due to the increased production of carbon dioxide; 72% to 30% and 55% to 25%. The negative percent decrease seen in the NEDC cycle simulated at 15°C and 70%RH condition is caused by the ambient temperature being lower than the set temperature in the cabin, as mentioned for the previous control strategies. The use of RC mode in this scenario increases the power to cool for the compressor, causing an increase in the compressor load compared to operating in the OSA mode condition. These results can emphasize once again that compressor load savings will be greater at higher ambient temperatures than at lower ambient temperatures due to the

increased power to cool savings experienced at higher ambient temperatures.

Table 4.23: NEDC Compressor Load Results with Fractional Control for 1 Occupant

Driving Cycle	Minimum Compressor Load kW	Maximum Compressor Load kW	Compressor Load Fractional Control kW	% Decrease from OSA
NEDC 1: 15°C, 70% RH	0.1284	0.1089	0.1153	-6%
NEDC 2: 28°C, 50% RH	0.3080	0.8465	0.3775	55%
NEDC 3: 35°C, 60% RH	0.4575	2.3324	0.6609	72%

Table 4.24: NEDC Compressor Load Results with Fractional Control for 4 Occupants

Driving Cycle	Minimum Compressor Load kW	Maximum Compressor Load kW	Compressor Load Fractional Control kW	% Decrease from OSA
NEDC 1: 15°C, 70% RH	0.1284	0.1089	0.1117	-5.5%
NEDC 2: 28°C, 50% RH	0.3080	0.8465	0.6326	25%
NEDC 3: 35°C, 60% RH	0.4575	2.3324	1.6420	30%

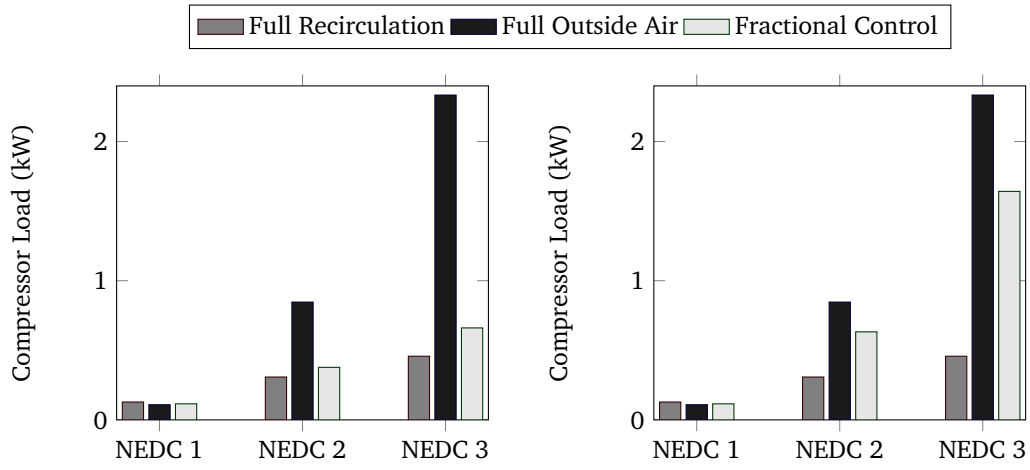

(a) 1 Occupant

(b) 4 Occupants

Figure 4.30: NEDC Compressor Load with Fractional Recirculation Control With 1 and 4 Occupants

Figures 4.31 and 4.32 show the details of carbon dioxide concentrations and relative humidity using the fractional control strategy under the NEDC cycle at

ambient conditions of 28°C and 50% relative humdity. As can be seen from Figure 4.31, the carbon dioxide concentrations are held at a limit of 1000 ppm for both 1 and 4 occupant scenarios ,complying with ASHRAE Standard 62. Figure 4.32 details the relative humidity over the cycle, verifying the succesful implementation of the additional relative humidity control featured in the fractional recirculation strategy for the 1 occupant scenario at 200 and 1050 seconds. Figure 4.33 shows the recirculation flap door position move to 100% OSA at these times, allowing the relative humidity in the cabin to rise. Although a decrease in the cabin carbon dioxide concentrations can be seen corresponding to the switch to OSA mode, the strategy ensures a cabin relative humidity that is within human comfort limits.

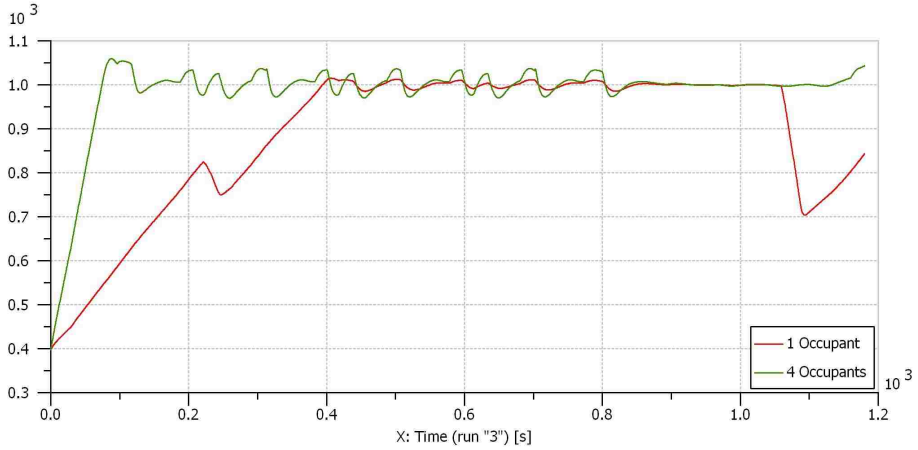

Figure 4.31: Cabin CO_2 Concentrations (ppm) for Fractional Control: NEDC Cycle- 28°C, 50% RH

Figures 4.34 and 4.35 show the carbon dioxide concentrations and cabin relative humidity during the FTP75 cycle at 22°C and 50% relative humidity. Similarly to the NEDC cycle shown above, the ability of the fractional control strategy's ability to maintain the cabin carbon dioxide concentration at the upper limit of 1000 ppm. The difference in the initial carbon dioxide build-up rate between 1 and 4 occupants can also be seen. The relative humidity in the cabin remained between 30-60% for both 1 occupant and 4 occupant scenarios. In these cases, the relative humidity control was

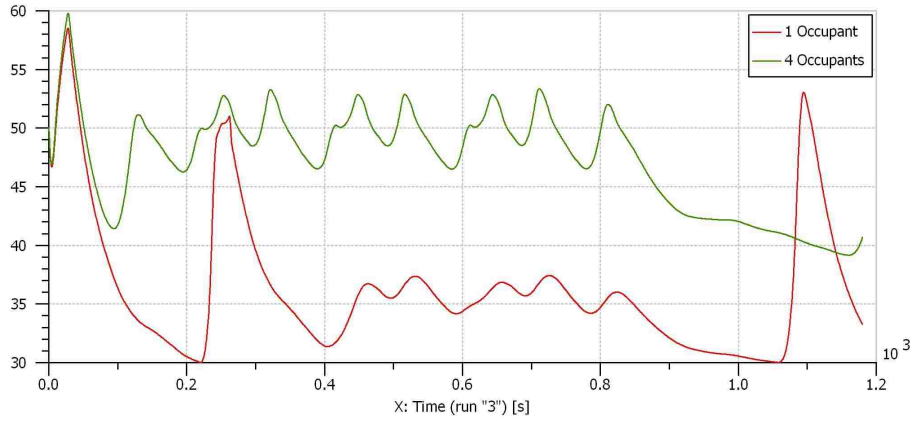

Figure 4.32: Cabin Relative Humidity (%) for Fractional Control: NEDC Cycle- 28°C, 50% RH

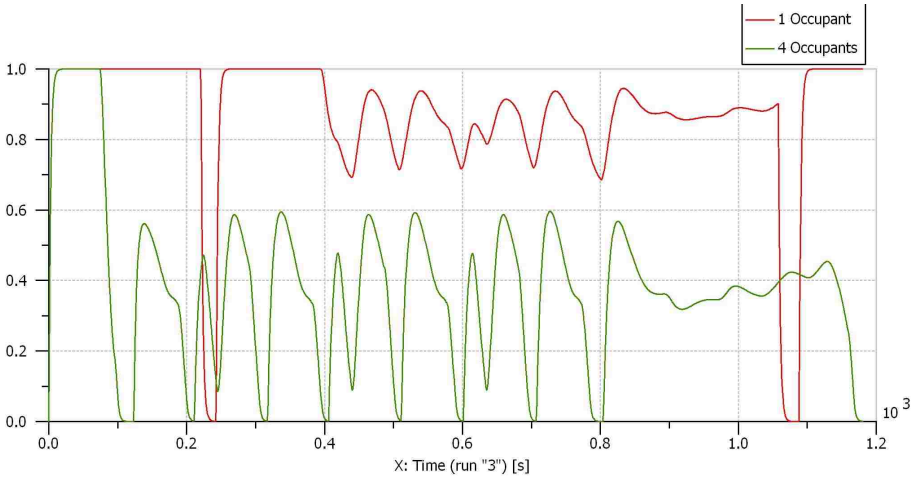

Figure 4.33: Recirculation Flap Response for Fractional Control: NEDC Cycle at 28°C, 50% RH

not triggered, as the relative humidity in the cabin never reached the lower limit of 30%. The relative humidity throughout the cycle can be seen to be higher for the 4 occupant scenario, due to the increased water vapor production of the passengers.

The temperature implications of the strategy can be seen in the most severe case during the NEDC cycle at 35°C and 60% relative humidity in Figure 4.36. Similarly to the on-off control and timed strategies, the temperature fluctuations become dependent on the amount of recirculated air being used and the transition from a low power to

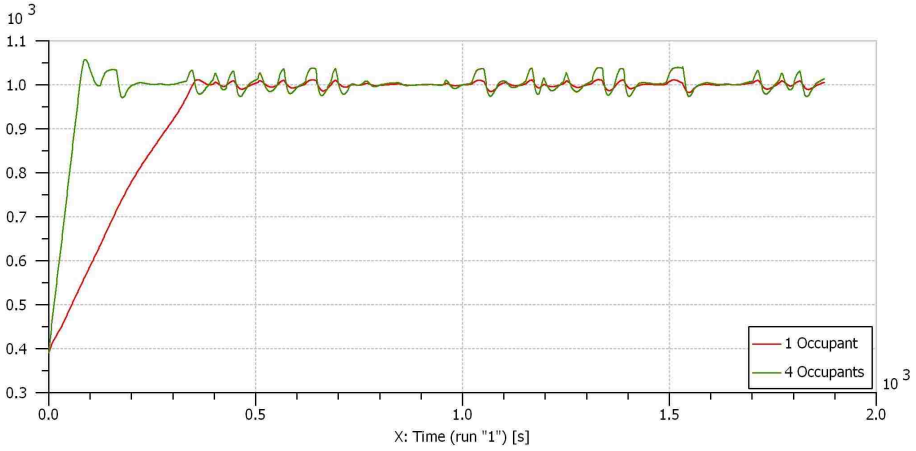

Figure 4.34: Cabin CO_2 Concentrations (ppm) for Fractional Control: FTP75 Cycle- 22°C, 50% RH

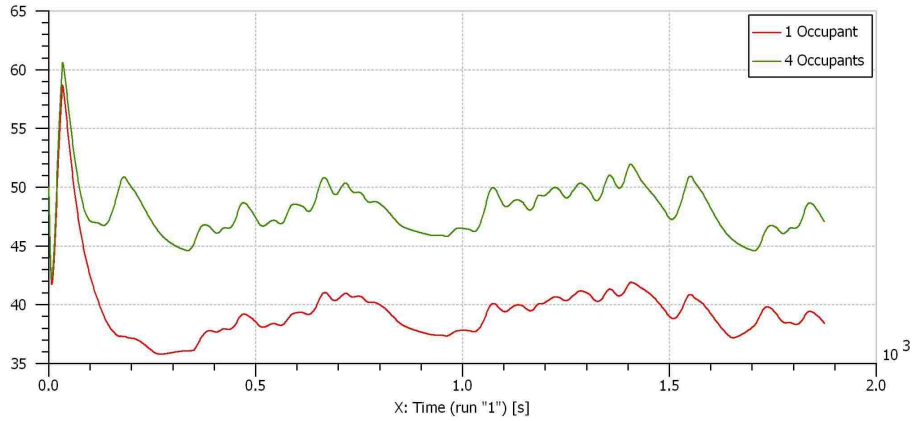

Figure 4.35: Cabin Relative Humidity (%) for Fractional Control: FTP75 Cycle- 22°C, 50% RH

cool scenario to a high power to cool scenario. With one occupant in the cabin, the amount of recirculated air remains higher than with 4 occupants, allowing the cabin temperature to remain more stable toward the set cabin temperature. Although the peaks for both occupant scenarios are more frequent than those for the timed control strategies and comparable to the on-off strategies, these peaks can be seen to be less severe than both the on-off and timed strategies due to the use of even the slightest fraction of recirculated air. In all other cycle simulations, all the cabin temperature was

able to be maintained at the set cabin temperature of 22°C.

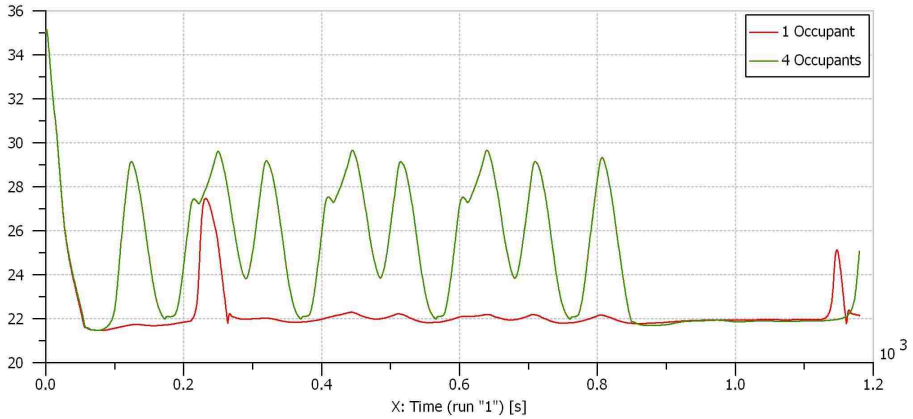

Figure 4.36: Cabin Temperature (°C) for Fractional Control: NEDC Cycle- 35°C, 60% RH

All of the driving cycle cases conducted at 22°C and 50% RH maintained cabin relative humidity between 30-60% throughout the entire duration of the cycle, without the need of active relative humidity control. Similarly to the other strategies, the relative humidity in the cabin remained lower for 1 occupant than for 4 occupants due to increased water vapor production of more passengers. With the use of active relative humidity control, cabin relative humidities of other NEDC cases at different ambient temperatures and humidity remained within the human comfort limits. An emphasis for the 1 occupant scenarios was to maintain the relative humidity above 30% using the active relative humidity control.

An interesting situation arose using the fractional control strategy under the NEDC case at 35°C and 60% relative humidity. During the 4 occupant scenario, the relative humidity in the cabin rose above 60% while the carbon dioxide concentrations were at a maximum limit shown in Figure 4.37 and Figure 4.38. In order to decrease the relative humidity in the cabin, there should be an increase in the amount of recirculated air; however increasing the amount of recirculated air would push the carbon dioxide concentrations above the upper limit. In this scenario, a trade-off must

be obtained between the relative humidity in the cabin and the permissible limit for carbon dioxide concentrations. In other ambient temperature and relative humidity cases where this scenario may be present, a choice must be made to either allow the relative humidity in the cabin to rise, or to sacrifice the air quality and let the carbon dioxide concentrations in the cabin surpass the limit of ASHRAE Standard 62.

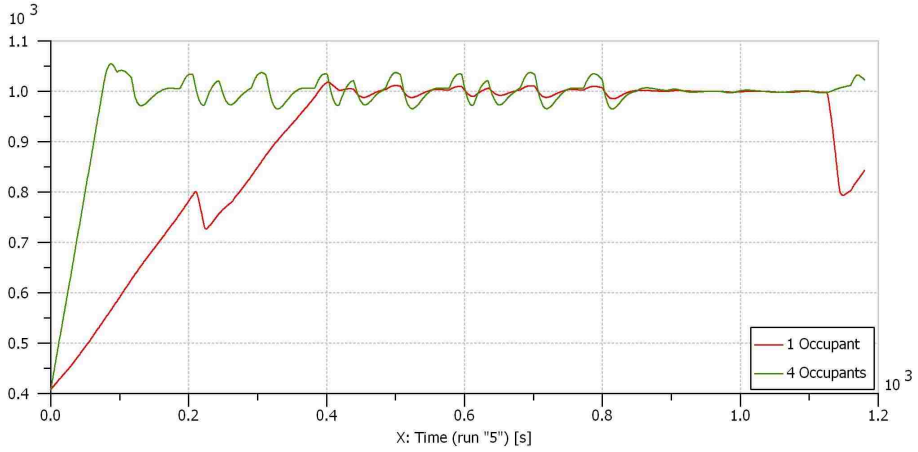

Figure 4.37: Cabin CO_2 Concentrations (ppm) for Fractional Control: NEDC Cycle- 35°C, 60% RH

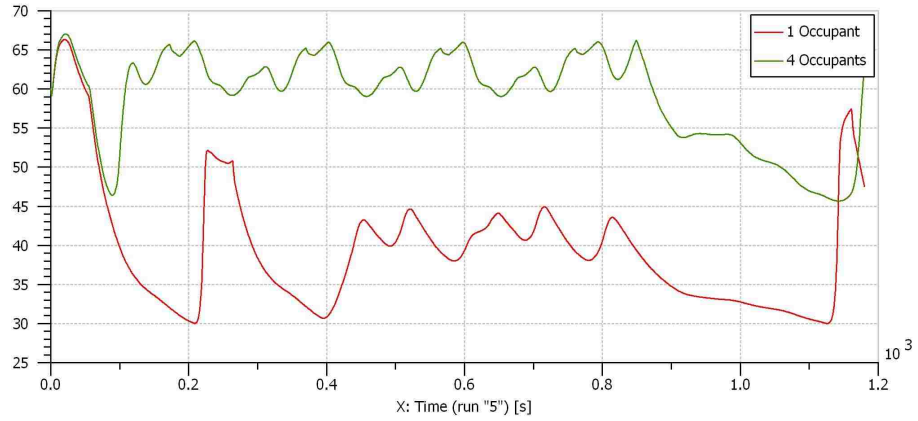

Figure 4.38: Cabin Relative Humidity (%) for Fractional Control: NEDC Cycle- 35°C, 60% RH

The results above showcase the fractional control strategy's ability to successfully adjust the recirculation flap door in order to maintain the carbon dioxide

concentrations at a limit corresponding to ASHRAE Standard 62. The strategy is able to combine aspects of the on-off control strategy by controlling carbon dioxide concentrations, and the timed strategy by using as much recirculated air as possible. The strategy's ability to control carbon dioxide concentrations means that the compressor load savings will ultimately be reduced as the number of occupants in the cabin increase (similarly to the on-off strategy), which has been seen for all cycles simulated above. The ability to also control the relative humidity in the cabin, with an exception to the 35°C, 60% case mentioned above, will have a positive effect on human comfort inside the cabin. Peak temperature fluctuations inside the cabin at high ambient temperatures have been shown to be less severe than both on-off and timed strategies, yet the frequency of fluctuations can be comparable to the on-off strategy and more frequent than the timed strategy. With reference to Figure 4.33, the recirculation flap door must ensure smooth operation and mechanical durability as it receives positional signals from the signal controller. Further testing would have to ensure the mechanical durability and reliability of the recirculation flap door featuring a fractional control strategy does not differ from the mechanical durability and reliability of a simple on-off or timed control strategy.

4.4 Model Limitations and Uncertainties

While the simple carbon dioxide build-up model shown in this thesis research has the ability to predict the carbon dioxide concentrations in a vehicle cabin based on several different vehicle parameters and air conditioning modes, there are several limitations and sources of uncertainties in the development of the model, and simulation studies. While these limitations and uncertainties may affect the results of individual recirculation strategies, the author acknowledges that relative comparisons between strategies should hold true.

4.4.1 Model Limitations

To begin with limitations of the model, the carbon dioxide and water vapor from the passengers were taken to be point sources; meaning there was no volume reduction taken into account from the passengers. Carbon dioxide concentrations from the model may be slightly lower than expected, due to the larger cabin volume when not considering the passengers taking up volumetric space inside the cabin. This slight volume change would have a primary effect on the time constant governing the build-up of carbon dioxide inside the cabin, and it could be hypothesized that the concentrations would be higher in comparison to the model. Since the volume displacement is higher for 4 occupants compared to 1 occupant, it can be expected that the 4 occupant scenarios will have a higher error.

The simple build-up model also assumes all passengers inside the cabin exhale carbon dioxide at the same constant rate. Since the exhalation rate of carbon dioxide can be affected, by age, metabolism and other personal factors, the model cannot differentiate between two or more passengers exhaling carbon dioxide at different rates. Cases such as adolescent children inside the cabin in addition to adults would have to be specifically modeled in order to account for the variability in carbon dioxide exhalation between passengers. A useful addition to the model would be to include the ability to further detail carbon dioxide exhalation details of all passengers separately; making it possible to include scenarios like the one mentioned above. Furthermore, the source of carbon dioxide in the cabin was entirely from passenger exhalation, and the build-up governed by the vehicle's air exchange rate. Any possible infiltration stemming from the exhaust gasses was not presented in this build-up model.

Equations 3.5 and 3.6 used for predicting the air exchange rate presented some further limitations to the model. Due to the method in which the equations were

developed by Hudda et al. [11], the model provides a generalized prediction of the air exchange rate based on a large sample of different vehicle manufacturers and models; the main parameters differentiating the large sample being vehicle volume, and age. The air exchange rate, especially when operating in RC mode, is highly dependent on the vehicle make and model, as discussed in Section 2.3. Manufacturing differences such as seals can especially vary from a higher end model to a lower end model, and between different vehicle manufacturers, potentially creating a large variation in air exchange rates between vehicles. Although there is an additional parameter representing the manufacturing adjustment, these prediction equations make it difficult to estimate the air exchange rate of any specific individual vehicle model, thus our results are limited to the accuracy of the prediction equations. In order to accurately represent a specific vehicle model and manufacturer, experimental testing of the specific model would have to be undertaken, in order to characterize the air exchange rates at multiple operating points. If possible, a predictive equation could be derived from the experimental testing to appropriately describe the specific model, further enhancing the accuracy of the model results.

The final limitation involved was the use of a proportional integral controller to control the recirculation flap door for fractional recirculation control. Further optimization of controller gains would result in increased performance of the strategy. Optimizing controllers to their full potential may result in better compressor load savings for the fractional strategy, pushing it closer to the compressor load savings seen in some of the timed control strategies.

Considering the multiple limitations of the model, the results obtained from simulations are more than satisfying. Since the recirculation strategies were compared on a relative basis, the differences between them should hold true, even with the changing of input parameters or improvement of the model. Any adjustment of the

carbon dioxide production inside the cabin, or air exchange rates would affect all strategies equally, leaving the relative comparison unchanged. Any enhancements to the model mentioned above would enhance the accuracy of individual recirculation strategies themselves.

4.4.2 Model Uncertainties

The model prediction equations that estimate the air exchange rate again represent a source of uncertainty in the model results. Although this source of uncertainty is also presented as a limitation to the model, (as the results are limited to the accuracy of these prediction equations) there are still uncertainties in how well the equations represent a certain vehicle class, or manufacturer. As stated above, this eliminated the ability to analyze any specific vehicle model. The prediction equations for the air exchange rate could have more accurate results for smaller or bigger or vehicles, or even have more accurate results for one vehicle manufacturer over another. As vehicle variations and parameters such as age were found to be extremely evident when it comes to the air exchange rate determination, experimental testing could provide additional data from which to base the prediction equations on. This could provide the ability to simulate recirculation strategies on one specific vehicle model and manufacturer rather than simulating on a generic vehicle mode.

Another assumption used in the creation of the build-up model was in determining the air exchange rate when fractional recirculation was involved. Equation 3.4b represents the assumption that when a fraction of recirculation is involved, the resultant air exchange rate is equal to the fraction of air exchange rate in RC mode plus the fraction of air exchange rate in OSA mode. Given the equations for both RC and OSA modes, a resultant air exchange rate could be determined for any fraction of recirculation from 0-100%. Given the magnitude difference between air exchange

rates in RC and OSA modes, this assumption indicated that even a small fraction of OSA (5-10%) had a considerable effect on decreasing the build-up of carbon dioxide inside the cabin. This scenario further described in Section 3.2. As there is no literature available on air exchange rates involving a fraction of recirculated air, an additional experimental study could provide useful data to improve the model's ability to simulate a fractional control strategy. Experimental testing could validate the use of this assumption, and provide further accuracy in predicting air exchange rates when fractional recirculation is utilized, or give light to an additional equation that could model the resultant air exchange rate more precisely.

The final sources of uncertainty involved in the creation of the model were the waste products exhaled by the occupants inside the vehicle, including the concentration and flow rates of carbon dioxide in addition to water vapor. Parameters used in the model were based on literature studies involving the range of carbon dioxide concentrations (38,000-57,000 ppm) and exhalation flow rates (5-7 L/m) based on the individual's metabolic state. Since the action of driving produces a higher metabolic state than resting, the flow rate of carbon dioxide was taken to be slightly higher than the resting state. As the concentration can vary from individual to individual, the concentration used in the model was taken to be an average value. The model had the potential to underestimate or overestimate the source production of carbon dioxide inside the cabin. Experimental testing of driving individuals could indicate a better source concentration and flow rate to improve the accuracy of the model. The water production of passengers was a parameter that could be introduced into the AMEsim cabin model. The water production of passengers was estimated based on literature to be 50g/h per person. This parameter can vary from person to person, as ASHRAE standards have indicated a slightly higher value of 90g/h per person. This estimation mainly affected the relative humidity in the cabin and how it

was influenced by the individual control strategies.

The results obtained from the simulation model are more than satisfying even when considering the uncertainties mentioned above. Most if not all of the above uncertainties involve estimations from literature, without the inclusion of additional experimental testing. Experimental testing coinciding with this thesis research would assist in improving the parameters mentioned, and the accuracy of the model simulation results.

Chapter 5
Conclusions and Recommendations

The following chapter is a reaffirmation of any significant conclusions resulting from this thesis research. The model generated was designed to offer a generalization of a large number of vehicle makes and manufacturers, and provide a simple prediction of the carbon dioxide build-up simulated to the utmost accuracy. Different recirculation strategies were to be implemented into the model and compared based on carbon dioxide build-up, compressor load reductions, and any effects on the thermal environment of the cabin. The research completed was based on an extensive literature review, which not only presented the lack of information on studying functional recirculation control strategies for controlling carbon dioxide, but also the shortage of cohesive experimental results for predicting the air exchange rate inside vehicles. The results of the study successfully achieved the objectives of the research and in addition, further recommendations for future work on related subjects are provided.

5.1 Conclusions

- Phenomena discussed in literature such as the reduction of equilibrium concentrations at higher speeds, and higher blower mass flow rates, in addition to the severity of build-up with increasing number of passengers were also experienced by the lumped parameter model.
- Using the derived equation for a fractional air exchange rate, simulations showed that small amounts of outside air (5-10%) were able to greatly reduce equilibrium carbon dioxide concentrations under steady state driving conditions.
- Both on-off and fractional recirculation strategies were able to successfully control the carbon dioxide build-up inside the vehicle cabin within ASHRAE Standard 62

for acceptable air quality. The high levels of carbon dioxide seen in the timed recirculation strategy remains to be am important factor diminishing air quality inside the cabin and causing potential health concerns over time.

- Compressor load savings were found to be directly related to the amount of recirculation involved in the strategy. As such, the timed control strategies were favorable for reducing the compressor load over both the on-off and fractional control strategies, as these cycles involving a CO_2 sensor were sensitive to the number of occupants in the vehicle.
- Timed recirculation control remains to be a better choice for any temperature implications, as both fractional and on-off control strategies experienced large and frequent cabin temperature fluctuations at high ambient conditions (35°C).
- The trade-off between carbon dioxide concentrations, and compressor load savings becomes the limiting factor when analyzing various control strategies. For acceptable air quality, health and safety of all passengers, a control strategy must find an appropriate balance between compressor load savings, and severity of carbon dioxide build-up inside the cabin.

Control strategies involved in this thesis research may be applied to the automatic function found in vehicle air conditioning systems. The ECU could select one or more control strategies for optimal compressor load savings, air quality or cabin temperature, depending on the user's priority. The thesis research managed to successfully address all goals outlined, and provide insight to carbon dioxide build-up and recirculation strategies to mitigate the severity.

5.2 Recommendations

The recommendations below offer insights to automatic recirculation control strategies based on a combination of previous studies, author based recommendations, and results obtained over the progression of this thesis research.

- If air quality becomes a focus for the automotive manufacturer, utilizing a fractional or on-off control strategy with the use of a carbon dioxide sensor is recommended for controlling carbon dioxide concentrations to maintain adequate air quality.
- Timed control strategies have been shown to be a poor choice when concerning cabin air quality. High carbon dioxide concentrations seen using these strategies have been shown to be well above ASHRAE Standard 62 and are alarming when considering occupant health and safety.
- For strategies that include a frequent oscillation from RC to OSA mode and even strategies involving fractional recirculation, experimental testing must ensure the durability and reliability of all mechanical components. Any recirculation flap door utilizing a specific recirculation strategy should be able to maintain the same lifespan as one not utilizing a specific strategy, thus not compromising the integrity of the recirculation flap door.

5.3 Opportunities for Future Work

While it is clear that the research goals were accomplished in the completion of this thesis work, there are opportunities to further investigate recirculation control strategies and to improve the simulation model. Experimental testing becomes an important factor in further understanding vehicle air exchange rates that affect the

build-up of pollutants inside the cabin. The following is an in-depth list of opportunities for future work to improve the accuracy of the build-up model and also the comparison of various recirculation control strategies.

- Further experimental testing in order to better quantify and predict the air exchange rates inside vehicles, with an emphasis on air exchange rates using fractional recirculation. Improved estimations can then be applied to a specific vehicle make or model.
- Experimental testing of recirculation control strategies to validate simulation model. Physical verification of the successful operation of various recirculation control strategies.
- Experimental investigation of carbon dioxide concentrations and flow rates of human exhalation for an improved estimation within the simulation model.
- Incorporate passenger jury testing to better understand subjective aspects of thermal comfort and air quality induced by various control strategies.
- Cost analysis of various recirculation strategies. This would consider any potential limitations or drawbacks of a specific recirculation strategy from a cost comparison perspective.
- RC mode has been shown to reduce particle pollution entering the cabin, and so a module which could predict cabin particle concentrations may be a useful tool. The addition of particle pollution implications of the recirculation strategies could improve the capability of the simulation model and provide a further base on which to compare the various strategies.
- Analyzing recirculation control strategies during winter conditions may be beneficial as winter conditions may present a more severe scenario for carbon

dioxide build-up inside the cabin (cabin tightly sealed ie. no windows open)

The creation of this carbon dioxide build-up model successfully identified main vehicle parameters and their effects on the carbon dioxide build-up in the cabin. This model was also able to simulate and compare various recirculation control strategies to control carbon dioxide and analyze any further vehicle implications of these strategies. If combined with the numerous opportunities for future work listed above, an improved model could provide more insight into the simulation of recirculation control strategies for improved vehicle cabin air quality.

Bibliography

[1] M. J. Fedoruk and B. D. Kerger, "Measurement of volatile organic compounds inside automobiles," *Journal of Exposure Science and Environmental Epidemiology*, vol. 13, no. 1, pp. 31–41, 2003.

[2] H. Jung, "Modeling co_2 concentrations in vehicle cabin," tech. rep., SAE Technical Paper, 2013.

[3] Y. Zhu, A. Eiguren-Fernandez, W. C. Hinds, and A. H. Miguel, "In-cabin commuter exposure to ultrafine particles on los angeles freeways," *Environmental Science & Technology*, vol. 41, no. 7, pp. 2138–2145, 2007.

[4] K. Galatsis, W. Wlodarski, B. Wells, and S. McDonald, "Vehicle cabin air quality monitor for fatigue and suicide prevention," *SAE transactions*, vol. 109, no. 6, pp. 55–59, 2000.

[5] G.-S. Zhang, T.-T. Li, M. Luo, J.-F. Liu, Z.-R. Liu, and Y.-H. Bai, "Air pollution in the microenvironment of parked new cars," *Building and Environment*, vol. 43, no. 3, pp. 315–319, 2008.

[6] A. V. Filho, "New vehicles cabin indoor air quality," tech. rep., SAE Technical Paper, 2010.

[7] G. D. Mathur, "Experimental investigation to monitor tailpipe emissions entering into vehicle cabin to improve indoor air quality (iaq)," tech. rep., SAE Technical Paper, 2007.

[8] G. D. Mathur, "Field tests to monitor build-up of carbon dioxide in vehicle cabin with ac system operating in recirculation mode for improving cabin iaq and safety," *SAE International Journal of Passenger Cars-Mechanical Systems*, vol. 1, no. 1, pp. 757–767, 2009.

[9] M. L. Grady, H. Jung, Y. chul Kim, J. K. Park, and B. C. Lee, "Vehicle cabin air quality with fractional air recirculation," tech. rep., SAE Technical Paper, 2013.

[10] S. A. Fruin, N. Hudda, C. Sioutas, and R. J. Delfino, "Predictive model for vehicle air exchange rates based on a large, representative sample," *Environmental Science & Technology*, vol. 45, no. 8, pp. 3569–3575, 2011.

[11] N. Hudda, S. P. Eckel, L. D. Knibbs, C. Sioutas, R. J. Delfino, and S. A. Fruin, "Linking in-vehicle ultrafine particle exposures to on-road concentrations," *Atmospheric Environment*, vol. 59, pp. 578–586, 2012.

[12] S. Huff, B. West, and J. Thomas, "Effects of air conditioner use on real-world fuel economy," tech. rep., SAE Technical Paper, 2013.

[13] A. Kemle, R. Manski, H. Riegel, and M. Weinbrenner, "Reduction of fuel consumption in air conditioning systems," *Training*, vol. 2014, pp. 04–10.

[14] S. A. Rice, "Human health risk assessment of co2: survivors of acute high-level exposure and populations sensitive to prolonged low-level exposure," *Environments*, vol. 3, no. 5, pp. 7–15, 2004.

[15] J. L. Scott, D. G. Kraemer, and R. J. Keller, "Occupational hazards of carbon dioxide exposure," *Journal of Chemical Health and Safety*, vol. 16, no. 2, pp. 18–22, 2009.

[16] Y. A. Cengel and Boles, *Thermodynamics: An Engineering Approach*, vol. 5. McGraw-Hill New York, 2011.

[17] R. T. Balmer, *Modern Engineering Thermodynamics*. Academic Press, 2010.

[18] A. Handbook-Fundamentals, "Chapter 6: Psychrometrics," *American Society of Heating Refrigeration and Air-Conditioning Engineers, Atlanta*, p. 17, 1997.

[19] A. Handbook-Fundamentals, "Chapter 8: Thermal comfort," *American Society of Heating Refrigeration and Air-Conditioning Engineers, Atlanta*, p. 28, 1997.

[20] ASHRAE, "Standard 55-2004," *Thermal environmental conditions for human occupancy*, 2004.

[21] A. V. Arundel, E. M. Sterling, J. H. Biggin, and T. D. Sterling, "Indirect health effects of relative humidity in indoor environments.," *Environmental Health Perspectives*, vol. 65, p. 351, 1986.

[22] H. Tsutsumi, Y. Hoda, S.-i. Tanabe, and A. Arishiro, "Effect of car cabin environment on driver's comfort and fatigue," *Human Factors*, vol. 1927, pp. 01–01, 2007.

[23] N. Hudda, E. Kostenidou, C. Sioutas, R. J. Delfino, and S. A. Fruin, "Vehicle and driving characteristics that influence in-cabin particle number concentrations," *Environmental Science & Technology*, vol. 45, no. 20, pp. 8691–8697, 2011.

[24] U. E. P. Agency, "Carbon dioxide as a fire suppressant: Examining the risks," Feb. 2000. `http://www.epa.gov/ozone/snap/fire/co2/co2report.pdf`.

[25] NIOSH, "Criteria for a recommended standard," *Occupational exposure to Carbon Dioxide (Pub. No. 76-194). Cincinnati, OH: NIOSH (DHHS)*, 1976.

[26] O. Safety, H. Administration, *et al.*, "Cfr 1910.1000 table z-1," *OSHA website www. osha. gov*, 29.

[27] ASHRAE, "Standard 62-2001, ventilation for acceptable indoor air quality," *American Society of Heating, Refrigerating, and Air-Conditioning Engineers, Atlanta, www. ASHRAE. org*, 2001.

[28] B. Fletcher and C. Saunders, "Air change rates in stationary and moving motor vehicles," *Journal of Hazardous Materials*, vol. 38, no. 2, pp. 243–256, 1994.

[29] L. D. Knibbs, R. De Dear, and S. E. Atkinson, "Field study of air change and flow rate in six automobiles," *Indoor Air*, vol. 19, no. 4, pp. 303–313, 2009.

[30] W. Ott, N. Klepeis, and P. Switzer, "Air change rates of motor vehicles and in-vehicle pollutant concentrations from secondhand smoke," *Journal of Exposure Science and Environmental Epidemiology*, vol. 18, no. 3, pp. 312–325, 2008.

[31] H. J. Krzywicki and K. S. Chinn, "Human body density and fat of an adult male population as measured by water displacement," *The American journal of clinical nutrition*, vol. 20, no. 4, pp. 305–310, 1967.

[32] A. TenWolde and C. L. Pilon, "The effect of indoor humidity on water vapor release in homes," *Proceedings of Thermal Performance of the Exterior Envelopes of Whole Buildings X*, 2007.

[33] G. Ashrae and D. Book, "Fundamentals and equipment," *New York: ASHRAE*, 1963.

[34] C. Malvicino, M. Markowitz, K. Schuermanns, A. Bergami, C. Arnaud, R. Haller, C. Petitjean, C. Strupp, N. Lemke, D. Clodic, *et al.*, "B-cool project-ford ka and fiat panda r-744 mac systems," *Gas*, vol. 4, p. 5, 2009.

Vita Auctoris

Name:	Teron Matton
Place of Birth:	Windsor, ON
Year of Birth:	1990
Education:	University of Windsor, B.A.Sc. Mechanical Engineering, Windsor, ON, 2012
	University of Windsor, M.A.Sc. Candidate Mechanical Engineering, Windsor, ON, 2015